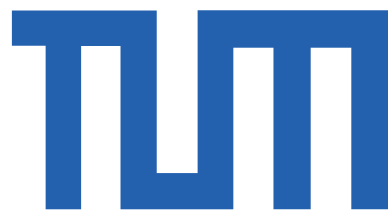


---

# Decoherence in a Disordered Quasi-1D Metallic Ring

Maximilian Treiber

---



München 2008



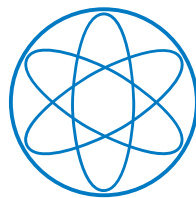
---

# Decoherence in a Disordered Quasi-1D Metallic Ring

Maximilian Treiber

---

Diplomarbeit  
am Physik Department  
der Technischen Universität  
München



vorgelegt von  
Maximilian Treiber

München, den 1. September 2008

Erstgutachter: Prof. Dr. Wilhelm Zwerger

Zweitgutachter: Prof. Dr. Jan von Delft

# Contents

<b>Summary</b>	<b>vii</b>
<b>1 Conductivity of disordered metals</b>	<b>1</b>
1.1 Introduction	1
1.2 Coherent backscattering	2
1.3 Weak localization	4
<b>2 Dephasing</b>	<b>13</b>
2.1 Infrared cutoff for weak localization	13
2.2 Cooperon in an external potential: Path integral representation	14
2.3 Decoherence due to electron-electron interactions	16
<b>3 Quasi-1d systems: Classical noise</b>	<b>19</b>
3.1 Fluctuation-Dissipation-Theorem and Johnson-Nyquist noise	19
3.2 Classical noise correlator in a quasi-1d system	21
3.3 Dephasing of the Cooperon due to electron-electron interactions	24
3.4 Electron-Electron interactions for quasi-1d systems in real space	24
3.5 Averaging over closed random walks	26
3.6 Exact results in an infinite quasi-1d wire	27
3.7 Calculation of the Cooperon decay function in a quasi-1d ring	28
3.7.1 Diffusion on a ring and winding numbers	28
3.7.2 Averaging over closed random walks on a ring	30
3.7.3 Results for the Cooperon decay function	32
3.7.4 Asymptotic behavior of the Cooperon decay function	34
3.7.5 Summary	36
<b>4 Quasi-1d systems: Quantum noise</b>	<b>39</b>
4.1 Quantum noise correlator including the Pauli principle	39
4.2 Cooperon decay and quantum noise	41
4.3 Calculation of the Cooperon decay function in a quasi-1d ring	42
4.3.1 Asymptotic behavior of the Cooperon decay function	42
4.3.2 Summary and results for the dephasing length	49

<b>5</b>	<b>Corrections to the conductivity</b>	<b>53</b>
5.1	Weak localization correction to the conductivity in a quasi-1d ring . . . . .	53
5.2	Magneto-conductance measurements . . . . .	57
5.3	Possible experimental realization . . . . .	59
5.3.1	The effect of connecting wires . . . . .	60
5.3.2	Recent experiments in a grid . . . . .	61
<b>6</b>	<b>Conclusions</b>	<b>63</b>
<b>A</b>	<b>Asymptotic evaluation of the Cooperon decay function</b>	<b>65</b>
A.1	Classical noise . . . . .	65
A.1.1	The long ring $l_t \ll 1$ : . . . . .	65
A.1.2	The short ring $1 \ll l_t$ : . . . . .	66
A.2	Quantum noise . . . . .	67
A.2.1	The long ring $l_T \ll l_t \ll 1$ . . . . .	67
A.2.2	The short ring $l_T \ll 1 \ll l_t$ . . . . .	68
A.2.3	The very short ring $1 \ll l_T \ll l_t$ . . . . .	70
<b>B</b>	<b>Comments on the numerical evaluation of the Cooperon decay function</b>	<b>71</b>
<b>C</b>	<b>Mathematical Formulas</b>	<b>73</b>
C.1	Table of integrals and sums . . . . .	73
C.2	Asymptotic expansions . . . . .	75
<b>D</b>	<b>Special functions</b>	<b>77</b>
D.1	The function $\tilde{\Omega}(x)$ . . . . .	77
D.2	The function $\tilde{z}_Q(x)$ . . . . .	79
	<b>Acknowledgments</b>	<b>84</b>

# Summary

In this thesis, we will calculate the correction to the conductivity of a disordered quasi one dimensional metallic ring in the weak localization regime, using an improved treatment of electron-electron interactions.

After a short introduction, we will start our discussion in chapter 1 with a review of the transport properties in this regime and explain the effect of coherent backscattering. We will then give an introduction to the formal perturbation theory, based on the so called Cooperon diagram, by which this effect can be described. This will allow us to connect the conductivity correction to the return probability of a random walk of the electrons in the disordered system.

In chapter 2 we will introduce electron dephasing in the context of this correction and explain how thermal fluctuations of the surrounding electrons lead to decoherence.

We will then consider the case of a disordered quasi one dimensional metallic ring, which is closely connected to the problem of the disordered infinite wire, first solved by Altshuler, Aronov and Khmelnitsky (AAK). In their celebrated paper [1] from 1982, these authors calculated the correction to the conductivity in the weak localization regime, due to electron-electron interactions in the framework of Johnson-Nyquist noise. We will discuss the basics of this correction in chapter 3 and will show that their results, in the absence of a magnetic field, can be well approximated by a Cooperon decay function of the form:

$$F(t) \sim Tt^{3/2}.$$

In 2004, Ludwig and Mirlin [2] and later Texier and Montambaux [3], were able show that in the geometry of a ring, the results are strongly modified. We will show in chapter 3 that the correction to the conductivity in a quasi one dimensional ring can be written in the form

$$\Delta\sigma \sim \int_0^\infty \sum_{n=-\infty}^\infty P_n(t) e^{-F_n(t)} \quad P_n(t) = \frac{1}{\sqrt{4\pi Dt}} e^{-(nL)^2/4Dt},$$

where  $n$  is the winding number of an electron trajectory and  $L$  is the size of the ring.

Then, we will calculate in the real space and time domain the function  $F_n(t)$  for classical noise and obtain a behavior similar to AAK for trajectories which are much shorter than  $L$ , while for trajectories that explore the system completely it is given by

$$F_n(t) \sim LTt,$$

confirming the known results. We will analyze this crossover in detail and calculate relevant correction terms.

Recently, Marquardt and von Delft suggested a more evolved treatment of the electronic noise in their papers [4] and [5] and proposed an effective replacement for the correlator of the corresponding fields.

They calculated corrections to the Cooperon decay function in an infinite wire and obtained a parametrically small deviation from the AAK result in the form:

$$F(t) \sim Tt^{3/2} \left( 1 - \frac{1}{\sqrt{Tt}} \right),$$

where, in the regime of weak localization, always  $Tt \gg 1$ . In chapter 4 we will confirm this result and calculate the correction due to this improved treatment in the ring geometry.

We will find that, as long as the thermal length  $L_T = \sqrt{D/T}$  stays much smaller than the ring size  $L$  and the average length of the trajectory  $L_t = \sqrt{Dt}$ , the correction remains parametrically small and we will give a detailed calculation of all relevant terms.

For the case of a thermal length larger than the size of the ring, on the other hand, we find a new regime, with a different size and temperature dependence:

$$F_n(t) \sim L^3 T^2 t.$$

Here, the decay is strongly suppressed, since, using the improved version of the correlator, the potential can be considered frozen on the time scale of  $\hbar/k_B T$ , describing the onset of strong localization. An overview of these results can be found in table 4.1.

In chapter 5 we will discuss the correction to the conductivity, obtained from the calculated decay function. We will find that in the new regime the correction will necessarily be too large to be treated in the framework of weak localization. Thus, we will concentrate on the possibility to measure deviations from the the classical results. For this, we will consider the presence of an external magnetic field and the effect of connecting the ring to leads and recent experiments in metallic grids.

# Chapter 1

## Conductivity of disordered metals

In the 1980s, the anomalous transport properties of electrons in disordered systems have been studied experimentally and theoretically in great detail. It has been found that the quantum-interference of electrons scattering at impurities can not be neglected in sufficiently disordered systems and gives rise to a correction to the conductivity generally called *weak localization*. For original reviews of this topic, see [6] and [7]. In this chapter, we will discuss the basic properties of this correction and the underlying concepts, which will be the foundation of our later calculations.

### 1.1 Introduction

The simplest model of electrical conduction in a metal is the Drude model, where one obtains a local isotropic current density originating from an external electric field of the form:

$$\mathbf{j}(x) = \sigma_0 \mathbf{E}(x), \quad \sigma_0 = \frac{ne^2\tau_{tr}}{m}. \quad (1.1)$$

The conductivity is here proportional to the electron charge density  $ne$ , to the ratio of the electron charge to its mass  $e/m$  (originating from the Lorentz force) and the transport time  $\tau_{tr}$ , given by the average time during which the electron is effectively accelerated. This is equivalent to the average time between collision of the electron with some scattering potential, which is given in a metal by impurities, defects, interstitials, etc. The assumptions on which this is based are

- Electrons behave as classical particles and do not interact with each other.
- Collisions of the electrons with impurities are instantaneous and independent events, which occur with a probability of  $1/\tau_{tr}$  per unit time.
- The electric field  $\mathbf{E}(x)$  is weak, so that the response can be treated in linear order, and varies only slowly on the length of the mean free path  $l_e$ . Any magnetic fields can be neglected.

In spite of the crude simplicity of this model, it is nevertheless sufficient to adequately describe several real systems.

One of the most remarkable features of the Drude model is that one may equally describe it in the context of a diffusion process of the electrons through the metal impurities. In steady state, the current is equivalent to a gradient of the electron charge density:

$$\sigma_0 E = -eD\nabla n. \quad (1.2)$$

The coefficient  $D$ , called the diffusion constant, can be obtained in the Drude model by the Einstein relation:

$$\sigma_0 = 2e^2\rho_0 D, \quad (1.3)$$

where  $\rho_0 = \partial n/\partial\epsilon|_{\epsilon_F} = 3n/4\epsilon_F$  is the electron density of states at the Fermi surface, so that

$$D = \frac{1}{3}v_F^2\tau_{tr}. \quad (1.4)$$

There have been several successful attempts to improve this simple picture. In the context of the *Boltzmann equation*, one is able to improve the treatment of the collision process and calculate the transport time from a microscopic scattering theory. Band structure effects of the metal can be included in an *effective electron mass* and the interactions of the electron with the surrounding Fermi-sea can be treated in the context of the *Fermi-liquid theory*.

But all these improvements have in common that the electron is described as a free (quasi-)particle, obeying some distribution function, totally neglecting the wave-like behavior of the electron as a quantum mechanical object. In fact, following Heisenberg's uncertainty relation, it follows that as long as

$$k_F l_e \gg 1 \quad (1.5)$$

the free particle description may be an adequate approximation.

But at high enough impurity concentrations, this cannot be correct any more. The quantum nature of the electrons manifests itself by a reduction of the conductivity due to coherent backscattering of the electron wave, interfering at the impurity positions. This correction is what is generally called weak localization and its theory is a perturbation theory in the small parameter  $1/k_F l_e$ .

In the opposite limit, when the wavelength of the electron gets comparable to its mean free path, the electron states become localized and the metal becomes insulating. In fact, in one or two dimensions, it has been shown that already at arbitrary small impurity densities, the correction due to this effect necessarily leads to localization at zero temperature. This is generally called Anderson localization.

## 1.2 Coherent backscattering

To describe the propagation of an electron in a disordered metal, we use a quasi-classical picture, corresponding to the limit  $k_F l_e \gg 1$ . We assume here that the electron travels on

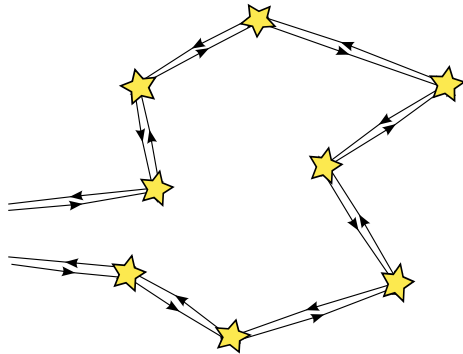


Figure 1.1: Two electron trajectories in a disordered metal, where one of the scattering sequences has been reversed. Both trajectories pick up the same phase if they are closed.

classical paths, but, in contrast to a particle, additionally has a phase factor that varies with time. Points in space having the same phase can then be considered a wavefront, similar to the rules of classical optics. In the presence of impurities, the paths may then be viewed as a sequence of free propagations, interrupted by scattering events.

Following the rules of quantum mechanics, the probability for an electron to travel some distance in the metal is given by the squared amplitude of two such paths. Therefore, consider the amplitudes of two paths  $\psi_a$  and  $\psi_b$  in this metal with the same start and end points. In a purely classical treatment, where one does not keep track of a phase, the probability would be given simply by the incoherent sum of the individual probabilities:

$$|\psi_a|^2 + |\psi_b|^2. \quad (1.6)$$

The wave-nature of the electron, on the other hand, will lead to a final probability of the form:

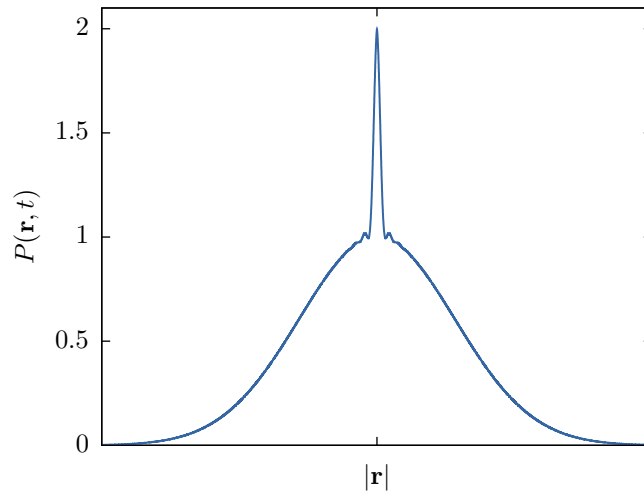
$$|\psi_a + \psi_b|^2 = |\psi_a|^2 + |\psi_b|^2 + \psi_a\psi_b^* + \psi_a^*\psi_b, \quad (1.7)$$

where the last two terms depend on the phase factor and describe the effect of interference.

Since the wavelength of the electron is very short, compared to the average distance between collisions, the interference will be very sensitive to the impurity positions. In our treatment of the problem, we are not interested in sample specific effects, thus, we consider an average over impurity positions. After this average has been done, the pairs of trajectories will dominate this probability, where collisions involve exactly the same impurities, since a variation of one impurity position (on the scale of the impurity distance) of only one of the trajectories will change its phase drastically and, after averaging over all impurity positions, cancel out.

As long as we only assume static, elastic scattering events, so that the system is symmetric with respect to time-reversing a trajectory, there are in fact two pairs of trajectories that survive averaging. The first one is given by the pair which scatters at the same impurities in the same order, while for the second, the scattering sequence of one of the trajectories is exactly reversed. The latter case is shown in figure 1.1. In fact, for the propagation probability for a closed trajectory, both contribute equally and thus the return probability is exactly doubled. The probability from a purely classical treatment here

Figure 1.2: The probability density for quantum diffusion is doubled close to the origin in a quantum mechanical treatment of diffusion. (Taken from [8])



yields  $2|\psi|^2$  while, because of the interference term, one obtains  $2|\psi|^2 + 2\psi^*\psi = 4|\psi|^2$  in this semi-classical treatment. On the other hand, when the start and end points are far away from each other, reversing one of the trajectories necessarily leads to opposite start and end points for each of the paths and the phase accumulated can not be the same any more. A detailed calculation of the quantum-mechanical diffusion probability density is shown in figure 1.2. This enhancement of the return probability due to the phase factor and due to this time-reversal symmetry of the system is called coherent backscattering. The weak localization correction to the conductivity, which we will calculate in this thesis, is due to this interference effect.

### 1.3 Weak localization

In this section we will formally derive the corrections to the conductivity, due to coherent backscattering. Within the scope of this thesis, this can only be a short sketch of well known results, for the reader who is not familiar with the theory of weak localization. Therefore, at several points in the derivation, we have to refer to a more careful introduction, given e.g. in chapter 1 of [9] or chapter 7 of [8]. Here, we will follow the argumentations of [10].

Starting from the Einstein relation (1.3), we write the (isotropic,  $\mathbf{q} = 0$ ) conductivity as:

$$\sigma = 2e^2 \rho_0 \frac{v_F^2}{3} \int_0^\infty dt \langle \hat{\mathbf{k}}'(t) \hat{\mathbf{k}}(0) \rangle, \quad (1.8)$$

where we replaced the transport time  $\tau_{tr}$  by the time-integrated momentum-momentum correlation function, describing the time an electron travels before losing its memory of the initial direction of its velocity. (A detailed derivation of this assumption from Kubo's formula can be found in appendix A of [7] or in chapter 1.2.3 of [9]. We assumed here that the wave-vectors have modulus  $k_F$ , i.e.  $\hat{\mathbf{k}}$  is normalized to 1.)

If the electron is in the state  $\psi$ , then this average is given by:

$$\langle \hat{\mathbf{k}}'(t) \hat{\mathbf{k}}(0) \rangle = \sum_{\mathbf{k}'} (\hat{\mathbf{k}}' \hat{\mathbf{k}}) \langle |\langle \mathbf{k}' | \psi(t) \rangle|^2 \rangle_{imp}, \quad (1.9)$$

where  $\langle \dots \rangle_{imp}$  denotes averaging over impurity positions, as has been discussed in the previous section.

The modulus squared of the overlap can be written in terms of the retarded electron Green's function:

$$|\langle \mathbf{k}' | \psi(t) \rangle|^2 = |\langle \mathbf{k}' | \hat{U}(t) | \mathbf{k} \rangle|^2 = |G_{\mathbf{k}'\mathbf{k}}^R(t)|^2, \quad (1.10)$$

where  $\hat{U}(t)$  is the time-evolution operator and

$$G_{\mathbf{k}'\mathbf{k}}^R(t) = -i\theta(t) \langle \mathbf{k}' | \hat{U}(t) | \mathbf{k} \rangle. \quad (1.11)$$

For a free electron with dispersion relation  $\epsilon_{\mathbf{k}}$ , the retarded Green's function and its Fourier transform are given by:

$$G_{\mathbf{k}'\mathbf{k}}^{R(0)}(t) = -i\theta(t) \delta_{\mathbf{k}'\mathbf{k}} e^{-i\epsilon_{\mathbf{k}}t} \quad \Rightarrow \quad G_{\mathbf{k}'\mathbf{k}}^{R(0)}(\omega) = \frac{\delta_{\mathbf{k}'\mathbf{k}}}{\omega - \epsilon_{\mathbf{k}} + i0^+}, \quad (1.12)$$

where, generally in this thesis, we will measure energy in units of frequency. We are interested in the impurity averaged product:

$$\langle |G_{\mathbf{k}'\mathbf{k}}^R(t)|^2 \rangle_{imp}. \quad (1.13)$$

Using an expansion in the impurity potential strength, this can be obtained using the diagrammatic technique. A comprehensive discussion of this technique can be found in [11]. Consider first the free retarded electron Green's function, which is a solution to the Schrödinger equation with  $\delta$ -inhomogeneity:

$$\begin{aligned} i\partial_t G_{\mathbf{k}'\mathbf{k}}^R(t) - \sum_{\tilde{\mathbf{k}}} H_{\mathbf{k}'\tilde{\mathbf{k}}} G_{\tilde{\mathbf{k}}\mathbf{k}}^R(t) &= \delta(t) \delta_{\mathbf{k}'\mathbf{k}} \quad (\text{for } t > 0) \\ \Rightarrow \omega G_{\mathbf{k}'\mathbf{k}}^R(\omega) - \sum_{\tilde{\mathbf{k}}} H_{\mathbf{k}'\tilde{\mathbf{k}}} G_{\tilde{\mathbf{k}}\mathbf{k}}^R(\omega) &= \delta_{\mathbf{k}'\mathbf{k}}, \end{aligned} \quad (1.14)$$

where  $H$  is the Hamilton operator of the system. Now, in the presence of the (static) potential of the impurities,  $V(\mathbf{q})$ , the Hamiltonian is given by the free part plus the potential:

$$H_{\mathbf{k}'\tilde{\mathbf{k}}} = \epsilon_{\mathbf{k}'} \delta_{\mathbf{k}'\tilde{\mathbf{k}}} + V(\mathbf{q} = \mathbf{k}' - \tilde{\mathbf{k}}). \quad (1.15)$$

From this, we obtain a Dyson equation for the full retarded Green's function (i.e. in the presence of the impurity potential) in terms of the free Green's function, given in (1.12):

$$G_{\mathbf{k}'\mathbf{k}}^R(\omega) = G_{\mathbf{k}'\mathbf{k}}^{R(0)}(\omega) + \sum_{\mathbf{q}} G_{\mathbf{k}'\mathbf{k}'}^R(\omega) V(\mathbf{q}) G_{\mathbf{k}'-\mathbf{q}\mathbf{k}}^R(\omega) \quad (1.16)$$

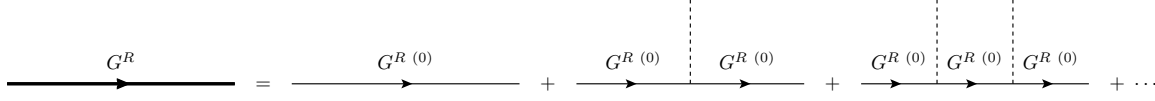


Figure 1.3: Diagrammatic representation of (1.17).

The solution of this equation can be obtained by iterative substitution:

$$\begin{aligned}
G_{\mathbf{k}'\mathbf{k}}^R(\omega) &= G_{\mathbf{k}'\mathbf{k}}^{R(0)}(\omega) + \sum_{\mathbf{q}} G_{\mathbf{k}'\mathbf{k}'}^{R(0)}(\omega) V(\mathbf{q}) G_{\mathbf{k}'-\mathbf{q}\mathbf{k}}^{R(0)}(\omega) \\
&+ \sum_{\mathbf{q}_1} \sum_{\mathbf{q}_2} G_{\mathbf{k}'\mathbf{k}'}^{R(0)}(\omega) V(\mathbf{q}_1) G_{\mathbf{k}'-\mathbf{q}_1\mathbf{k}'-\mathbf{q}_1}^{R(0)}(\omega) V(\mathbf{q}_2) G_{\mathbf{k}'-\mathbf{q}_1-\mathbf{q}_2\mathbf{k}}^{R(0)}(\omega) \\
&+ \dots
\end{aligned} \tag{1.17}$$

This iteration can be represented diagrammatically, see figure 1.3, where horizontal bold lines correspond to the full retarded Green's functions and thin horizontal lines to the free Green's functions, while impurity potentials are symbolized by dashed, vertical lines.

We are interested now in the impurity averaged version of this Green's function, thus we need an explicit model for the impurities. A particularly simple model, which is commonly used in this context is the so-called Edwards model, which assumes that  $V(\mathbf{r})$  is a Gaussian random process. Here, we assume the following form:

$$\langle V(\mathbf{r}) \rangle_{imp} = 0 \tag{1.18}$$

$$\langle V(\mathbf{r}) V(\mathbf{r}') \rangle_{imp} = \delta(\mathbf{r} - \mathbf{r}') \frac{1}{2\pi\rho_0\tau}. \tag{1.19}$$

The impurity potential here is thus an example of *white noise*, i.e. delta correlated in space, whose average over the whole system is vanishing. The factor  $2\pi\rho_0\tau$  is here simply a parameter, describing the strength of the impurity potential, which can be obtained from a microscopic theory in the limit of a high density of weak scatterers, see chapter 2.2.2 of [8]. In  $\mathbf{k}$ -space, the second term reads:

$$\langle V(\mathbf{k}) V(\mathbf{k}') \rangle_{imp} = \delta_{\mathbf{k}\mathbf{k}'} \frac{1}{2\pi\rho_0\tau V}, \tag{1.20}$$

where  $V$  is the volume of our system. Gaussian processes have the very important property that higher order correlators can always be factorized in terms of the two-point correlator, e.g.:

$$\begin{aligned}
\langle V(\mathbf{k}_1) V(\mathbf{k}_2) V(\mathbf{k}_3) V(\mathbf{k}_4) \rangle_{imp} &= \langle V(\mathbf{k}_1) V(\mathbf{k}_2) \rangle_{imp} \langle V(\mathbf{k}_3) V(\mathbf{k}_4) \rangle_{imp} \\
&+ \langle V(\mathbf{k}_1) V(\mathbf{k}_3) \rangle_{imp} \langle V(\mathbf{k}_2) V(\mathbf{k}_4) \rangle_{imp} \\
&+ \langle V(\mathbf{k}_1) V(\mathbf{k}_4) \rangle_{imp} \langle V(\mathbf{k}_2) V(\mathbf{k}_3) \rangle_{imp}
\end{aligned} \tag{1.21}$$

(i.e. all possible pairings in analogy to Wick's theorem for a bosonic, free quantum field theory), where the probability distribution of the values  $V(\mathbf{k})$  evaluated at different points  $\mathbf{k}$  has to be Gaussian.

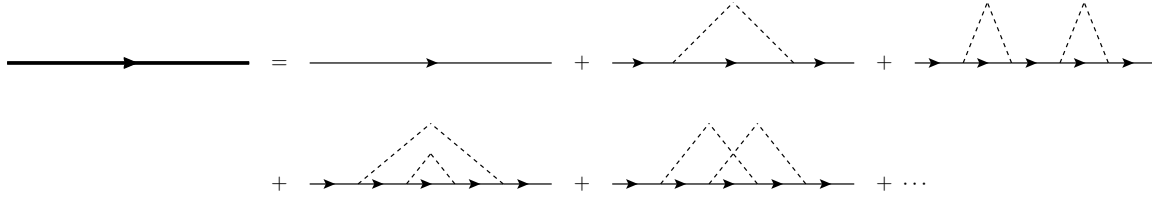
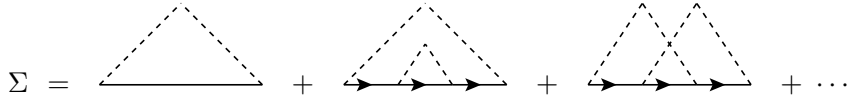


Figure 1.4: Diagrammatic representation of the impurity averaged Green's function.

Figure 1.5: Diagrammatic representation of the irreducible self-energy  $\Sigma(\mathbf{k}, \omega)$  from (1.22).

The effect of the delta correlation and the gaussian factorization is best seen in the diagrammatic representation, figure 1.4, which is the impurity averaged version of 1.3 (but, to higher order in the potential). All the impurity lines have to be connected now, because of (1.18), in all possible ways, because of (1.21). And with each impurity line, one has to associate the term given by (1.19).

The diagrams can be summed up using a geometric series:

$$\begin{aligned}
 \langle G_{\mathbf{k}}^R(\omega) \rangle_{imp} &= G_{\mathbf{k}}^{R(0)}(\omega) + G_{\mathbf{k}}^{R(0)}(\omega) \Sigma(\mathbf{k}, \omega) G_{\mathbf{k}}^{R(0)}(\omega) \\
 &\quad + G_{\mathbf{k}}^{R(0)}(\omega) \Sigma(\mathbf{k}, \omega) G_{\mathbf{k}}^{R(0)}(\omega) \Sigma(\mathbf{k}, \omega) G_{\mathbf{k}}^{R(0)}(\omega) \\
 &\quad + \dots \\
 &= \frac{G_{\mathbf{k}}^{R(0)}(\omega)}{1 - \Sigma(\mathbf{k}, \omega) G_{\mathbf{k}}^{R(0)}(\omega)},
 \end{aligned} \tag{1.22}$$

where we used the shorthand notation  $G_{\mathbf{k}}^R = G_{\mathbf{k}\mathbf{k}}^R$ , since, after averaging over impurities, the system will be translationally invariant. Here,  $\Sigma(\mathbf{k}, \omega)$  is the so-called irreducible self energy, given by all diagrams, indicated in figure 1.5, which cannot be divided into separate pieces by cutting a single  $G_{\mathbf{k}}^{R(0)}$ -line.

Inserting the result for the free Green's function (1.12) into (1.22), we obtain:

$$\langle G_{\mathbf{k}}^R(\omega) \rangle_{imp} = \frac{1}{\omega - \epsilon_{\mathbf{k}} + i0^+ - \Sigma(\mathbf{k}, \omega)}. \tag{1.23}$$

The self energy is a complex quantity and its real part can be absorbed into a renormalization of  $\epsilon_{\mathbf{k}}$ , while its imaginary part is the physically important scattering rate. Since  $\Sigma$  is already given by an infinite number of diagrams, one commonly only considers the first order term, given by the first diagram of figure 1.5:

$$\text{Im} [\Sigma(\mathbf{k}, \omega)] = \frac{1}{2\pi V \rho_0 \tau} \sum_{\mathbf{q}} \text{Im} \left[ G_{\mathbf{k}-\mathbf{q}}^{R(0)}(\omega) \right] = -\frac{1}{2\tau}, \tag{1.24}$$

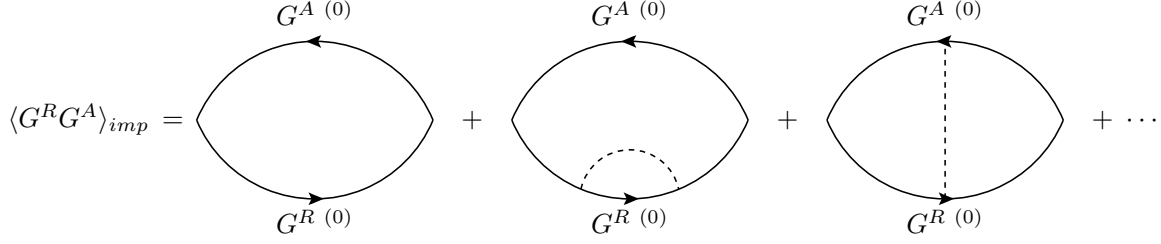


Figure 1.6: Averaging the product  $G^R G^A$  over impurity positions. Thin lines represent the free Green's function  $G^{(0)}$ .

since  $\text{Im} \left[ G_{\mathbf{k}}^R(\omega) \right] = -\pi \delta(\omega - \epsilon_{\mathbf{k}})$ . We conclude that the retarded Green's function after impurity averaging is given by

$$\langle G_{\mathbf{k}}^R(\omega) \rangle_{imp} = \frac{1}{\omega - \epsilon_{\mathbf{k}} + \frac{i}{2\tau}}. \quad (1.25)$$

The free Green's function is thus broadened in  $\mathbf{k}$  space, describing the fact that in a random potential plane wave states  $|\mathbf{k}\rangle$  are no longer eigenstates of  $H$  but have finite lifetime, given by  $\tau$ , corresponding, at least for isotropic scattering events, to a scattering time.

Actually, we were interested in the impurity average of the product (1.13):

$$\begin{aligned} \langle |G_{\mathbf{k}'\mathbf{k}}^R(t)|^2 \rangle_{imp} &= \langle G_{\mathbf{k}'\mathbf{k}}^R(t) G_{\mathbf{k}\mathbf{k}'}^A(-t) \rangle_{imp} \\ &= \int \frac{d\omega}{2\pi} e^{-i\omega t} \int \frac{d\epsilon}{2\pi} \langle G_{\mathbf{k}'\mathbf{k}}^R(\epsilon + \omega) G_{\mathbf{k}\mathbf{k}'}^A(\epsilon) \rangle_{imp}, \end{aligned} \quad (1.26)$$

where we defined the advanced Green's function:

$$[G_{\mathbf{k}'\mathbf{k}}^R(t)]^* = G_{\mathbf{k}\mathbf{k}'}^A(-t). \quad (1.27)$$

Averaging this product can be done in the same way as for the single Green's function, i.e. draw the retarded and advanced electron lines (denoted diagrammatically by arrows pointing in the opposite direction) and then connect them in all possible ways by impurity lines. This is shown schematically in figure 1.6.

The leading contributions in this expansion are given by the diagrams of figure 1.7. They can be put into 3 categories:

1. The **Drude** part, given by the first diagram of figure 1.7, which corresponds to the replacement

$$\langle G_{\mathbf{k}'\mathbf{k}}^R(t) G_{\mathbf{k}'\mathbf{k}}^A(-t) \rangle_{imp} \rightarrow \langle G_{\mathbf{k}'\mathbf{k}}^R(t) \rangle_{imp} \langle G_{\mathbf{k}'\mathbf{k}}^A(-t) \rangle_{imp} \quad (1.28)$$

The impurity lines here are connected only to one and the same electron propagator. In the quasi-classical picture, this corresponds to the case, where both electron trajectories never collide with the same impurity. Successive collisions are thus totally

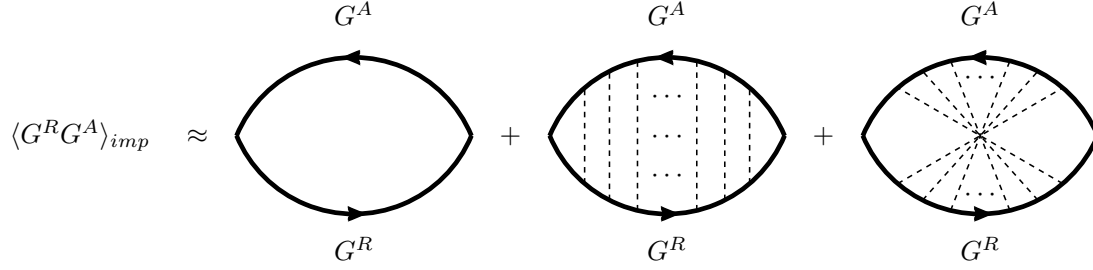


Figure 1.7: The 3 classes of diagrams dominating the impurity averaged product  $G^R G^A$ . Thick lines represent the impurity averaged Green's functions  $G$ .

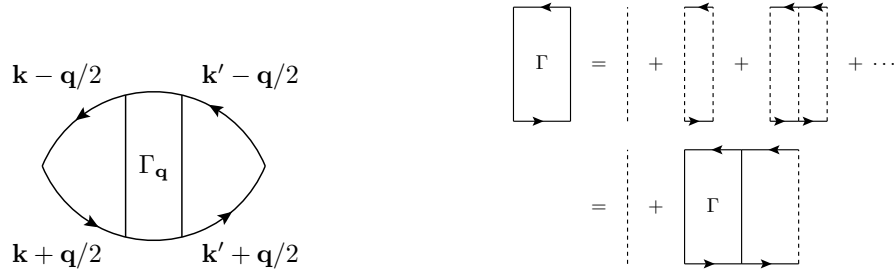


Figure 1.8: The diagrams corresponding to the diffuson and the structure factor.

uncorrelated. For this contribution, we obtain from (1.9), (1.10) and (1.25):

$$\begin{aligned}
 \sum_{\mathbf{k}'} (\hat{\mathbf{k}}' \hat{\mathbf{k}}) \langle |G_{\mathbf{k}'\mathbf{k}}^R(t)|^2 \rangle_{imp} &\approx \int \frac{d\omega}{2\pi} e^{-i\omega t} \sum_{\mathbf{k}'} (\hat{\mathbf{k}}' \hat{\mathbf{k}}) \int \frac{d\epsilon}{2\pi} \langle G_{\mathbf{k}'\mathbf{k}}^R(\epsilon + \omega) \rangle_{imp} \langle G_{\mathbf{k}'\mathbf{k}}^A(\epsilon) \rangle_{imp} \\
 &= \int \frac{d\omega}{2\pi} e^{-i\omega t} \sum_{\mathbf{k}} \hat{\mathbf{k}}^2 \int \frac{d\epsilon}{2\pi} \frac{1}{\epsilon - \epsilon_{\mathbf{k}} + \omega + \frac{i}{2\tau}} \frac{1}{\epsilon - \epsilon_{\mathbf{k}} - \frac{i}{2\tau}} \\
 &= \int \frac{d\omega}{2\pi} e^{-i\omega t} \frac{1}{\frac{1}{\tau} - i\omega} \\
 &= e^{-t/\tau},
 \end{aligned} \tag{1.29}$$

where the integral has been done using the residue theorem. Using this in (1.8) for the conductivity, we obtain:

$$\sigma = 2e^2 \rho_0 \frac{v_F^2}{3} \tau, \tag{1.30}$$

which coincides with the Drude result (1.3) and a posteriori identifies the parameter  $\tau$  with the transport time, here, coinciding with the elastic scattering time for our simple model of isotropic scatterers.

2. The so called **diffuson**, given by the second diagram of figure 1.7. Here, the Green's functions correspond to two trajectories with the exact same impurity scattering sequences, which we already identified in the previous section as a contribution that

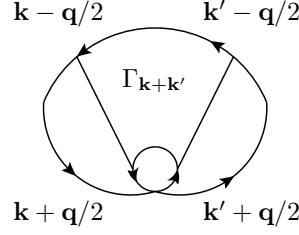


Figure 1.9: The diagram corresponding to the Cooperon, where one electron line has been twisted around. In this form, the structure factor of the diffuson and the Cooperon are identical.

survives impurity averaging. This diagram can be evaluated by considering the structure factor  $\Gamma$ , shown on the right, which is given by a so-called ladder diagram. In the case of the diffuson, this factor does not depend on  $\mathbf{k}$  and  $\mathbf{k}'$ , thus, the contribution to the conductivity due to the diffuson vanishes, because of the factor  $(\hat{\mathbf{k}}\hat{\mathbf{k}})$  of (1.8). The vector  $\mathbf{q}$ , shown in the diagram is the spatial dependence of the conductivity itself, thus in the case of anisotropic scattering, the diffuson plays an important role. A detailed discussion of these results and a careful reasoning of why it does not contribute to isotropic transport can be found in chapter 7.2.2 of [8].

3. The so called **Cooperon**, given by the third diagram of figure 1.7, which is given by the sum of all, so-called, *maximally crossed diagrams*, first discussed by Langer and Neal. This corresponds to trajectory pairs, where, for one of them, the sequence of scattering processes is the exact opposite of the other. To calculate the contribution of this diagram to the conductivity, consider figure 1.9, where one of the electron lines has been twisted, to show that the structure factor is actually the same as for the diffuson, but now depending on  $\mathbf{Q} = \mathbf{k} + \mathbf{k}'$ . From the figure 1.8 of the structure factor, we read off:

$$\Gamma_{\mathbf{Q}}(\omega) = \frac{1}{2\pi\rho_0\tau} + \frac{1}{2\pi\rho_0\tau V} \sum_{\mathbf{k}} \Gamma_{\mathbf{Q}}(\omega) \langle G_{\mathbf{k}}^R(\epsilon) \rangle_{imp} \langle G_{\mathbf{k}-\mathbf{Q}}^A(\epsilon - \omega) \rangle_{imp} \quad (1.31)$$

(Such types of equations are known in the literature as Bethe-Salpeter-Equations.), where  $\Gamma$  does not depend on  $\mathbf{k}$  for fixed  $\mathbf{Q}$ . Thus, we can calculate the value of the sum over the Green's functions alone:

$$\begin{aligned} & \frac{1}{2\pi\rho_0\tau V} \sum_{\mathbf{k}} \langle G_{\mathbf{k}}^R(\epsilon) \rangle_{imp} \langle G_{\mathbf{k}-\mathbf{Q}}^A(\epsilon - \omega) \rangle_{imp} \\ &= \frac{1}{2\pi\rho_0} \int d\Omega d\eta \frac{1}{\epsilon - \eta + \frac{i}{2\tau}} \frac{1}{\epsilon - \omega - \eta + \mathbf{v}\mathbf{Q} - \frac{i}{2\tau}}, \end{aligned} \quad (1.32)$$

where we turned the sum over  $\mathbf{k}$  into an integral over the energy variable  $\eta = \epsilon_k$  and angle  $\Omega$  using the density of states  $\rho_0$  and linearized the dispersion relation, assuming

$Q \ll k$ :

$$\epsilon_{\mathbf{k}-\mathbf{Q}} \approx \epsilon_{\mathbf{k}} - \mathbf{v}\mathbf{Q} \quad \mathbf{v} = \nabla_{\mathbf{k}}\epsilon. \quad (1.33)$$

The integral over  $\eta$  can be done using the residue theorem and we obtain:

$$\frac{1}{2\pi\rho_0\tau V} \sum_{\mathbf{k}} \langle G_{\mathbf{k}}^R(\epsilon) \rangle_{imp} \langle G_{\mathbf{k}-\mathbf{Q}}^A(\epsilon - \omega) \rangle_{imp} = \int d\Omega \frac{1}{1 - i\omega\tau + i\mathbf{v}\mathbf{Q}\tau}. \quad (1.34)$$

In the so called *diffusive regime* (i.e. high impurity concentrations), which we are considering here, we have

$$Ql_e \ll 1 \quad \omega\tau \ll 1. \quad (1.35)$$

Which means that we can expand the denominator, and using the relations

$$\int d\Omega \mathbf{v}\mathbf{Q} = 0 \quad \int d\Omega (\mathbf{v}\mathbf{Q})^2 = \frac{1}{d} v_F^2 Q^2 \quad (1.36)$$

in  $d = 3$ , we obtain:

$$\frac{1}{2\pi\rho_0\tau V} \sum_{\mathbf{k}} \langle G_{\mathbf{k}}^R(\epsilon) \rangle_{imp} \langle G_{\mathbf{k}-\mathbf{Q}}^A(\epsilon - \omega) \rangle_{imp} \approx 1 + i\omega\tau - DQ^2\tau + \dots \quad (1.37)$$

From this, we obtain the structure factor:

$$\Gamma_{\mathbf{Q}}(\omega) = \frac{1}{2\pi\rho_0\tau} \frac{1}{DQ^2\tau - i\omega\tau}, \quad (1.38)$$

which can be checked by inserting (1.38) and (1.37) into (1.31). For the corrections to the conductivity, we read off from figure 1.9 (we consider the isotropic  $\mathbf{q} = 0$  case):

$$\begin{aligned} & \sum_{\mathbf{k}'} \langle \hat{\mathbf{k}}\hat{\mathbf{k}}' \rangle \int \frac{d\epsilon}{2\pi} \langle G_{\mathbf{k}'\mathbf{k}}^R(\epsilon + \omega) G_{\mathbf{k}'\mathbf{k}}^A(\epsilon) \rangle_{cooperon} \\ &= \sum_{\mathbf{k}'} \langle \hat{\mathbf{k}}\hat{\mathbf{k}}' \rangle \int \frac{d\epsilon}{2\pi} \langle G_{\mathbf{k}}^R(\epsilon + \omega) \rangle_{imp} \langle G_{\mathbf{k}}^A(\epsilon) \rangle_{imp} \Gamma_{\mathbf{k}+\mathbf{k}'}(\omega) \langle G_{\mathbf{k}'}^R(\epsilon + \omega) \rangle_{imp} \langle G_{\mathbf{k}'}^A(\epsilon) \rangle_{imp}. \end{aligned} \quad (1.39)$$

$\Gamma$  diverges for *backscattering*,  $\mathbf{k} = -\mathbf{k}'$ , and  $\omega = 0$ , so that

$$\approx - \sum_{\mathbf{Q}} \Gamma_{\mathbf{Q}}(\omega) \int \frac{d\epsilon}{2\pi} [\langle G_{\mathbf{k}}^R(\epsilon) \rangle_{imp} \langle G_{\mathbf{k}}^A(\epsilon) \rangle_{imp}]^2 \approx -2\tau^3 \frac{1}{V} \sum_{\mathbf{Q}} \Gamma_{\mathbf{Q}}(\omega), \quad (1.40)$$

where the integral has been calculated in the same way as in (1.29). The full conductivity correction, using (1.8) and (1.26), due to the Cooperon, now gives

$$\begin{aligned} \Delta\sigma &= -2e^2\rho_0 \frac{v_F^2}{3} \int_0^\infty dt \int \frac{d\omega}{2\pi} e^{-i\omega t} 2\tau^3 \frac{1}{V} \sum_{\mathbf{Q}} \frac{1}{2\pi\rho_0\tau} \frac{1}{DQ^2\tau - i\omega\tau} \\ &= -\frac{2e^2D}{\pi} \int_0^\infty dt \int \frac{d\omega}{2\pi} e^{-i\omega t} \frac{1}{V} \sum_{\mathbf{Q}} P(\mathbf{Q}, \omega), \end{aligned} \quad (1.41)$$

with

$$P(\mathbf{Q}, \omega) = \frac{1}{DQ^2 - i\omega}. \quad (1.42)$$

As can be easily checked,  $P$  is in fact the Fourier transform of the solution to the diffusion equation:

$$\left[ \frac{\partial}{\partial t} - D\Delta_{\mathbf{r}'} \right] P(\mathbf{r}, \mathbf{r}') = \delta(\mathbf{r} - \mathbf{r}')\delta(t), \quad (1.43)$$

where

$$P(\mathbf{r}, \mathbf{r}', t) = \frac{1}{(4\pi Dt)^{d/2}} e^{-|\mathbf{r}-\mathbf{r}'|/4Dt}. \quad (1.44)$$

Thus, the corrections may equally be written in the form:

$$\Delta\sigma = -\frac{2e^2 D}{\pi} \int_0^\infty dt P(\mathbf{r}, \mathbf{r}, t). \quad (1.45)$$

Note the same space arguments of  $P$ , corresponding to the probability density to return to the origin in a diffusion process, which we will also refer to as a *closed random walk*.

# Chapter 2

## Dephasing

### 2.1 Infrared cutoff for weak localization

In the previous chapter, we argued that the weak localization correction to the conductivity in one dimension can be written in the form

$$\Delta\sigma = -\frac{2e^2D}{\pi} \int_0^\infty dt P(r, r, t), \quad (2.1)$$

where  $P(r, r, t)$  is the probability density associated with the Cooperon. For a free, one dimensional diffusion process, we obtain from the diffusion equation (1.44):

$$P(r, r, t) = \frac{1}{\sqrt{4\pi Dt}}. \quad (2.2)$$

This probability density is obtained by the square amplitude of two time reversed random walks in the metal. Formally, we can assume diffusive motion only for trajectories much longer than the mean free path, which is commonly ensured by a lower cutoff at  $\tau_{tr}$ . But since the integral (2.1) is well behaved at the lower integration boundary and dominated by large values of  $t$ , the lower cutoff may equally be set to zero, giving just a small correction. Note that this is not the case for higher dimensions, which we do not consider here.

Having said this, the correction to the conductivity is formally diverging, which is due to the fact that a random walk in one dimension is recurrent. The assumptions in the last chapter that lead to this correction were that impurity collisions are elastic and that electron-electron interactions can be neglected, leading to fully coherent propagation of the electrons, corresponding to the case  $T = 0$ .

In a real metal though, electrons dissipate energy in numerous ways, leading to the destruction of phase coherence and thereby regularize the integral (2.1). To be precise, the requirement for the decoherence of the Cooperon is breaking the symmetry of time-reversing an electron trajectory, as has been explained in the previous chapter. Thus, generally, we assume that after some time the propagation will become incoherent and will

not contribute to the corrections in the weak localization regime any more. In this thesis we will write the resulting regularization in the form:

$$\Delta\sigma = -\frac{2e^2D}{\pi} \int_0^\infty dt P(r, r, t) e^{-F(t)}, \quad (2.3)$$

defining the Cooperon decay function  $F(t)$ . The typical timescale, describing the duration of coherent transport, may then be extracted from:

$$F(\tau_\phi) = 1, \quad (2.4)$$

where we defined the decoherence time  $\tau_\phi$ . The central goal of this thesis will be, to calculate  $F(t)$  in the geometry of a quasi one dimensional metallic ring, using an improved treatment of electron-electron interactions.

## 2.2 Cooperon in an external potential: Path integral representation

Although a calculation of the Cooperon in the presence of external fields is possible using purely diagrammatic techniques (for a review of this in the case of electron-electron interactions, see [12]), we will here take the path integral approach. Following Feynman [13], the propagator of the Schrödinger equation can be written as a path integral over the corresponding action. For a detailed introduction to this topic, see e.g. [14]. In the presence of an external potential  $V$ , depending on space and time, the one-particle Green's function obeys the equation

$$\left[ -i\frac{\partial}{\partial t} - \frac{1}{2m}\nabla_{\mathbf{r}'}^2 + V(\mathbf{r}', t) \right] G(\mathbf{r}, \mathbf{r}', t) = \delta(\mathbf{r} - \mathbf{r}')\delta(t). \quad (2.5)$$

Feynman showed that the solution to this differential equation can be written as:

$$G(\mathbf{r}, \mathbf{r}', t) = \int_{r(0)=\mathbf{r}}^{r(t)=\mathbf{r}'} \mathcal{D}[\mathbf{r}] e^{i\int_0^t d\tau \mathcal{L}(\mathbf{r}, \dot{\mathbf{r}}, \tau)}, \quad (2.6)$$

where  $\mathcal{L}(\mathbf{r}, \dot{\mathbf{r}}, t)$  is the Lagrangian given by

$$\mathcal{L}(\mathbf{r}, \dot{\mathbf{r}}, \tau) = \frac{1}{2}m\dot{\mathbf{r}}^2 - V(\mathbf{r}, \tau). \quad (2.7)$$

The relevant spatial scale associated with the action, is the Fermi wavelength. If we assume that the potential is varying only slowly on this scale, we can make use of the

so-called eikonal approximation to separate out the potential, assuming that the effect of the potential can be included in an envelope function  $\phi(\mathbf{r}, \mathbf{r}', t)$ :

$$G(\mathbf{r}, \mathbf{r}', t) = G_0(\mathbf{r}, \mathbf{r}', t) e^{\phi(\mathbf{r}, \mathbf{r}', t)}, \quad (2.8)$$

where  $G_0$  is the Green's function in the absence of the external potential. This approximation has first been used by Gorkov in the context of superconductivity. For a detailed discussion, see [15].

The probability density  $P(\mathbf{r}, \mathbf{r}', t)$  associated to the Cooperon is also a solution to a differential equation, the diffusion equation (1.43):

$$\left[ \frac{\partial}{\partial t} - D\Delta_{\mathbf{r}'} \right] P(\mathbf{r}, \mathbf{r}', t) = \delta(\mathbf{r} - \mathbf{r}')\delta(t), \quad (2.9)$$

where we require  $\mathbf{r}' \rightarrow \mathbf{r}$  in the end.

In the same way as for the Schrödinger equation, we can write the solution to this equation as

$$P(\mathbf{r}, \mathbf{r}', t) = \int_{r(0)=\mathbf{r}}^{r(t)=\mathbf{r}'} \mathcal{D}[\mathbf{r}] e^{-\int_0^t d\tau \mathcal{L}(\mathbf{r}, \dot{\mathbf{r}}, \tau)}, \quad (2.10)$$

but now with the Lagrangian:

$$\mathcal{L}(\mathbf{r}, \dot{\mathbf{r}}, \tau) = \frac{\dot{\mathbf{r}}^2}{4D}. \quad (2.11)$$

In contrast to the one-particle Green's function, this probability density consists of the product of an amplitude and its complex conjugate. Both amplitudes correspond to multiple scattering sequences between the impurities of the metal, forming a forward and a backward trajectory. If both sequences were exactly equal, they would both pick up the same phase and the probability density would be unaffected by any external fields. Here, on the other hand,  $P$  is obtained, by reversing the temporal sequence of one of the trajectories, corresponding to backscattering. Thus, both trajectories effectively see a different potential, leading to a phase difference  $\phi$ , which is non-zero as long as the potential is not invariant under the time reversal of one trajectory. This implies that a constant external field cannot lead to decoherence.

Formally, this phase difference is due to the structure factor (1.31). If we include a potential in the retarded and advanced Green's functions of (1.34) and assume that the potential is only slowly varying, so that we can apply the eikonal approximation, then we can expand the denominator in the diffusive regime just as before and obtain a modified differential equation for  $P$ , given now by

$$\left[ \frac{\partial}{\partial t} - D\Delta_{\mathbf{r}'} - i(V(\mathbf{r}', t) - V(\mathbf{r}', t')) \right] P(\mathbf{r}, \mathbf{r}', t, t') = \delta(\mathbf{r} - \mathbf{r}')\delta(t - t'). \quad (2.12)$$

For a detailed derivation and discussion of this equation, see chapter A6.3 of [8]. Note the fact that the Cooperon has a non-local temporal structure in a time-dependent field.

The solution of this equation may now be written as the path integral (2.10) with the modified Lagrangian

$$\mathcal{L}(\mathbf{r}, \dot{\mathbf{r}}, \tau) = \frac{\dot{\mathbf{r}}^2}{4D} - i[V(\mathbf{r}(\tau), \tau) - V(\mathbf{r}(\tau), t - \tau)]. \quad (2.13)$$

The phase difference, i.e. the Cooperon phase, is thus given by:

$$i\phi = i \int_0^t d\tau [V(\mathbf{r}(\tau), \tau) - V(\mathbf{r}(\tau), t - \tau)]. \quad (2.14)$$

Since we know the probability density of a free diffusion process, it is convenient to write the return probability, i.e.  $P(\mathbf{r}' \rightarrow \mathbf{r})$ , in the form:

$$P(\mathbf{r}, \mathbf{r}, t) = \int_{\mathbf{r}(0)=\mathbf{r}}^{\mathbf{r}(t)=\mathbf{r}} \mathcal{D}[\mathbf{r}] (e^{i\phi}) e^{-\int_0^t dt \frac{\dot{\mathbf{r}}^2}{4D}} \quad (2.15)$$

$$\approx P_0(\mathbf{r}, \mathbf{r}, t) \langle e^{i\phi} \rangle_{R_t}, \quad (2.16)$$

where  $\langle \dots \rangle_{R_t}$  stands for averaging over all closed random walks  $R$  of duration  $t$  and  $P_0(\mathbf{r}, \mathbf{r}, t)$  is the probability density of a closed random walk, which is in one dimension given by (2.2). In the last approximation, we thus used the assumption that the external potential is varying slow enough, so that it does not affect the dynamics of the electron at the classical level. Note that  $P(\mathbf{r}, \mathbf{r}, t)$  will not depend on  $\mathbf{r}$ , if we assume translationally invariant systems.

By comparing (2.16) with (2.3) we can express the Cooperon decay function in terms of the external potentials:

$$e^{-F(t)} = \langle e^{i \int_0^t d\tau [V(\mathbf{r}(\tau), \tau) - V(\mathbf{r}(\tau), t - \tau)]} \rangle_{R_t}. \quad (2.17)$$

## 2.3 Decoherence due to electron-electron interactions

As seen from (2.14), any process that destroys the time reversal symmetry of the forward and backward trajectory gives rise to decoherence of the Cooperon.

The typical example for such a process is the effect of an external magnetic field, which we will discuss in chapter 5.2.

In the isolated metal, the two dominating sources for decoherence are interactions between electrons and lattice vibrations (electron-phonon interactions) and between electrons with each other (electron-electron interactions), simply because both processes correspond to inelastic collision events (the total energy is conserved, but the energy of each electron is modified).

At low enough temperatures, the modes of the lattice vibrations are frozen and the dominating phase breaking mechanism is given by electron-electron interactions. We will

see in the next chapter that the effect of this interaction can be understood as resulting from a fluctuating electromagnetic field that dephases the forward and the backward path of the Cooperon.

This equivalence is due to the so called Fluctuation-Dissipation-Theorem, which will allow us to write down a potential-potential correlation function  $\langle VV \rangle$  of the fields, effectively describing the effect of electron-electron collisions in the metal and depending on the temperature of the system.

The reason why such a correlator (a two point function) will be enough to describe the effect of the surrounding electrons is that in the standard *random phase approximation*, which we shall adopt throughout, electronic noise effectively behaves like Gaussian noise.

Gaussian processes have the property that higher order correlators factorize in terms of the two-point correlator, which we already discussed in our disorder model, see (1.21). Another property of such a process is that the average over the exponential of a Gaussian random variable  $\phi$  is given by

$$\langle e^{i\phi} \rangle = e^{-\frac{1}{2}\langle \phi^2 \rangle}, \quad (2.18)$$

as long as  $\langle \phi \rangle = 0$ , which we can safely assume since a constant potential cannot contribute to dephasing. The cooperon decay  $F(t)$  may thus be calculated from:

$$e^{-F(t)} = \langle e^{-\frac{1}{2}\langle \phi^2 \rangle_V} \rangle_{R_t}, \quad (2.19)$$

where

$$\begin{aligned} \frac{1}{2}\langle \phi^2 \rangle_V = \frac{1}{2} \int_0^t d\tau_1 \int_0^t d\tau_2 & \langle V(\mathbf{r}(\tau_1), \tau_1)V(\mathbf{r}(\tau_2), \tau_2) + V(\mathbf{r}(\tau_1), t - \tau_1)V(\mathbf{r}(\tau_2), t - \tau_2) \\ & - V(\mathbf{r}(\tau_1), \tau_1)V(\mathbf{r}(\tau_2), t - \tau_2) - V(\mathbf{r}(\tau_1), t - \tau_1)V(\mathbf{r}(\tau_2), \tau_2) \rangle_V. \end{aligned} \quad (2.20)$$

The average  $\langle \dots \rangle_V$  denotes averaging over different realizations of the noise potential  $V$ .



# Chapter 3

## Quasi-1d systems: Classical noise

In the previous chapter we learned how to obtain the Cooperon decay function from a potential-potential correlator for electron-electron interactions, see (2.19), which were assumed to be Gaussian distributed.

In this chapter we will derive this correlator, effectively describing these interactions as thermal noise, in the *high temperature* regime, which is known in the literature as Johnson-Nyquist noise. Then we will calculate the Cooperon decay from the obtained result in quasi one dimensional systems.

### 3.1 Fluctuation-Dissipation-Theorem and Johnson-Nyquist noise

We will start here, by deriving a current-current correlator of the random thermal currents for arbitrary metal geometries. In the next section, we will then analyze the correlator of the corresponding potentials in the quasi one dimensional case.

Assume that we have small thermal fluctuations in the Fourier modes of the electrical field  $\delta\mathbf{A}(\mathbf{k}, \omega)$ , leading to a small current  $\delta\mathbf{j}(\mathbf{k}, \omega)$  of the form:

$$\delta\mathbf{j}_\alpha(\mathbf{k}, \omega) = i\omega\sigma^{\alpha\beta}(\mathbf{k}, \omega) \delta\mathbf{A}_\beta(\mathbf{k}, \omega). \quad (3.1)$$

Then, according to Kubo's formula (see [16]), the conductivity tensor is given by

$$i\omega\sigma^{\alpha\beta}(\mathbf{k}, \omega) = i \int_{-\infty}^{\infty} dt e^{i\omega t} \langle [\delta\hat{\mathbf{j}}_\alpha(\mathbf{k}, t), \delta\hat{\mathbf{j}}_\beta(-\mathbf{k}, 0)] \rangle \theta(t) \quad (3.2)$$

and we introduced Gibbs averaging over temperature:

$$\langle \dots \rangle = \text{Tr} [e^{(\Omega-H)/T} \dots]. \quad (3.3)$$

(Note that in this thesis, we will measure temperature and all other energy scales in units of frequency.) (3.2) identifies the AC conductivity with the retarded current-current

correlation function that governs the dissipative response of the system to the external perturbation.

If we assume an isotropic metal in the limit of small frequencies, the conductivity is given by

$$\sigma^{\alpha\beta}(\mathbf{k}, \omega) \approx \sigma_0 \delta_{\alpha\beta}, \quad (3.4)$$

where  $\sigma_0$  is the Drude conductivity of the metal, given by (1.1). Thus, (3.2) reduces here to

$$\int_0^{\infty} dt e^{i\omega t} \langle [\delta\hat{\mathbf{j}}_{\alpha}(\mathbf{k}, t), \delta\hat{\mathbf{j}}_{\beta}(-\mathbf{k}, 0)] \rangle = \omega \sigma_0 \delta_{\alpha\beta}. \quad (3.5)$$

Now, consider the average anti-commutator of these current densities, given by:

$$\langle \{\delta\hat{\mathbf{j}}, \delta\hat{\mathbf{j}}\} \rangle(\mathbf{k}, \omega) = \int_{-\infty}^{\infty} dt e^{i\omega t} \left( \langle \delta\hat{\mathbf{j}}(\mathbf{k}, t) \delta\hat{\mathbf{j}}(-\mathbf{k}, 0) \rangle + \langle \delta\hat{\mathbf{j}}(-\mathbf{k}, 0) \delta\hat{\mathbf{j}}(\mathbf{k}, t) \rangle \right). \quad (3.6)$$

In thermodynamic equilibrium we can use the Kubo-Martin-Schwinger identity:

$$\langle \hat{A}(t) \hat{B}(0) \rangle = \text{Tr} \left[ e^{(\Omega-H)/T} e^{iHt} \hat{A}(0) e^{-iHt} \hat{B}(0) \right] = \langle \hat{A}(0) \hat{B}(t + i/T) \rangle \quad (3.7)$$

for any operators  $\hat{A}$  and  $\hat{B}$ , not explicitly depending on time. Then we can rewrite the anti-commutator in thermal equilibrium as

$$\langle \{\delta\hat{\mathbf{j}}, \delta\hat{\mathbf{j}}\} \rangle(\mathbf{k}, \omega) = (e^{\omega/T} + 1) \int_{-\infty}^{\infty} dt e^{i\omega t} \langle \delta\hat{\mathbf{j}}(-\mathbf{k}, 0) \delta\hat{\mathbf{j}}(\mathbf{k}, t) \rangle. \quad (3.8)$$

The same can be done for the commutator:

$$\langle [\delta\hat{\mathbf{j}}, \delta\hat{\mathbf{j}}] \rangle(\mathbf{k}, \omega) = (e^{\omega/T} - 1) \int_{-\infty}^{\infty} dt e^{i\omega t} \langle \delta\hat{\mathbf{j}}(-\mathbf{k}, 0) \delta\hat{\mathbf{j}}(\mathbf{k}, t) \rangle. \quad (3.9)$$

Combining these two equations we obtain

$$\langle \{\delta\hat{\mathbf{j}}, \delta\hat{\mathbf{j}}\} \rangle(\mathbf{k}, \omega) = \coth\left(\frac{\omega}{2T}\right) \langle [\delta\hat{\mathbf{j}}, \delta\hat{\mathbf{j}}] \rangle(\mathbf{k}, \omega). \quad (3.10)$$

The commutator on the right hand side is defined as

$$\langle [\delta\hat{\mathbf{j}}, \delta\hat{\mathbf{j}}] \rangle(\mathbf{k}, \omega) = - \int_0^{\infty} dt e^{-i\omega t} \langle \delta\hat{\mathbf{j}}(\mathbf{k}, t) \delta\hat{\mathbf{j}}(-\mathbf{k}, 0) \rangle + \int_0^{\infty} dt e^{i\omega t} \langle \delta\hat{\mathbf{j}}(\mathbf{k}, t) \delta\hat{\mathbf{j}}(-\mathbf{k}, 0) \rangle, \quad (3.11)$$

which is simply two times the dissipative response, given by the conductivity in (3.5). Thus, we obtain:

$$\boxed{\langle \{\delta\hat{\mathbf{j}}_{\alpha}, \delta\hat{\mathbf{j}}_{\beta}\} \rangle(\mathbf{k}, \omega) = 2\omega\sigma_0 \coth\left(\frac{\omega}{2T}\right) \delta_{\alpha\beta}}. \quad (3.12)$$

which is the so called Fluctuation-Dissipation-Theorem (or Callen-Welton's formula [17]) for random currents in a metal. In the classical limit, for high temperatures, this simplifies to:

$$\boxed{\langle \delta \mathbf{j}_\alpha \delta \mathbf{j}_\beta \rangle(\mathbf{k}, \omega) = 2T\sigma_0 \delta_{\alpha\beta}}, \quad (3.13)$$

where we replace the non-commuting quantum-mechanical operators by their classical equivalences:

$$\frac{1}{2} \langle \{ \delta \hat{\mathbf{j}}_\alpha, \delta \hat{\mathbf{j}}_\beta \} \rangle(\mathbf{k}, \omega) \longrightarrow \langle \delta \mathbf{j}_\alpha \delta \mathbf{j}_\beta \rangle(\mathbf{k}, \omega). \quad (3.14)$$

(3.13) is known in the literature as the classical Johnson-Nyquist-Theorem, see [18]. Note that the expression on the right-hand side does not depend on frequency, which means that Johnson-Nyquist-Noise is white noise, i.e. delta-correlated in time. Furthermore there is generally no dependence on  $\mathbf{k}$  of the current-current correlator, as long as the conductivity is isotropic.

As can be seen from (3.12), however, a quantum mechanical treatment of the electron-electron interactions necessarily leads to a more complicated time dependence, which we will consider in the next chapter. Here, we will only consider the high temperature regime, characterized by (3.13)

## 3.2 Classical noise correlator in a quasi-1d system

In the previous section we have derived a correlator of the random currents in an isotropic metal. What we are really interested in, is the average correlator of the potentials  $\langle VV \rangle_V$ , induced by these currents in a quasi one dimensional system. Here we face the subtle issue that the fluctuations are distributed randomly in all directions, but we consider only a current flow parallel to the direction of the wire. (Our derivation of this correlator will be along the lines of [1], but in a different gauge.)

The total current density in a wire is given (to linear order) by the response to an electric field and by the response to a gradient in the electron density  $\rho$  (for details, see chapter 3.7 of [19]). Therefore, we can write the total current density in our wire as

$$\mathbf{j}^{tot} = \sigma_0 \mathbf{E} - D \nabla \rho + \delta \mathbf{j}, \quad (3.15)$$

where  $\delta \mathbf{j}$  is the additional current originating from thermal fluctuations, whose correlator is given by (3.13). In quasi one dimension, the total current has only one component, thus we are interested in the electric field parallel to the direction of the wire,  $\mathbf{E}_\parallel$ . To calculate this, we transform to Fourier space and decompose the wave vector into the sum  $\mathbf{k} + \mathbf{q}$ , where  $\mathbf{k}$  is pointing in the direction of the wire, while  $\mathbf{q}$  is perpendicular to it. Using Gauss's law:

$$\nabla \cdot \mathbf{E} = \frac{\rho}{\epsilon_0}, \quad (3.16)$$

we obtain:

$$\mathbf{E}(\mathbf{k}, \mathbf{q}) = \frac{-i\rho(\mathbf{k}, \mathbf{q})}{\epsilon_0} \frac{\mathbf{k} + \mathbf{q}}{k^2 + q^2}. \quad (3.17)$$

Note that at  $qa \ll 1$ ,  $a$  being the transverse size of the wire,  $\rho(\mathbf{k}, \mathbf{q})$  does not depend on  $\mathbf{q}$ , meaning that in our quasi one dimensional system, we may neglect its transverse spatial dependence. The field in the direction  $\mathbf{k}$  of the wire,  $\mathbf{E}_{\parallel}$ , is now given by

$$\mathbf{E}_{\parallel}(\mathbf{k}) = \int \frac{d^2q}{(2\pi)^2} \mathbf{E}(\mathbf{k}, \mathbf{q}) \quad (3.18)$$

$$= \frac{-i\rho(\mathbf{k})\mathbf{k}}{2\pi\epsilon_0} \int_0^{1/a^2} dq \frac{q}{k^2 + q^2} \quad (3.19)$$

$$\approx \frac{-i\rho(\mathbf{k})\mathbf{k}}{2\pi\epsilon_0} \ln\left(\frac{1}{ka}\right). \quad (3.20)$$

In quasi one dimension we may thus follow from (3.15):

$$j^{tot}(k) = \sigma_0 E(k) - iDk\rho(k) + \delta j(k), \quad (3.21)$$

with

$$E(k) = \frac{-i\rho(k)k}{2\pi\epsilon_0} \ln\left(\frac{1}{ka}\right). \quad (3.22)$$

Using the continuity equation

$$kj^{tot}(k) = \omega\rho(k), \quad (3.23)$$

we obtain the charge density:

$$\rho(k) = \frac{1}{\omega + iDk^2} k (\sigma_0 E(k) + \delta j(k)). \quad (3.24)$$

Plugging in this result in (3.20), we find

$$E(k) = \frac{\ln(1/ka)}{2\pi\epsilon_0} \frac{k^2}{i\omega - Dk^2} (\sigma_0 E(k) + j(k)). \quad (3.25)$$

From this, we finally obtain the field  $E(k)$  of the current fluctuations:

$$E(k) = -\delta j \left( 2\pi\epsilon_0 \frac{-i\omega + Dk^2}{k^2 \ln(1/ka)} + \sigma_0 \right)^{-1}. \quad (3.26)$$

At sufficiently small  $k$ ,  $\omega$ , we can neglect the first term in brackets (as long as  $1/ka$  is large) and obtain approximately:

$$E(k) = -\frac{\delta j(k)}{\sigma_0}, \quad (3.27)$$

corresponding to Ohm's law in a real one dimensional system. For the correlator of these fields, this becomes:

$$\langle EE \rangle(k, \omega) = \frac{1}{\sigma_0^2} \langle \delta j \delta j \rangle(k, \omega). \quad (3.28)$$

In one dimension we obtain for Johanson-Nyquist noise (3.13):

$$\langle \delta j \delta j \rangle(k, \omega) = 2T\sigma_0. \quad (3.29)$$

Finally we find the correlator of the fields:

$$\langle EE \rangle(k, \omega) = \frac{2T}{\sigma_0}. \quad (3.30)$$

For the corresponding potential, defined by

$$E = -\frac{1}{e} \text{grad}V, \quad (3.31)$$

this becomes

$$\boxed{\langle VV \rangle_V(k, \omega) = \frac{2Te^2}{\sigma_0 k^2}}, \quad (3.32)$$

which is the form of the correlator we were interested in and which is used frequently in the literature. (We added the index  $V$  to connect the result with our previous considerations and to distinguish this average from the random walk average in the next sections.)

Note, that this expression, just like the current-current correlation function, does not depend on frequency and is thus delta correlated in time.

The spatial dependence  $1/k^2$  on the other hand, was originating from the relation of the electric field to its potential, (3.31), and can be assumed to hold generally. This correlator can also be interpreted as the Fourier transform of the solution to the equation

$$-D\Delta_r \langle VV \rangle(r, \omega) = \delta(r) \quad (3.33)$$

with  $D = \frac{\sigma_0}{2Te^2}$ , in analogy to the diffusion equation (1.43). It is thus the time integrated probability density of a diffusion process, which corresponds to the assumption that the potential is a random walk in space.

From now on, we will conveniently and for the sake of a more transparent description do our calculations in real space and time, where we write the correlator in the factorized form:

$$\boxed{\langle VV \rangle_V(r, t) = -\frac{e^2}{\sigma_0} Q(r)W(t)}. \quad (3.34)$$

By comparison, we have:

$$Q(r) = -2 \frac{1}{(2\pi)^d} \int dk \frac{1}{k^2} e^{ikr}, \quad (3.35)$$

with proper boundary conditions and

$$W(t) \equiv W_C(t) = T\delta(t), \quad (3.36)$$

where the index  $C$  stands for ‘classical’ noise.

This factorized way of writing the correlator gives us the opportunity to calculate the average over random walks more easily, since only  $Q(r)$  depends on the trajectory position. In the next chapter, we will discuss how  $W(t)$  is modified at low temperatures. In this way we will be able to take over most of the results from this chapter to the next and only modify terms depending on  $W(t)$ .

### 3.3 Dephasing of the Cooperon due to electron-electron interactions

Using the factorized form of the correlator (3.34), we obtain from (2.20) an expression for the additional phase of the Cooperon:

$$\frac{1}{2}\langle\Phi^2\rangle_V = -\frac{e^2}{\sigma_0} \int_0^t d\tau_1 \int_0^t d\tau_2 (W(\tau_1 - \tau_2) - W(\tau_1 + \tau_2 - t)) Q(r(\tau_1) - r(\tau_2)). \quad (3.37)$$

We assumed  $Q(r) = Q(-r)$ , because of translational symmetry around zero and  $W(t) = W(-t)$ , which holds for all explicit forms of the correlator we are going to consider in this thesis.

To calculate the Cooperon decay, we now have to do the average over random walks  $R_t$  of duration  $t$  in the form

$$e^{-F(t)} = \langle e^{-\frac{1}{2}\langle\Phi^2\rangle_V} \rangle_{R_t}. \quad (3.38)$$

This average can be calculated exactly only for the infinite wire, see section 3.6. In this thesis, we will instead calculate the much easier quantity

$$\boxed{e^{-F(t)} \approx e^{-\frac{1}{2}\langle\Phi^2\rangle_{V,R_t}}}, \quad (3.39)$$

i.e. we will lift the average into the exponent. This approximation, first used and discussed in [20], is unfortunately not controlled by a small parameter, but is known to give very accurate results.

Using this approximation, we can calculate the Cooperon decay from

$$\boxed{F(t) = -\frac{e^2}{\sigma_0} \int_0^t d\tau_1 \int_0^t d\tau_2 (W(\tau_1 - \tau_2) - W(\tau_1 + \tau_2 - t)) \langle Q(r(\tau_1) - r(\tau_2)) \rangle_{R_t}}, \quad (3.40)$$

because only  $Q$  depends on the trajectory positions.

### 3.4 Electron-Electron interactions for quasi-1d systems in real space

The  $k = 0$  mode of the correlator in (3.32) diverges. This comes as no surprise, since long-wavelength modes of the noise cost only little energy. On the other hand, it is clear,

that this mode can not contribute to the dephasing of the Cooperon, because it gives just a constant contribution to the potential, which is the same for the forward and the backward path.

This can be verified by the transformation  $\tau_2 \rightarrow t - \tau_2$  in (3.40). The decay function then becomes:

$$F(t) = -\frac{e^2}{\sigma_0} \int_0^t d\tau_1 \int_0^t d\tau_2 W(\tau_1 - \tau_2) (\langle Q(r(\tau_1) - r(\tau_2)) \rangle_{R_t} - \langle Q(r(\tau_1) - r(t - \tau_2)) \rangle_{R_t}), \quad (3.41)$$

where it is evident that terms of  $Q$  which do not depend on the trajectory  $r(t)$  cancel out. Thus, the  $k = 0$  Fourier component of  $Q$  will be dropped henceforth.

Now, consider a quasi one dimensional system of size  $L$  with periodic boundary conditions, which corresponds to the geometry of a ring (R). Then the space dependent part of the correlator (before averaging over random walks  $R_t$ ) can be written from (3.35) as:

$$Q_R(r) = -2 \left( \frac{1}{L} \sum_{k>0} \frac{1}{k^2} e^{ikr} + c.c \right) \quad (3.42)$$

with  $k = \frac{2\pi n}{L}$ ,  $n = \{1, \dots, \infty\}$  and, as discussed above, we omitted the  $k = 0$  mode.

Evidently,  $Q_R(r) = Q_R(-r)$ , hence we replace  $r$  by  $|r|$ . To perform the sum, it is convenient to consider

$$\frac{\partial}{\partial |r|} Q_R(|r|) = -\frac{i}{\pi} \left( \sum_{n=1}^{\infty} \frac{e^{\frac{2\pi i}{L}|r|n}}{n} - \sum_{n=1}^{\infty} \frac{e^{-\frac{2\pi i}{L}|r|n}}{n} \right) \quad (3.43)$$

$$= \frac{i}{\pi} \left( \ln \left( \frac{1 - e^{\frac{2\pi i}{L}|r|}}{1 - e^{-\frac{2\pi i}{L}|r|}} \right) \right) \quad (3.44)$$

$$= \left( 1 - \frac{2|r|}{L} \right), \quad (3.45)$$

where we used the series expansion of the logarithm:

$$-\ln(1-x) = x + \frac{x^2}{2} + \frac{x^3}{3} + \frac{x^4}{4} + \dots \quad (3.46)$$

We conclude that

$$\boxed{Q_R(r) = |r| \left( 1 - \frac{|r|}{L} \right)}. \quad (3.47)$$

In the limit of the infinite wire (W),  $L \rightarrow \infty$ , this simply becomes

$$\boxed{Q_W(r) = |r|}. \quad (3.48)$$

### 3.5 Averaging over closed random walks

To calculate the decay function  $F(t)$  in the approximation (3.39), we have to average the phase over closed random walks  $R_t$  of duration  $t$  in one dimension. This average is defined by the path integral (2.15):

$$\langle \dots \rangle_{R_t} = \int_{r(0)=r}^{r(t)=r} \mathcal{D}r(t) \dots \exp \left( - \int_0^t d\tau \frac{\dot{r}(\tau)}{4D} \right), \quad (3.49)$$

where  $r$  is some arbitrary point, since the systems we are considering are translationally invariant. Equivalently, we may write for an arbitrary function  $f(r)$ :

$$\langle f(r(\tau)) \rangle_{R_t} = \int_{-\infty}^{\infty} dr' \frac{P(r, r', \tau) P(r', r, t - \tau)}{P(r, r, t)} f(r'), \quad (3.50)$$

where the probability density  $P(r, r', t)$  that a random walk starting from  $r$  reaches point  $r'$  in time  $t$  is a solution of the diffusion equation (1.43). In one dimension, for an infinite system, it is given by

$$P(r, r', t) = \frac{1}{\sqrt{4\pi Dt}} e^{-(r-r')^2/4Dt}. \quad (3.51)$$

The factor  $P(r, r, t)$  in (3.50) ensures the normalization condition  $\langle 1 \rangle_{R_t} \equiv 1$ .

Note that the phase we have to average over depends not only on the position of the random walk at some time  $\tau$ , but also at the time  $t - \tau$  from the backward path of the Cooperon, making our problem non-local in time.

Thus, consider a function  $f$ , depending on the coordinate difference of a random walk taken at different times:

$$\langle f(r(\tau_1) - r(\tau_2)) \rangle_{R_t}, \quad (3.52)$$

where we assume  $0 < \tau_1 < \tau_2 < t$ . Then this average can be calculated in the infinite system by

$$\langle f(r(\tau_1) - r(\tau_2)) \rangle_{R_t} = \int_{-\infty}^{\infty} dr_1 \int_{-\infty}^{\infty} dr_2 \frac{P(r, r_1, \tau_1) P(r_1, r_2, \tau_2) P(r_2, r, t - \tau_1 - \tau_2)}{P(r, r, t)} f(r_1 - r_2). \quad (3.53)$$

As an example for this prescription, we calculate the closed random walk average of (3.48). Using (3.53) and performing the double integral, one readily finds:

$$\langle |r(\tau_1) - r(\tau_2)| \rangle_{R_t} = \sqrt{\frac{4D(\tau_2 - \tau_1)}{t\pi}} (t - (\tau_2 - \tau_1)). \quad (3.54)$$

For future reference, it is useful to note that the calculation of a double integral can be avoided using the following trick: Since the point  $r$  was chosen arbitrarily, we can exploit

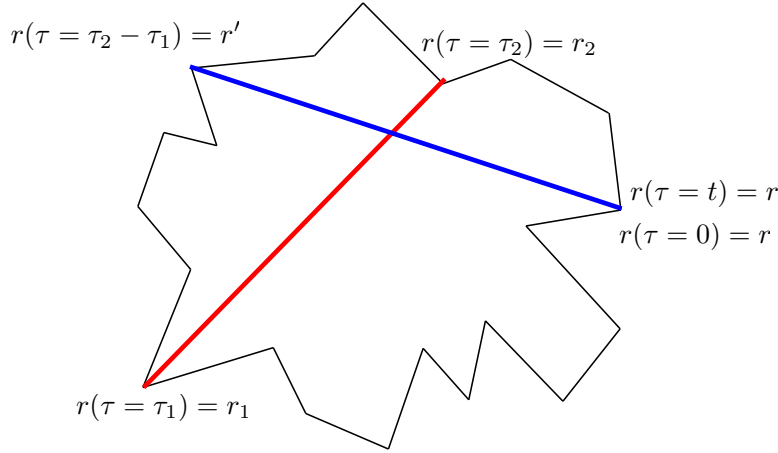


Figure 3.1: After averaging over all possible closed random walks, the distances  $|r - r'|$  and  $|r_1 - r_2|$  are equivalent.

the symmetry of problem. Instead of calculating the average distance between two points of the closed random walk, located at times  $\tau_1$  and  $\tau_2$ , we can equally well just calculate the average distance covered by a closed random walk after time  $\tau_{21} = \tau_2 - \tau_1$ , see Figure 3.1. Using (3.50), we obtain:

$$\langle |r(\tau_1) - r(\tau_2)| \rangle_{R_t} \equiv \langle |r(\tau_{21})| \rangle_{R_t} = \sqrt{\frac{4D\tau_{21}}{t\pi}}(t - \tau_{21}). \quad (3.55)$$

in agreement with (3.54). We will show later that a similar replacement can be done in the ring. In fact, in all translationally invariant systems,  $\langle |r(\tau_1) - r(\tau_2)| \rangle_{R_t}$  is always a function of  $\tau_2 - \tau_1$  only.

Note that the expression (3.55) is vanishing for  $\tau_{21} = 0$  and  $\tau_{21} = t$ , corresponding to a closed random walk. For  $\tau_{21} \ll t$  it is  $\sim \sqrt{D\tau_{21}}$  corresponding to an unrestricted random walk in one dimension. Also note for further reference that the integral over all times  $\tau_{21}$  has the same dependence on the total time  $t$ , independent of whether the random walk is closed or unrestricted:

$$\int_0^t d\tau_{21} \sqrt{\frac{4D\tau_{21}}{t\pi}}(t - \tau_{21}) \sim \sqrt{D}t^{3/2} \sim \int_0^t d\tau_{21} \sqrt{D\tau_{21}}. \quad (3.56)$$

Only the prefactor is changed.

## 3.6 Exact results in an infinite quasi-1d wire

In an infinite wire and using classical Johnson-Nyquist noise (3.13), it is possible to calculate the corrections to the conductivity including an external magnetic field exactly, i.e. without the need of approximation (3.39). The effect of the magnetic field is characterized by the additional decoherence time  $\tau_B$ , which we will explain in more detail in chapter (5.2).

This calculation has been done first by Altshuler, Aronov and Khmelnitsky (AAK), see [1]. They were able to decouple the forward and backward trajectories  $r(\tau)$  and  $r(t-\tau)$  by a coordinate transform in a path integral representation, thus making the problem local in time and derived an exactly solvable differential equation for the Cooperon. They obtained:

$$\Delta\sigma = -\frac{e^2}{\pi} \sqrt{D\tau_N} \frac{\text{Ai}(\tau_N/\tau_B)}{\text{Ai}'(\tau_N/\tau_B)}. \quad (3.57)$$

where the Nyquist time  $\tau_N$  is defined by:

$$\tau_N = \left( \frac{\sigma_0}{e^2 T \sqrt{D}} \right)^{2/3}. \quad (3.58)$$

In this thesis, we are actually only interested in the effect of the fluctuating environment, characterized by the phase  $\phi$ , in which case we can write the left hand side of (3.57) as follows:

$$\int_0^\infty dt P_0(r, r, t) \langle e^{i\phi} \rangle_{V, R_t} e^{-t/\tau_B} = -\frac{1}{2} \sqrt{\frac{\tau_N}{D}} \frac{\text{Ai}(\tau_N/\tau_B)}{\text{Ai}'(\tau_N/\tau_B)}, \quad (3.59)$$

where we assumed that the magnetic field accounts for an independent exponential decay. It has been shown in [21] that  $\langle e^{i\phi} \rangle_{V, R_t}$  can be extracted from (3.59) by an inverse Laplace transform. Using an approximation formula for the zeros of the Airy function, the decay due to electron-electron interactions can then be approximated:

$$\langle e^{i\phi} \rangle_{V, R_t} \approx e^{-\sqrt{\pi}/4 (t/\tau_N)^{3/2}}. \quad (3.60)$$

For the Cooperon decay function this implies:

$$F(t) = \frac{e^2}{\sigma_0} \frac{\sqrt{\pi D}}{4} T t^{3/2}. \quad (3.61)$$

We will see below that this result is recovered by using approximation (3.39).

## 3.7 Calculation of the Cooperon decay function in a quasi-1d ring

### 3.7.1 Diffusion on a ring and winding numbers

Diffusive motion on a ring is substantially different from the infinite medium. Electron trajectories can be classified by a winding number  $n$ , counting the number of closed loops around the ring. In this way, the position along a trajectory may be represented by the tuple  $(n, r)$ , where  $r$  is measured clockwise around the ring. Given a specific length  $L$  of the ring we have  $r \in [0, L]$ .

To proceed further, we start by calculating the probability density  $P(r, r', t)$  of free diffusive motion on a ring. We have to solve the diffusion equation

$$\left( \frac{\partial}{\partial t} - D\nabla_{r'}^2 \right) P(r, r', t) = \delta(r - r')\delta(t), \quad (3.62)$$

implying periodic boundary conditions

$$P(r, r', t) = P(r + L, r' + L, t). \quad (3.63)$$

For this, consider the equation

$$-D\Delta\psi_n(r) = E_n\psi_n(r), \quad (3.64)$$

for which we assume a full set of solutions  $\psi_n$  to be known. We can then construct a general solution for (3.62) simply by:

$$P(r, r', t) = \theta(t) \sum_n \psi_n(r)^\dagger \psi_n(r') e^{-E_n t}. \quad (3.65)$$

A full set of solutions to (3.64), implementing the boundary conditions (3.63), is given by

$$\psi_q(r) = \frac{1}{\sqrt{L}} e^{iqr}, \quad (3.66)$$

where  $q = \frac{2\pi n}{L}$ ,  $n \in \mathbb{Z}$  and  $E_q = Dq^2$ . Thus,

$$P(r, r', t) = \frac{1}{L} \theta(t) \sum_q e^{-Dq^2 t} e^{-iq(r-r')} \quad (3.67)$$

$$= \frac{1}{L} \sum_{n=-\infty}^{\infty} e^{-\frac{4\pi^2 n^2 D t}{L^2}} e^{\frac{2\pi i n (r-r')}{L}}. \quad (3.68)$$

Using the Poisson transform, (C.1), we obtain:

$$P(r, r', t) = \frac{1}{L} \sum_{n=-\infty}^{\infty} \int_{-\infty}^{\infty} dy e^{-\frac{4\pi^2 D t y^2}{L^2}} e^{\frac{2\pi i (r-r') y}{L}} e^{2\pi i m y} \quad (3.69)$$

$$= \frac{1}{\sqrt{4\pi D t}} \sum_{n=-\infty}^{\infty} e^{-\frac{1}{4D t} (r-r'+nL)^2}, \quad (3.70)$$

which should be compared to the result (3.51) of the infinite system.

Instead of calculating the sum over all winding numbers together, we will conveniently consider each mode separately:

$$P_n(r, r', t) = \frac{1}{\sqrt{4\pi D t}} e^{-\frac{1}{4D t} (r-r'+nL)^2}. \quad (3.71)$$

and do the sum in the very end:

$$P(r, r', t) = \sum_{n=-\infty}^{\infty} P_n(r, r', t). \quad (3.72)$$

Because of the obvious translational invariance, we define the probability with only one space-argument as

$$P_n(r - r', t) = \frac{1}{\sqrt{4\pi Dt}} e^{-\frac{1}{4Dt}(r-r'+nL)^2}, \quad (3.73)$$

which we will use in later formulas.

Since the probability is now a sum over winding numbers, the correction to the conductivity (2.1) becomes

$$\Delta\sigma = -\frac{2e^2 D}{\pi} \sum_{n=-\infty}^{\infty} \int_0^{\infty} dt P_n(r, r, t) e^{-F_n(t)}, \quad (3.74)$$

where, using approximation (3.39), we defined

$$F_n(t) = \frac{1}{2} \langle \phi^2 \rangle_{V, R_{t,n}}. \quad (3.75)$$

The average has to be done now with respect to closed random walks  $R_{t,n}$  of duration  $t$  and winding number  $n$ .

### 3.7.2 Averaging over closed random walks on a ring

Recalling (3.47), we will now calculate the average

$$\langle Q_R(r(\tau_1) - r(\tau_2)) \rangle_{R_{t,n}} = \left\langle |r(\tau_1) - r(\tau_2)| \left( 1 - \frac{|r(\tau_1) - r(\tau_2)|}{L} \right) \right\rangle_{R_{t,n}} \quad (3.76)$$

over closed random walks  $R_{t,n}$  having duration  $t$  and winding number  $n$  on a ring of size  $L$ , following [3].

The probability for a random walk of winding number  $n$  to cover the distance  $r$  in time  $t$  is given by (3.71). Doing the average in the same way as in section 3.5, compare (3.53), we obtain for  $0 < \tau_1 < \tau_2 < t$ :

$$\begin{aligned} \langle Q_R \rangle_{R_{t,n}} &= \int_0^L \int_0^L dr_1 dr_2 \left( |r_1 - r_2| \left( 1 - \frac{|r_1 - r_2|}{L} \right) \right) \\ &\times \sum_{i+j+k=n} \frac{P_i(r_0 - r_1, \tau_1) P_j(r_1 - r_2, \tau_2 - \tau_1) P_k(r_2 - r_0, t - \tau_2)}{P_n(0, t)}. \end{aligned} \quad (3.77)$$

The sum  $\sum_{i+j+k=n}$  has the following meaning: take the sum over all possible products of functions  $P_i, P_j, P_k$  with winding numbers  $i, j$  and  $k$ , which constitute a random walk of total winding number  $n$ , over which we have to average.

Note, that the case  $\tau_1 > \tau_2$  can be calculated similarly, by interchanging  $r_0 - r_1$  with  $r_2 - r_0$  in the arguments of the diffusion probabilities.

Now, take  $\frac{1}{L} \int_0^L dr_0$  on both sides of (3.77) and use the semi-group property of the probabilities on a ring:

$$\int_0^L dr_2 \sum_m P_m(r_1 - r_2, t_1) \sum_n P_n(r_2 - r_3, t_2) = \sum_m P_m(r_1 - r_3, t_1 + t_2), \quad (3.78)$$

which can be verified by inserting (3.71). One readily obtains for all  $\tau_1$  and  $\tau_2$ :

$$\begin{aligned} \langle Q_R \rangle_{R_{t,n}} &= \frac{1}{2L} \int_{-L}^L dr_{12} \int_{L-(L-|r_{12}|)}^{L+(L-|r_{12}|)} d\bar{r}_{12} \left( |r_{12}| \left( 1 - \frac{|r_{12}|}{L} \right) \right) \\ &\times \sum_{m=-\infty}^{\infty} \frac{P_m(r_{12}, |\tau_{12}|) P_{n-m}(r_{12}, t - |\tau_{12}|)}{P_n(0, t)}, \end{aligned} \quad (3.79)$$

where we introduced  $\tau_{12} = \tau_1 - \tau_2$  and  $r_{12} = r_1 - r_2$ ,  $\bar{r}_{12} = r_1 + r_2$ . The physical transparent picture of this transformations is same as explained in Figure 3.1, but now applied to the ring geometry. Doing the  $\bar{r}_{12}$  integral, we obtain:

$$\langle Q_R \rangle_{R_{t,n}} = \int_{-L}^L dr_{12} \left( |r_{12}| \left( 1 - \frac{|r_{12}|}{L} \right)^2 \right) \sum_{m=-\infty}^{\infty} \frac{P_m(r_{12}, |\tau_{12}|) P_{n-m}(r_{12}, t - |\tau_{12}|)}{P_n(0, t)}. \quad (3.80)$$

Because  $P_m(r, t) = P_{-m}(-r, t)$ , the integral can be split into two parts:

$$\begin{aligned} \langle Q_R \rangle_{R_{t,n}} &= \int_0^L dr_{12} L \Omega\left(\frac{r}{L}\right) \sum_{m=-\infty}^{\infty} \frac{P_m(r_{12}, |\tau_{12}|) P_{n-m}(r_{12}, t - |\tau_{12}|)}{P_n(0, t)} \\ &+ \frac{P_{-m}(r_{12}, |\tau_{12}|) P_{-n+m}(r_{12}, t - |\tau_{12}|)}{P_n(0, t)}. \end{aligned} \quad (3.81)$$

where we introduced the function

$$\Omega(x) = x(1-x)^2. \quad (3.82)$$

To do the sum over  $m$ , we define the function  $\tilde{\Omega}$  as the periodic continuation of  $\Omega$ :

$$\tilde{\Omega}(x) = \Omega(\tilde{x}), \quad x = \tilde{x} + k \in \mathbb{R} \quad (3.83)$$

where  $k \in \mathbb{Z}$  is chosen, such that always  $\tilde{x} \in [0, 1]$ . (Some properties of the function  $\tilde{\Omega}(x)$  are summarized in appendix D.1) Using this, we can extend the integral in (3.81) to  $\pm\infty$ :

$$\int_{-\infty}^{\infty} dr_{12} L \tilde{\Omega}\left(\frac{r_{12}}{L}\right) \frac{P_0(r_{12}, |\tau_{12}|)P_n(r_{12}, t - |\tau_{12}|) + P_0(r_{12}, |\tau_{12}|)P_{-n}(r_{12}, t - |\tau_{12}|)}{P_n(0, t)}, \quad (3.84)$$

because  $P_m(r, t) = P_0(r - mL, t)$ . Inserting (3.71), we get:

$$\begin{aligned} \langle Q_R \rangle_{R_{t,n}}(\tau_{12}) &= \frac{L}{\sqrt{\pi}} \left( 4D \frac{|\tau_{12}|}{t} (t - |\tau_{12}|) \right)^{-\frac{1}{2}} \\ &\times \int_{-\infty}^{\infty} dr_{12} \tilde{\Omega}\left(\frac{r_{12}}{L}\right) \left( \exp\left(-\frac{\left(r_{12} - nL \frac{|\tau_{12}|}{t}\right)^2}{4D \frac{|\tau_{12}|}{t} (t - |\tau_{12}|)}\right) + (n \rightarrow -n) \right). \end{aligned} \quad (3.85)$$

With (3.85), we have recovered a result of [3].

### Limit of the infinite wire: $\sqrt{Dt} \ll L$

Because of (3.71), in the limit  $\sqrt{Dt} \ll L$  only the decay function for the  $n = 0$  mode will give a non-zero contribution to the conductivity corrections. Since inside the integral  $\frac{r_{12}}{L} \ll 1$  for  $\sqrt{Dt} \ll L$ , we can approximate  $\tilde{\Omega}$  using (D.3), and do the integral:

$$\langle Q_W \rangle_{R_{t,n=0}}(\tau_{12}) = \sqrt{\frac{4D|\tau_{12}|}{\pi t} (t - |\tau_{12}|)}. \quad (3.86)$$

As anticipated, this expression coincides with (3.55) for an infinite wire.

### 3.7.3 Results for the Cooperon decay function

The full Cooperon decay function is now given by (3.40) with (3.85) averaged over random walks having winding number  $n$ , as explained in (3.75). Inserting and going to sum and difference coordinates  $\tau_{12} = \tau_1 - \tau_2$  and  $\bar{\tau}_{12} = \tau_1 + \tau_2$ , we obtain:

$$\begin{aligned} F_n(t) &= -\frac{e^2}{\sigma_0} \int_0^t d\tau_{12} \left( 2(t - \tau_{12})W(\tau_{12}) - \left( \int_{-(t-\tau_{12})}^{+(t-\tau_{12})} d\bar{\tau}_{12} W(\bar{\tau}_{12}) \right) \right) \\ &\times \frac{1}{\sqrt{\pi}} \left( 4D \frac{|\tau_{12}|}{t} (t - |\tau_{12}|) \right)^{-\frac{1}{2}} \\ &\times \int_{-\infty}^{\infty} dr_{12} L \tilde{\Omega}\left(\frac{r_{12}}{L}\right) \left( \exp\left(-\frac{\left(r_{12} - nL \frac{|\tau_{12}|}{t}\right)^2}{4D \frac{|\tau_{12}|}{t} (t - |\tau_{12}|)}\right) + (n \rightarrow -n) \right), \end{aligned} \quad (3.87)$$

because the integrant is symmetric in  $\tau_{12}$ . To simplify this expression, we introduce the dimensionless variables  $x = \tau_{12}/t$  and  $y = r_{12}/L$  and obtain:

$$F_n(t) = \frac{1}{g(L)} \frac{l_t}{l_T^2} \int_0^1 dx \frac{z(x)}{\sqrt{\pi x(1-x)}} \int_{-\infty}^{\infty} dy \tilde{\Omega}(y) \frac{1}{2} \left[ \exp\left(-\frac{1}{l_t^2} \frac{\pi}{4} \frac{(y-nx)^2}{\pi x(1-x)}\right) + (n \rightarrow -n) \right], \quad (3.88)$$

where the time kernel  $z(x)$  is given by:

$$z(x) = -\frac{t}{T} \left[ 2(1-x)W(xt) - \int_{-(1-x)}^{+(1-x)} d\tilde{x} W(\tilde{x}t) \right]. \quad (3.89)$$

In (3.88), we introduced the ratio of the relevant length scales: the diffusive length of the trajectory  $L_t = \sqrt{Dt}$ , the thermal length  $L_T = \sqrt{D/T}$  and the length of the ring  $L$ :

$$l_t = \frac{L_t}{L} = \frac{\sqrt{Dt}}{L} \quad l_T = \frac{L_T}{L} = \frac{\sqrt{D/T}}{L}. \quad (3.90)$$

Furthermore, we introduced the dimensionless conductance on the length  $L$  in the form:

$$g(L) = \frac{\sigma_0}{e^2 L}. \quad (3.91)$$

In the metallic regime, which we consider here, we can always assume  $g(L) \gg 1$ .

It is convenient to use a Fourier representation of the function  $\tilde{\Omega}(x)$ , given by (D.6), and insert it into (3.88). Since terms antisymmetric in  $y$  give zero, we obtain:

$$F_n(t) = \frac{1}{g(L)} \frac{l_t}{l_T^2} \int_0^1 dx \frac{z(x)}{\sqrt{\pi x(1-x)}} \times \int_{-\infty}^{\infty} dy \left( \frac{1}{12} - \frac{1}{2} \sum_{k=1}^{\infty} \frac{\cos(2\pi ky) \cos(2\pi knx)}{(\pi k)^2} \right) \exp\left(-\frac{1}{l_t^2} \frac{\pi}{4} \frac{y^2}{\pi x(1-x)}\right). \quad (3.92)$$

Now, we can do the integral over  $y$  using (C.2):

$$F_n(t) = \frac{1}{g(L)} \frac{l_t^2}{l_T^2} \int_0^1 dx z(x) \left( \frac{1}{6} - \sum_{k=1}^{\infty} \frac{\cos(2\pi knx)}{(k\pi)^2} e^{-(\pi k)^2 (2l_t)^2 x(1-x)} \right). \quad (3.93)$$

This formula will be the basis for all our further calculations.

For classical noise (C), the time dependence of the correlator,  $W(t)$ , is given by a delta function, see (3.36), hence:

$$z_C(x) = 1 - 2(1-x)\delta(x) \quad (3.94)$$

From this we obtain:

$$F_n^C(t) = \frac{1}{g(L)} \frac{l_t^2}{l_T^2} \left[ \frac{1}{6} - \int_0^1 dx \left( \sum_{k=1}^{\infty} \frac{\cos(2\pi k n x)}{(k\pi)^2} e^{-(\pi k)^2 (2l_t)^2 x(1-x)} \right) \right]. \quad (3.95)$$

Note, that the only parameters affecting the form of this function are  $l_t$  and  $n$ . We will now evaluate its asymptotic limits and compare the results to a straightforward numerical evaluation.

### 3.7.4 Asymptotic behavior of the Cooperon decay function

#### Expected behavior

For classical Johnson-Nyquist noise we obtained in (3.36) a delta correlation for the temporal dependence of the correlator:  $W(t) = T\delta(t)$ . Thus, in formula (3.40) for the Cooperon decay, we can replace the double integral by a single one:

$$F_n(t) \sim T \int_0^t d\tau \langle Q \rangle_{R_{t,n}}(\tau). \quad (3.96)$$

We expect here two different regimes depending on  $l_t$  and  $n$ :

1. The **long ring** regime:  $\sqrt{Dt} \ll L$  implies  $l_t \ll 1$  and  $\mathbf{n} = \mathbf{0}$ : Here, the average trajectories are shorter than the system size and we expect a behavior for  $Q$  similar to the infinite wire, which has been calculated in (3.86). Qualitatively, the average over closed random walks can be replaced by an unrestricted random walk, which has been discussed in (3.56). Thus, we expect here:

$$F_{n=0}(t) \sim T \int_0^t d\tau \sqrt{D\tau} \sim \sqrt{DT} t^{3/2}. \quad (3.97)$$

For  $\mathbf{n} > \mathbf{0}$  on the other hand, the trajectories explore the system completely, by definition of  $n$ . Thus we replace the random walk average over  $Q$ , defined in (3.47), by its spacial average, giving:

$$\frac{1}{L} \int_0^L dx x \left(1 - \frac{x}{L}\right) \sim L. \quad (3.98)$$

For the decay, we conclude:

$$F_{n>0}(t) \sim T \int_0^t d\tau L \sim LTt. \quad (3.99)$$

2. The **short ring** regime:  $L \ll \sqrt{Dt}$  implies  $1 \ll l_t$ : Here, the average trajectories are always longer than the ring size, regardless of the winding number. With the same arguments as before we expect

$$F_n(t) \sim LTt \quad (3.100)$$

for **all n**.

## Results

A detailed calculation of the asymptotic behavior of the Cooperon decay function is given in appendix A.1. The results are:

$n = 0$  **mode**: We obtain for the **long ring**, i.e.  $l_t \ll 1$ , see (A.2):

$$F_{n=0}^C(t)_{l_t \ll 1} = \frac{1}{g(L)} \frac{\sqrt{\pi}}{4} \frac{l_t^3}{l_T^2} \left( 1 - \frac{4l_t}{3\sqrt{\pi}} \right). \quad (3.101)$$

In the original variables, this reads:

$$\boxed{F_{n=0}^C(t)_{\sqrt{Dt} \ll L} = \frac{e^2}{\sigma_0} \frac{\sqrt{D\pi}}{4} T t^{3/2} \left( 1 - \frac{4}{3\sqrt{\pi}} \sqrt{\frac{Dt}{L^2}} \right)}. \quad (3.102)$$

The leading term coincides with the result (3.57) for the infinite wire. For increasing  $l_t$ , we see a crossover to the **short ring** regime, i.e. at  $1 \ll l_t$ , see (A.5):

$$F_{n=0}^C(t)_{1 \ll l_t} = \frac{1}{g(L)} \frac{1}{6} \frac{l_t^2}{l_T^2} \left( 1 - \frac{1}{30l_t^2} \right) \quad (3.103)$$

or

$$\boxed{F_{n=0}^C(t)_{L \ll \sqrt{Dt}} = \frac{e^2}{\sigma_0} \frac{1}{6} LTt \left( 1 - \frac{1}{30} \frac{L^2}{Dt} \right)}. \quad (3.104)$$

This crossover is shown in figure 3.2.

$n > 0$  **modes**: The leading behavior for the long and the short ring is identical, but the first correction term is different. We obtain for the **long ring** regime, i.e. at  $l_t \ll 1$ , see (A.4):

$$F_{n>0}^C(t)_{l_t \ll 1} = \frac{1}{g(L)} \frac{1}{6} \frac{l_t^2}{l_T^2} \left( 1 - 2 \frac{l_t^2}{n^2} \right) \quad (3.105)$$

or

$$\boxed{F_{n>0}^C(t)_{\sqrt{Dt} \ll L} = \frac{e^2}{\sigma_0} \frac{1}{6} LTt \left( 1 - 2 \frac{Dt}{n^2 L^2} \right)}, \quad (3.106)$$

and for the **short ring** regime, i.e. at  $1 \ll l_t$ , see (A.8):

$$F_{n>0}^C(t)_{1 \ll l_t} = \frac{1}{g(L)} \frac{1}{6} \frac{l_t^2}{l_T^2} \left( 1 - \frac{1}{30l_t^2} \right). \quad (3.107)$$

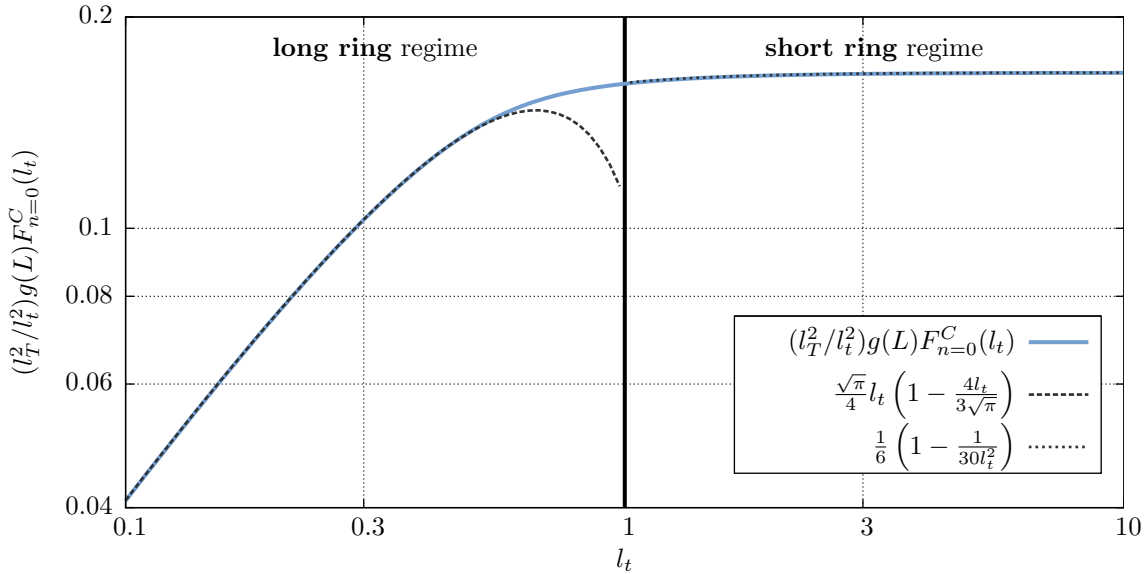


Figure 3.2: Numerical evaluation of the Cooperon decay function for the  $n = 0$  mode and classical noise. For comparison, we show the asymptotic expressions (3.101) and (3.103). A crossover between the long and the short ring regime is clearly visible.

or

$$F_{n>0}^C(t)_{L \ll \sqrt{Dt}} = \frac{e^2}{\sigma_0} \frac{1}{6} L T t \left( 1 - \frac{1}{30} \frac{L^2}{Dt} \right). \quad (3.108)$$

This behavior is shown in figure 3.3. The dependence on  $n$  is weak.

### 3.7.5 Summary

We obtained a change in the time dependence of the decay function from non-exponential ( $\sim t^{3/2}$ ) in the infinite system to exponential ( $\sim t$ ) when trajectories are longer than the size of the ring, thus agreeing with our expectations and confirming the results of [2] and [3]. Additionally, we calculated the leading correction terms at the crossover point. Recently, this dimensional crossover has been measured in metallic square networks, see [22]. We will review this experimental situation in more detail in chapter 6.

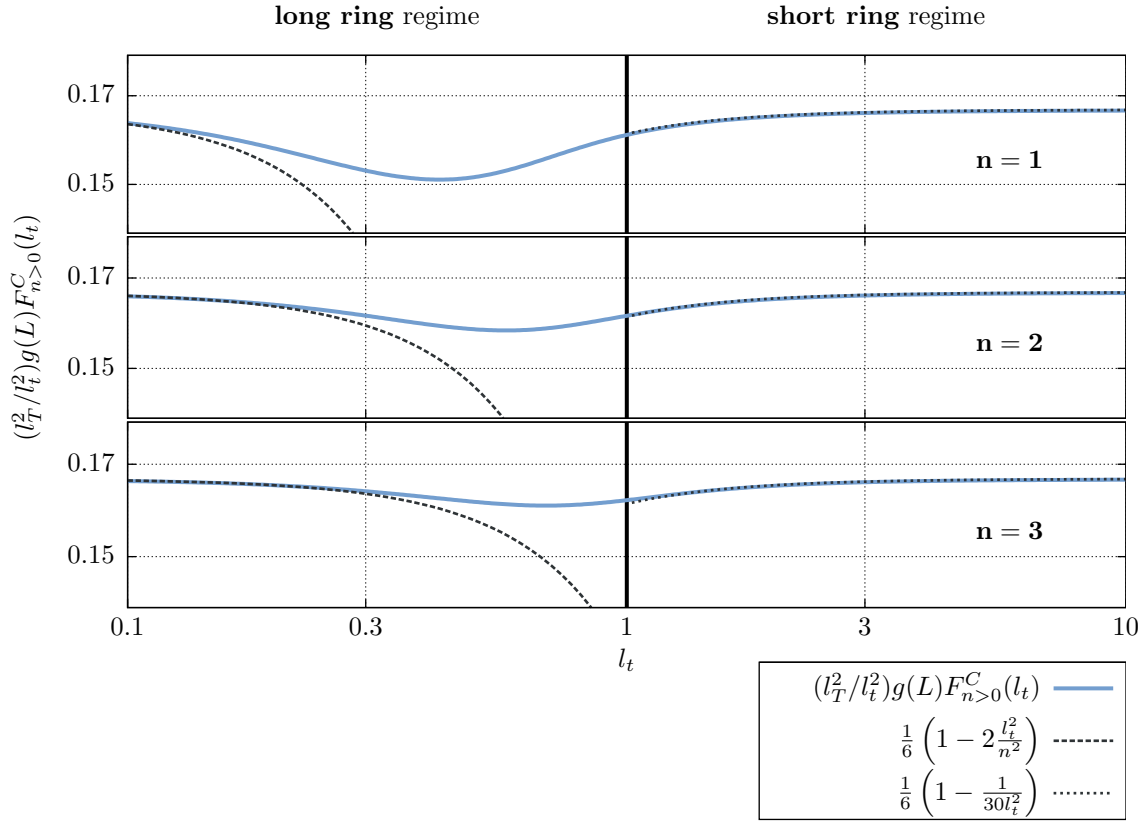


Figure 3.3: Numerical evaluation of the Cooperon decay function for the modes  $n > 0$  and classical noise. For comparison, we show the asymptotic expressions (3.105) and (3.107). We obtain no crossover between the long and the short ring regimes. Essentially, there is no dependence on  $n$  at all, except for small deviations close to  $l_t = 1$  for small  $n$ .



# Chapter 4

## Quasi-1d systems: Quantum noise

### 4.1 Quantum noise correlator including the Pauli principle

In the last chapter we used the noise obtained from the Fluctuation-Dissipation-Theorem, in the high temperature limit, cf. (3.13), (3.32) and (3.36). This correlator had no dependence on frequency and the noise was assumed white in time. As has been anticipated in our derivation of Johnson-Nyquist noise, a full quantum-mechanical treatment is possible, by replacing the correlation function by the anti-commutator:

$$\langle VV \rangle(\mathbf{k}, \omega) \rightarrow \frac{1}{2} \langle \{V, V\} \rangle(\mathbf{k}, \omega) = \coth(\omega/2T) \frac{1}{2} \langle [V, V] \rangle(\mathbf{k}, \omega) \quad (4.1)$$

and by taken into account a finite temperature, thus obtaining a factor of  $\coth(\omega/2T) = 2n(\omega) + 1$  (where  $n$  is the Bose function) instead of the linear temperature dependence.

However, this is not the full story. The derivation of this correlator describes the motion of a *single* electron in the presence of quantum noise, but in the *absence* of the Fermi sea of the metal.

The most striking physical difference in the metal is the effect of Pauli blocking. While a single electron (e.g. propagating in a vacuum), having energy  $\epsilon$ , may loose its energy by spontaneous emission at any time as long as  $\epsilon > 0$ , in a metal, the phase space for such a transition is reduced by the lack of available final states, occupied by the surrounding electrons. As the temperature increases, the number of free states increases and the blocking effect is reduced. In the limit  $T \rightarrow \infty$  one should recover the behavior discussed in the previous chapter.

Recently, von Delft, Marquardt et al. were able to include the effect of the Fermi sea in an effective correlator, which they presented in a series of two papers: [4] and [5]. They based their argumentation on a Feynman-Vernon influence functional approach, backed up by a careful diagrammatic calculation in Keldysh space (see also [23], for a detailed calculation. For an introduction to the influence functional approach, see [24], where the authors derive the classical Johnson-Nyquist theorem).

Their main result, was to propose an effective noise correlator in the presence of the Fermi sea, which they checked against available exact results and obtained only small corrections due to quantum noise at low temperatures.

They proposed replacing the coth factor by

$$2n(\omega) + 1 \rightarrow 2n(\omega) + 1 + f(\epsilon + \omega) - f(\epsilon - \omega). \quad (4.2)$$

Here,  $f$  is the Fermi function and  $\epsilon$  is the average energy, measured with respect to the fermi energy  $\epsilon_F$ , of the pair of propagating electron trajectories. This combination ensures that processes which would violate the Pauli principle ( $\omega \gg \max(T, \epsilon)$ ) are suppressed.

For the correlator, this replacement leads to

$$\langle VV \rangle(\mathbf{k}, \omega) \rightarrow [2n(\omega) + 1 + f(\epsilon + \omega) - f(\epsilon - \omega)] \frac{1}{2} \langle [V, V] \rangle(\mathbf{k}, \omega). \quad (4.3)$$

Thus we may retain our factorized form of the correlator (3.34):

$$\langle VV \rangle(\mathbf{r}, \omega) = \frac{2e^2}{\sigma_0} Q(\mathbf{r}) W_Q(\omega), \quad (4.4)$$

since the new factor affects the energy dependence of the correlator,  $W(\omega)$ , but leaves the spacial dependence  $Q(r)$  unchanged. The energy dependence is now given by  $W_Q(\omega)$ , defined by

$$W_Q(\omega, \epsilon) = \frac{\omega}{2} [2n(\omega) + 1 + f(\epsilon + \omega) - f(\epsilon - \omega)]. \quad (4.5)$$

(The factor  $\frac{\omega}{2}$  originates from the Fluctuation-Dissipation-Theorem, compare with (3.12).)

The correlator is now a function of the average energy  $\epsilon$  of the forward and backward electron trajectories. Following the steps of Marquardt et al., we average over this energy using the usual derivative of the Fermi function  $f(\epsilon)$ :

$$\langle \dots \rangle_\epsilon = \int d\epsilon [-f'(\epsilon)] \dots \quad (4.6)$$

The integral over the correlator occurs in the decay function in the exponent. Again, following Marquardt et al., we lift this average into the exponent:

$$\langle e^{-F(t)} \rangle_\epsilon \simeq e^{-\langle F(t) \rangle_\epsilon}, \quad (4.7)$$

then we can evaluate the  $\epsilon$ -integral and obtain:

$$W_Q(\omega) = \langle W_Q(\omega, \epsilon) \rangle_\epsilon = T \left( \frac{\omega/2T}{\sinh(\omega/2T)} \right)^2. \quad (4.8)$$

Fourier transforming yields

$$\boxed{W_Q(t) = \pi T^2 w(\pi T t), \quad w(x) = \frac{x \coth(x) - 1}{\sinh(x)^2}}, \quad (4.9)$$

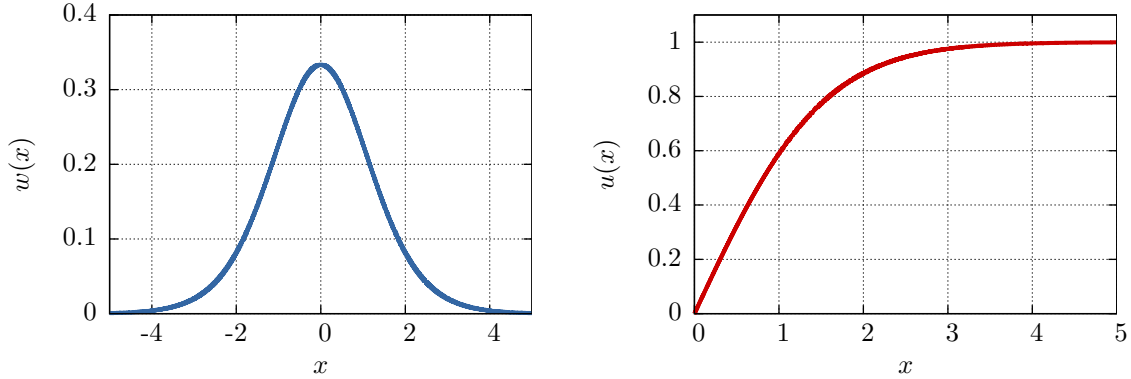


Figure 4.1: The function  $w(x)$ , defined by (4.9): A positive, peak-shaped function, and its integral  $u(x) = \int_{-x}^x dy w(y)$ , which tends to 1 for  $x \rightarrow \infty$ .

instead of the classical form  $W_C(t) = T\delta(t)$ , which we obtained for Johnson-Nyquist noise.

Note that  $W_Q$  equals  $T$  times a broadened delta function of width  $1/T$ , since  $w(x)$  is a positive, peak-shaped function with weight 1, see Figure 4.1. Thus, in the limit  $T \rightarrow \infty$  we recover the classical results.

The diffusive length scale of thermal fluctuations is given by the thermal length:  $L_T = \sqrt{D/T}$ . It has been shown in [4], that if the average length of the trajectory,  $L_t = \sqrt{Dt}$ , is shorter than this scale, the corrections to the conductivity cannot be in the regime of weak localization any more. Interaction effects become dominant and the results are fundamentally different, since different diagrams become important. Thus, in the following, we will require:

$$\boxed{L_t \gg L_T \quad \Leftrightarrow \quad Tt \gg 1} . \quad (4.10)$$

## 4.2 Cooperon decay and quantum noise

The Cooperon decay function is still given by (3.93):

$$F_n(t) = \frac{1}{g(L)} \frac{l_t^2}{l_T^2} \int_0^1 dx z(x) \left( \frac{1}{6} - \sum_{k=1}^{\infty} \frac{\cos(2\pi knx)}{(k\pi)^2} e^{-(\pi k)^2 (2l_t)^2 x(1-x)} \right), \quad (4.11)$$

but now the function  $z(x)$ , defined in (3.89), is given by

$$z_Q(x) = u(\alpha(1-x)) - 2\alpha(1-x)w(\alpha x). \quad (4.12)$$

where  $\alpha = \pi Tt = \pi l_t^2/l_T^2$ ,

$$w(x) = \frac{x \coth(x) - 1}{\sinh^2(x)} \quad \text{and} \quad u(x) = \int_{-x}^x dy w(y) = \coth(x) - \frac{x}{\sinh(x)^2}. \quad (4.13)$$

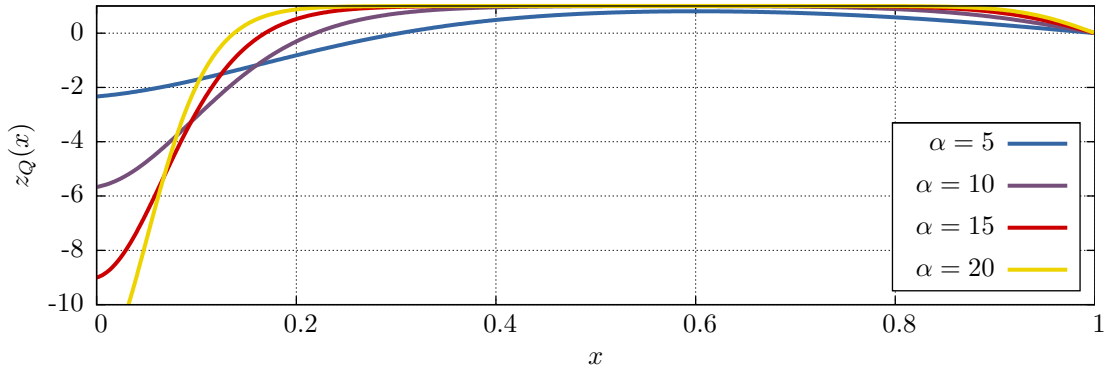


Figure 4.2: The function  $z_Q(x)$  defined by (4.12): In the limit  $T \rightarrow \infty$  it approaches the classical result (3.94).

Note that because of the symmetry of the integrand in (4.11), we may replace  $1 - x$  by  $x$  in the first term of (4.12) and thus replace  $z(x)$  by  $\tilde{z}(x)$ , defined by:

$$\tilde{z}_Q(x) = u((\pi l_t^2/l_T^2)x) - 2(\pi l_t^2/l_T^2)(1-x)w((\pi l_t^2/l_T^2)x). \quad (4.14)$$

Some of the properties and integrals of this function are given in (D.2)

### 4.3 Calculation of the Cooperon decay function in a quasi-1d ring

The Cooperon decay function is given by:

$$F^Q(t) = -\frac{1}{g(L)} \frac{l_t^2}{l_T^2} \int_0^1 dx \tilde{z}_Q(x) \left( \sum_{k=1}^{\infty} \frac{\cos(2\pi knx)}{(k\pi)^2} e^{-(\pi k)^2 (2l_t)^2 x(1-x)} \right), \quad (4.15)$$

where  $\tilde{z}_Q$  is given by (4.14).

We will now directly continue with an evaluation of its asymptotic behavior and compare the results to a numerical evaluation. For details on the latter, see appendix B. Note that in contrast to the case of classical noise,  $l_T$  now directly affects its form, instead of being just a prefactor, since  $\tilde{z}(x)$  depends on it in a non-trivial way.

#### 4.3.1 Asymptotic behavior of the Cooperon decay function

##### Expected behavior

In (4.10), we argued that the thermal length  $L_T$  should always be shorter than the average trajectory length  $L_t$ . Thus, as long as the thermal length of the system is also much shorter than the system size  $L$ , our improved treatment of the noise should give small

correction terms due to the smeared delta function, depending on temperature. However, modified behavior can be expected for the case of very low temperatures and a very short ring:  $L_T \gg L$ . Here, the decay should be much weaker than predicted using classical noise, since the potential can be considered frozen during the the scale  $1/T$ . Therefore, we expect 3 regimes:

1. The **long ring** regime:  $\sqrt{D/T} \ll \sqrt{Dt} \ll L$  implying  $l_T \ll l_t \ll 1$ : Just like in section 3.7.4, we expect for the  $\mathbf{n} = \mathbf{0}$  mode:

$$F_{n=0}(t) \sim Tt^{3/2} \quad (4.16)$$

and

$$F_{n>0}(t) \sim LTt \quad (4.17)$$

for  $\mathbf{n} > \mathbf{0}$ .

2. The **short ring** regime:  $\sqrt{D/T} \ll L \ll \sqrt{Dt}$  implying  $l_T \ll 1 \ll l_t$ : Also, just like in section 3.7.4, we expect:

$$F_n(t) \sim LTt, \quad (4.18)$$

for **all**  $\mathbf{n}$ .

3. The **very short ring** regime:  $L \ll \sqrt{D/T} \ll \sqrt{Dt}$  implying  $1 \ll l_T \ll l_t$ : Here, just like in the short ring regime, the trajectories are much longer than the ring size  $L$ , thus we expect no dependence on  $n$ , with the same arguments as in section 3.7.4.

Furthermore, the potential is effectively frozen during the time  $\tau_T = 1/T$ . Since this time is already much longer than the average time an electron needs for encircling the ring once, which is given by the Thouless time  $\tau_{Th} = L^2/D$ , we can assume from  $Q(r(\tau)) \sim L$  and  $W(\tau) \sim T^2$  for some fixed time  $\tau < \tau_T$ :

$$\langle V(\tau)V(0) \rangle \sim T^2L. \quad (4.19)$$

Now, since during the time  $\tau_T$ , the trajectories already explore the system completely, we can write the the phase accumulated during the time  $\tau_T$  as an integral over the ring size:

$$\delta\varphi = \tau_T \int_0^L dx V(x)(p^L(x) - p^R(x)), \quad (4.20)$$

where  $p(x)dx$  is the fraction of time spent by the particular realization of the trajectory in the interval  $[x, x + dx]$ . Here, for the Cooperon phase, we need the phase difference of two trajectories and therefore the difference  $p^L(x) - p^R(x)$  enters.  $p^{R/L}(x)$  generally differs from the simple constant  $1/L$ , since we are considering the finite interval  $\tau_T < t$ . Generally, in the simple picture of convergence of the empirical mean to its expectation value, the standard deviation scales like  $\sim 1/\sqrt{N}$  where  $N$  is the

number of samples. In our case, this number is proportional to the time  $\tau_T$ , as can also be confirmed in a more detailed derivation. We follow for the Gaussian average:

$$\langle \delta\varphi \rangle \sim \tau_T^2 (T^2 L) \frac{L^2}{\tau_T} \sim \tau_T T^2 L^3. \quad (4.21)$$

For the total phase of the Cooperon, which is then given by  $\frac{t}{\tau_T}$  segments of length  $\tau_T$ :

$$F_n(t) \sim \frac{t}{\tau_T} \tau_T T^2 L^3 \sim L^3 T^2 t. \quad (4.22)$$

Also note that the crossover from the short to the very short regime might also be interpreted as a transition from a quasi one dimensional to a zero dimensional system. The latter has been described in [25].

## Results

A detailed calculation of the asymptotic limits of the Cooperon decay function for quantum noise can be found in appendix A.2. The results are:

**long ring regime**  $l_T \ll l_t \ll 1$ : We obtain for the  $n = 0$  mode, see (A.14):

$$F_{n=0}^Q(t)_{l_T \ll l_t \ll 1} = \frac{1}{g(L)} \frac{\sqrt{\pi}}{4} \frac{l_t^3}{l_T^2} \left( 1 - \frac{2^{3/2}}{\pi} |\zeta(1/2)| \frac{l_T}{l_t} - \frac{4l_t}{3\sqrt{\pi}} \right). \quad (4.23)$$

The numerical factor of the first correction term is given by  $\frac{2^{3/2}}{\pi} |\zeta(1/2)| \approx 1.3$ . Expressed in the original variables this is given by:

$$\boxed{F_{n=0}^Q(t)_{l_T \ll l_t \ll 1} = \frac{e^2}{\sigma_0} \frac{\sqrt{D\pi}}{4} T t^{3/2} \left( 1 - \frac{2^{3/2}}{\pi} |\zeta(1/2)| \frac{1}{\sqrt{tT}} - \frac{4}{3\sqrt{\pi}} \sqrt{\frac{Dt}{L^2}} \right)}. \quad (4.24)$$

The first two terms of (4.24) reproduce the results obtained by Marquardt et al. ([4], Eq. 12a) for the case of an infinitely long wire. The first relative correction is  $\sim 1/\sqrt{Tt}$  and thus, parametrically small, see (4.10). The last term is the correction already obtained for classical noise, see (3.101) at the crossover to the short ring regime. The corrections have been checked numerically, see figures 4.3 (upper) for the dependence on  $l_T$  and 4.4 (upper left) for the dependence on  $l_t$ .

For modes  $n > 0$ , we find, see (A.18) (, for  $n \ll l_T^2/l_t^2$ ):

$$F_{n>0}^Q(t)_{l_T \ll l_t \ll 1} = \frac{1}{g(L)} \frac{1}{6} \frac{l_t^2}{l_T^2} \left( 1 - \frac{6}{\pi} \frac{n l_T^2}{l_t^2} - 2 \frac{l_t^2}{n^2} - \frac{12}{\pi} l_T^2 \right), \quad (4.25)$$

or expressed in the original variables:

$$\boxed{F_{n>0}^Q(t)_{\sqrt{D/T} \ll \sqrt{Dt} \ll L} = \frac{e^2}{\sigma} \frac{1}{6} L T t \left( 1 - \frac{6}{\pi} \frac{n}{tT} - 2 \frac{Dt}{n^2 L^2} - \frac{12}{\pi} \frac{D}{TL^2} \right)}. \quad (4.26)$$

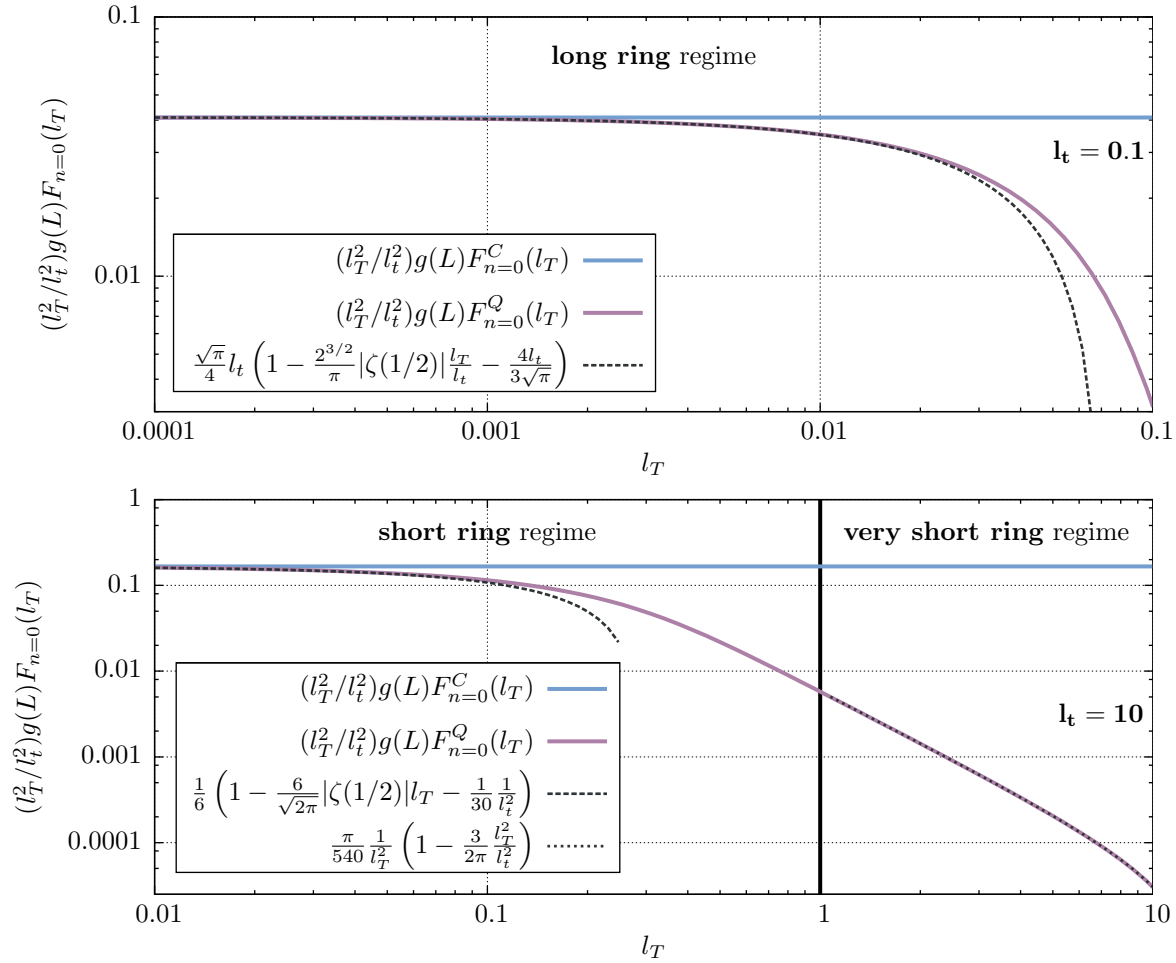


Figure 4.3: The decay function for quantum noise  $F_Q$  in comparison to classical noise  $F_C$  of the parameter  $l_T$  for  $n = 0$ . Upper figure:  $l_t = 0.1$ : the long ring regime and its asymptotic formula (4.23). Lower figure:  $l_t = 10$ : the short and very short ring regimes, shown with (4.27) and (4.29).

The second correction term has already been found for classical noise, see (3.105). The first term is the leading correction due to quantum noise. It depends on the winding number  $n$  and is proportional to  $1/Tt$  and thus also parametrically small. The last term is smaller than the first as long as  $n/l_t^2 > 2$  and is only required for small  $n$  and relatively large  $l_t \ll 1$ . For a numerical evaluation of this regime, see figures 4.5 for the dependence on  $l_T$  and 4.7 (left) for the dependence on  $l_t$ . As it was the case for classical noise, we confirm the result that in the long ring regime, the curve for  $n = 0$  and the curves for  $n > 0$  are fundamentally different, as can be seen when comparing figures 4.4 and 4.7. For higher modes, the crossover to the short ring regime is essentially absent.

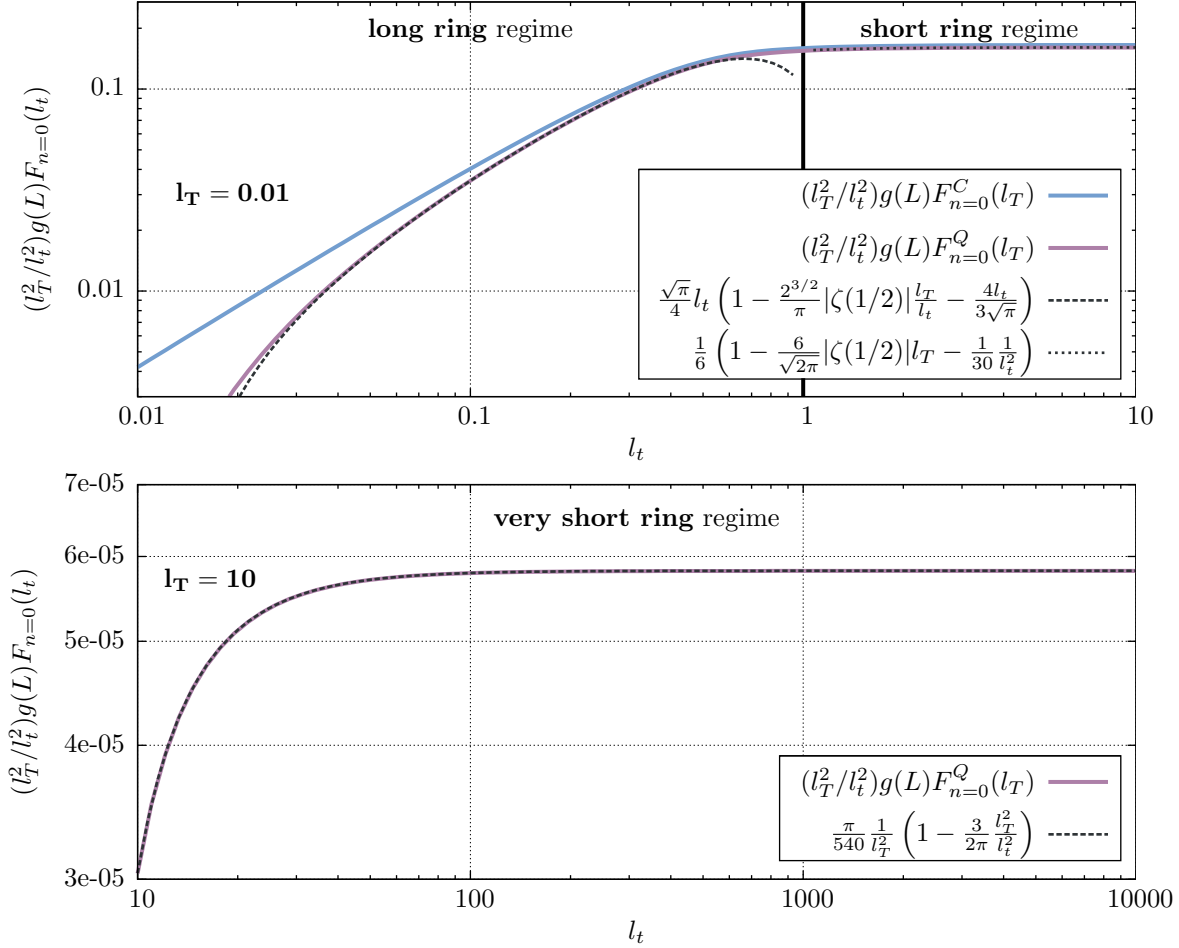


Figure 4.4: The decay function for quantum noise  $F_Q$  in comparison to classical noise  $F_C$  of the parameter  $l_t$  for  $n = 0$ . Upper figure:  $l_t = 0.01$ : the long and short ring regimes shown with (4.23) and (4.27). Lower figure:  $l_t = 10$ : the very short ring regime and its asymptotic formula (4.29).

**short ring regime**  $l_T \ll 1 \ll l_t$ : Here, the results for the  $n = 0$  and  $n > 0$  modes are identical, see (A.22) and (A.26):

$$F_n^Q(t)_{l_T \ll 1 \ll l_t} = \frac{1}{g(L)} \frac{1}{6} \frac{l_t^2}{l_T^2} \left( 1 - \frac{6}{\sqrt{2\pi}} |\zeta(1/2)| l_T - \frac{1}{30} \frac{l_t}{l_T^2} \right). \quad (4.27)$$

with  $\frac{6}{\sqrt{2\pi}} |\zeta(1/2)| \approx 3.5$ . Or in the original variables:

$$F_n^Q(t)_{\sqrt{D/T} \ll L \ll \sqrt{Dt}} = \frac{e^2}{\sigma} \frac{1}{6} LTt \left( 1 - \frac{6}{\sqrt{2\pi}} \sqrt{\frac{D}{TL^2}} - \frac{1}{30} \frac{L^2}{Dt} \right). \quad (4.28)$$

The last correction term coincides with the classical correction (3.107). The leading quantum correction is proportional to  $l_T$ , which is the ratio of the thermal length to the system

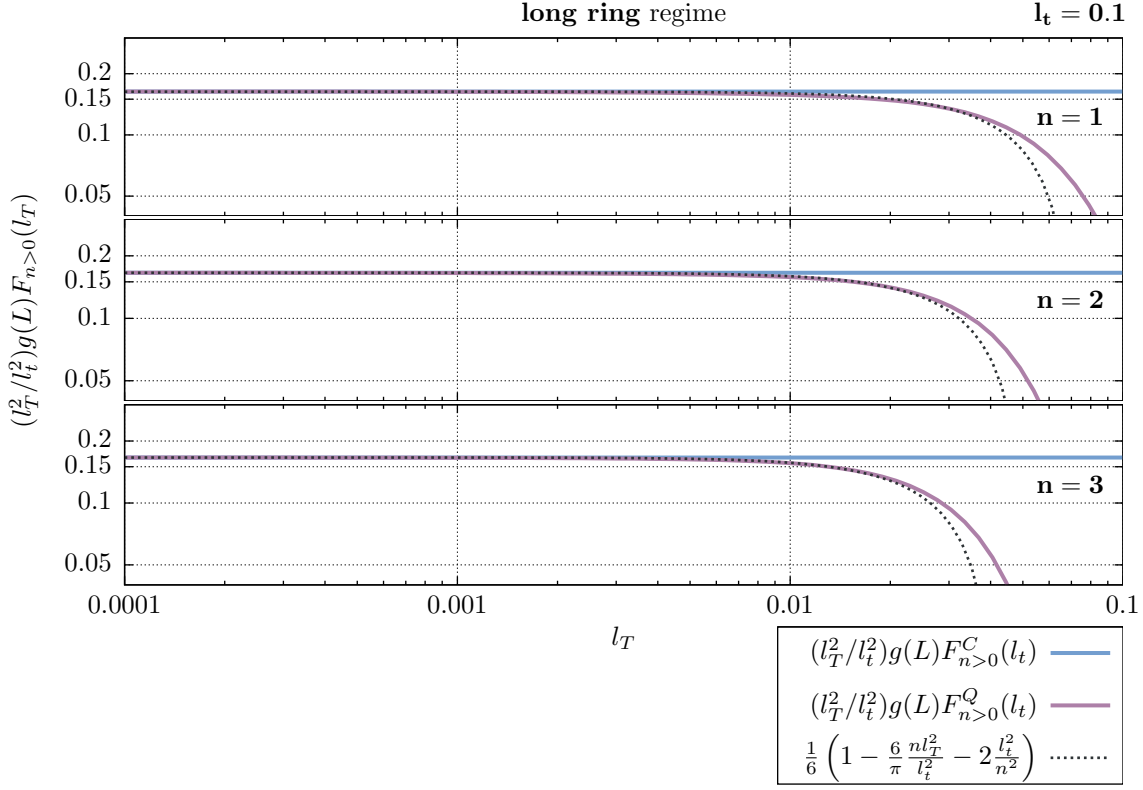


Figure 4.5: The decay function of the parameter  $l_T$  for  $l_t = 0.1$ , i.e. the long ring regime for modes  $n > 0$ . Shown in comparison to the asymptotic expression (4.25).

size. Note that this correction does not depend on the winding number  $n$ , as it has been the case for the long ring. Instead this correction marks the onset to the very small ring regime. For the  $n = 0$  mode, the decay function in this regime is shown in figure 4.3 (lower left) as a function of  $l_T$  and in 4.4 (upper right) as a function of  $l_t$ . For modes  $n > 0$ , see figures 4.6 (left) and 4.7 (right) respectively. In fact, one sees that the results for the zero mode and higher modes coincide.

**very short ring regime**  $1 \ll l_T \ll l_t$ : We obtain, also for all  $n$ , see (A.29):

$$F_n^Q(t)_{1 \ll l_T \ll l_t} = \frac{1}{g(L)} \frac{l_t^2}{l_T^4} \frac{\pi}{540} \left( 1 - \frac{3}{2\pi} \frac{l_T^2}{l_t^2} \right). \quad (4.29)$$

or

$$F_n^Q(t)_{L \ll \sqrt{D/T} \ll \sqrt{Dt}} = \frac{e^2}{\sigma} \frac{\pi}{540} \frac{1}{D} L^3 T^2 t \left( 1 - \frac{3}{2\pi} \frac{1}{Tt} \right). \quad (4.30)$$

This regime was totally absent in the classical calculation. The decay in this regime is drastically reduced, as can be seen in figures 4.3 (lower right) and 4.4 (lower). Also note the small prefactor  $\pi/540$ , which accounts for a further reduction of the decay. In the

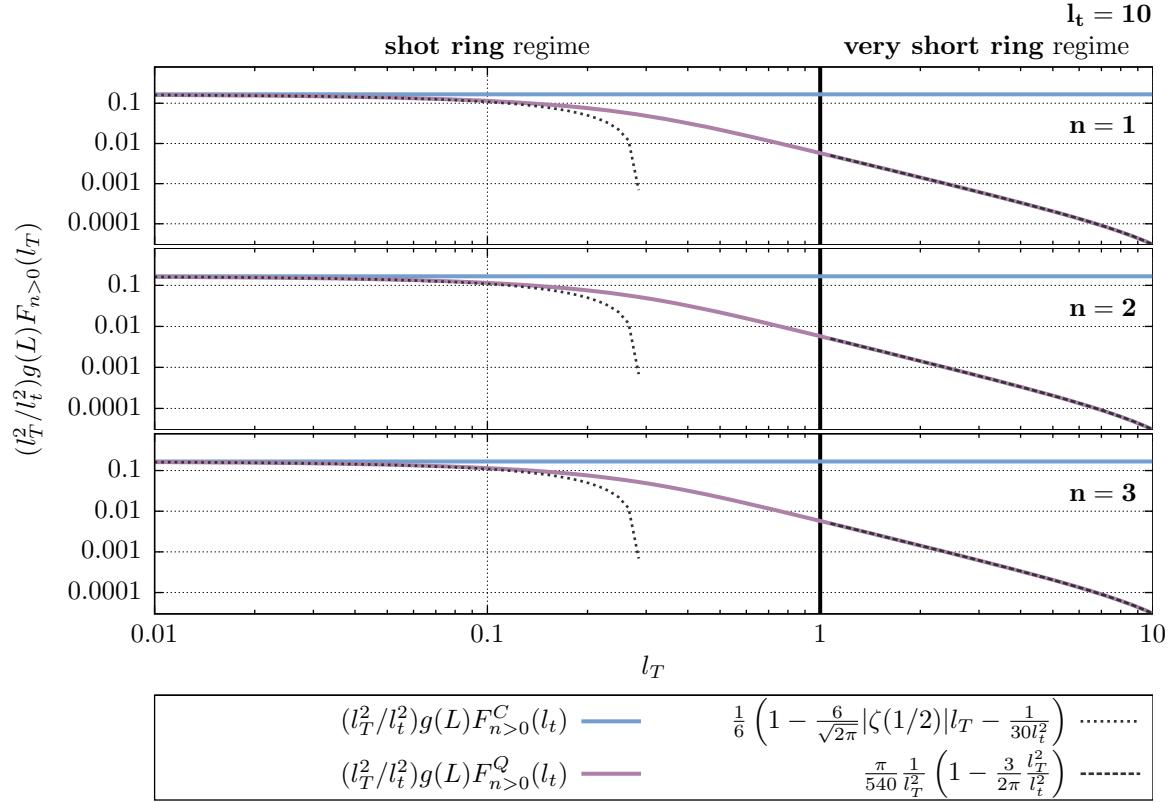


Figure 4.6: The decay function of the parameter  $l_T$  for  $l_t = 10$ , i.e. the short and very short ring regimes for modes  $n > 0$ . Shown in comparison to the asymptotic expressions (4.27) and (4.29).

latter plot, only the decay function calculated with quantum noise has been shown since the corresponding function using classical noise would be more than 3 orders of magnitude larger. In fact, it is given by the constant value  $(l_T^2/l_t^2)g(L)F_n^C(l_t) = 1/6$ , see (3.107). In the first plot, the transition from the small to the very small ring regime can be seen. Note the early onset of the new regime and the strong reduction of the decay in comparison to the classical calculation. The same is true for figures 4.6 (right) and 4.8, which show the dependence of the decay function in this regime on  $l_T$  and  $l_t$ , respectively, for modes  $n > 0$ . These figures confirm the result, that the winding number  $n$  is irrelevant in this regime.

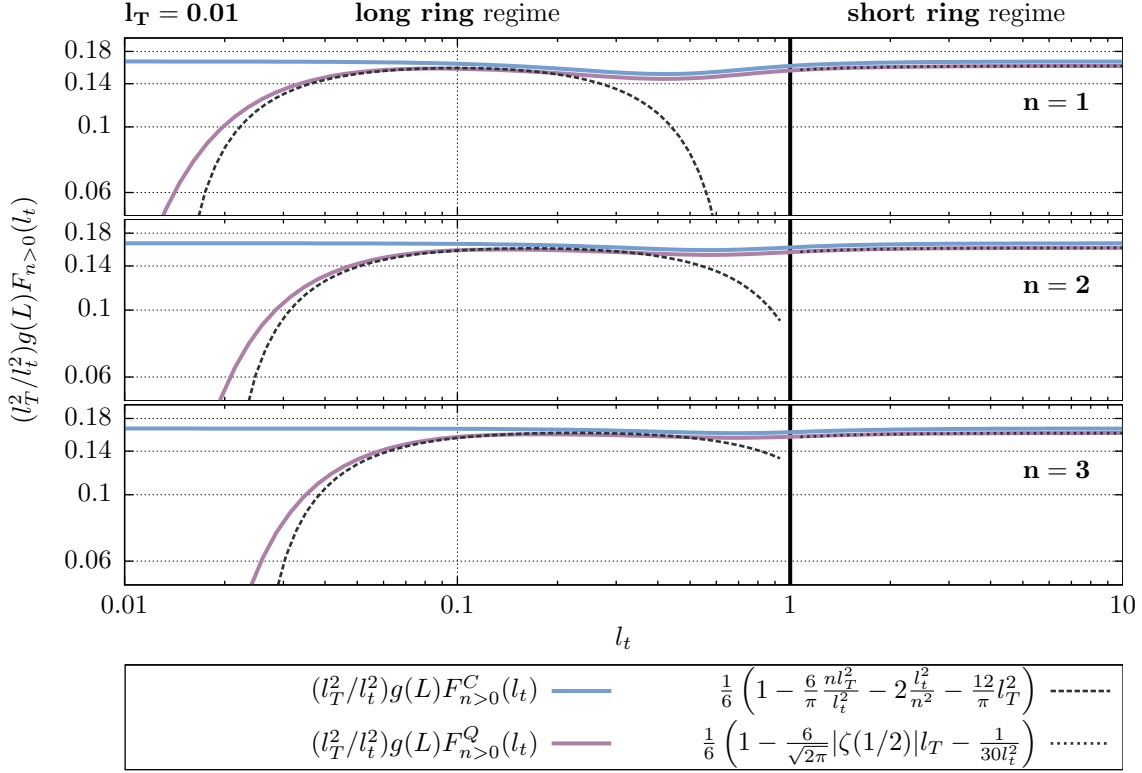


Figure 4.7: The decay function of the parameter  $l_t$  for  $l_T = 0.01$ , i.e. the long and the short ring regimes for modes  $n > 0$ . Shown in comparison to the asymptotic expressions (4.25) and (4.27).

### 4.3.2 Summary and results for the dephasing length

For completeness of our presentation we will extract here the dephasing length of the Cooperon due to electronic quantum noise. We define the decoherence time  $\tau_\phi$  and the relative decoherence length  $l_\phi$  simply by requiring:

$$F_n(\tau_\phi) \equiv 1 \quad l_\phi = \frac{L_\phi}{L} = \frac{\sqrt{D\tau_\phi}}{L}. \quad (4.31)$$

It's behavior may easily be extracted from the asymptotic expressions in the last section and is summarized in Table 4.1.

It shall be emphasized though, that the time corresponding to this decoherence length  $\tau_\phi = L_\phi^2/D$  is not the decoherence time of the Cooperon in the traditional sense, since it applies only to one specific winding number. We cannot simply use this time as an infrared cutoff for the conductivity integral. Instead, the summation over  $n$  has to be done first. Nevertheless, this quantity is accessible to the experimentalist using magneto-conductance measurements, which we will discuss in the next chapter.

The relative dephasing length is shown in figure 4.9 for several values of  $g(L) \gg 1$  and

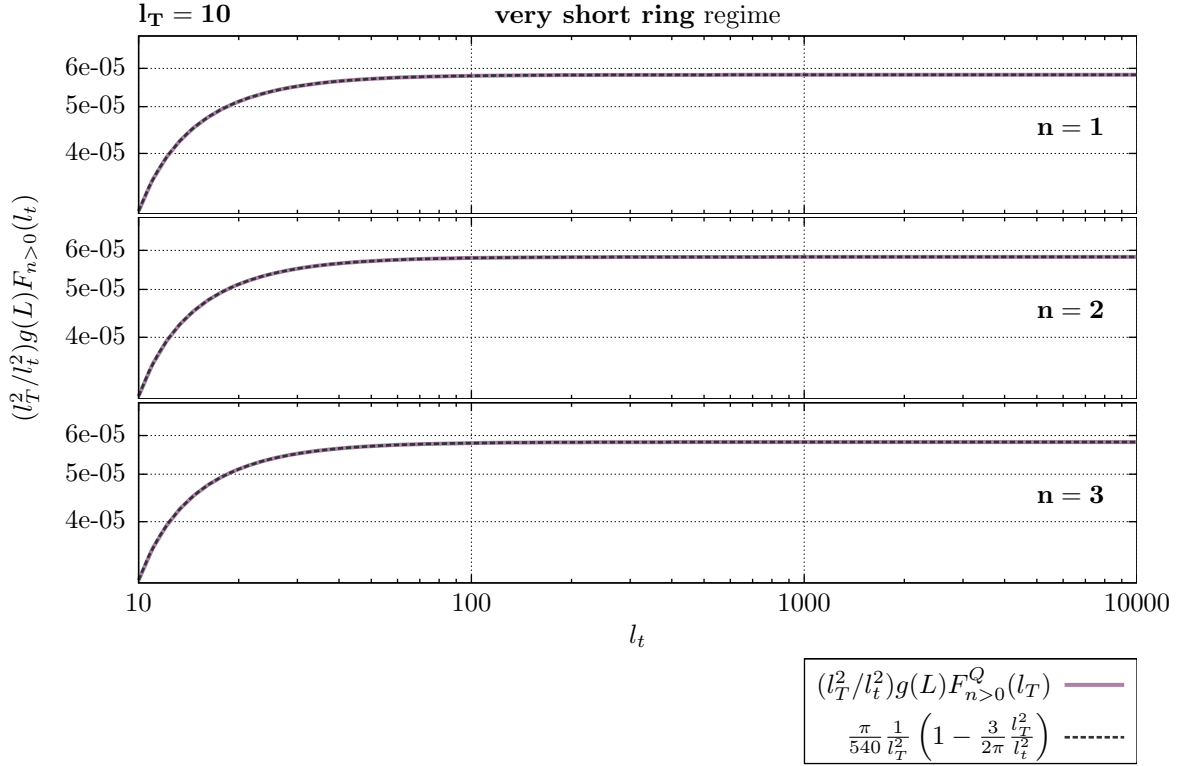


Figure 4.8: The decay function of the parameter  $l_t$  for  $l_T = 10$ , i.e. the very short ring regime for modes  $n > 0$ . Shown in comparison to the asymptotic expression (4.29).

for the zeroth and first mode. As it has been shown in the previous section, higher modes will behave similar to  $n = 1$ .

The figure 4.10 for  $n = 0$  shows all 3 regimes, obtained in the last section. Note that the crossover point from the long to the short ring regime is now given at  $l_\phi = 1$  while the crossover point from the short to the very short regime is at  $l_T = 1$ .

	Condition	Decay function	Relative correction	Dephasing length
<b>long ring</b> ( $n = 0$ )	$L_T \ll L_t \ll L$ $l_T \ll l_t \ll 1$	$F(t) \sim Tt^{3/2}$ $F(l_t) \sim \frac{1}{g(L)} \frac{l_t^3}{l_T^2}$	$\sim -1/\sqrt{tT}$ $\sim -l_T/l_t$	$L_\phi \sim T^{-1/3}$ $l_\phi \sim \sqrt[3]{g(L)l_T^2}$
<b>long ring</b> ( $n > 0$ )	$L_T \ll L_t \ll L$ $l_T \ll l_t \ll 1$	$F(t) \sim LTt$ $F(l_t) \sim \frac{1}{g(L)} \frac{l_t^2}{l_T^2}$	$\sim -n/tT$ $\sim -nl_T^2/l_t^2$	$L_\phi \sim (TL)^{-1/2}$ $l_\phi \sim \sqrt{g(L)l_T^2}$
<b>short ring</b> (all $n$ )	$L_T \ll L \ll L_t$ $l_T \ll 1 \ll l_t$	$F(t) \sim LTt$ $F(l_t) \sim \frac{1}{g(L)} \frac{l_t^2}{l_T^2}$	$\sim -\sqrt{1/TL^2}$ $\sim -l_T$	$L_\phi \sim (TL)^{-1/2}$ $l_\phi \sim \sqrt{g(L)l_T^2}$
<b>very short ring</b> (all $n$ )	$L \ll L_T \ll L_t$ $1 \ll l_T \ll l_t$	$F(t) \sim L^3T^2t$ $F(l_t) \sim \frac{1}{g(L)} \frac{l_t^2}{l_T^4}$	$\sim -1/Tt$ $\sim -l_T^2/l_t^2$	$L_\phi \sim (T^2L^3)^{-1/2}$ $l_\phi \sim \sqrt{g(L)l_T^4}$

Table 4.1: The 3(+1) regimes obtained from the Cooperon decay function in dimensionfull and dimensionless units. (The dimensionfull expressions are missing factors of  $[D] = m^2/s$  and  $[e^2/\sigma_0] = 1/m$ .)

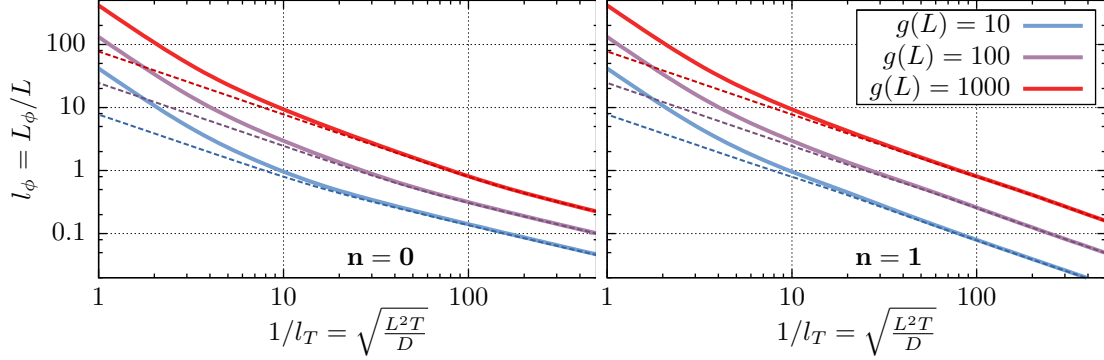


Figure 4.9: The dephasing length  $L_\phi$  calculated using quantum noise (solid lines) and classical noise (dotted lines) for several values of  $g(L)$  in units of the ring size  $L$  for  $n = 0$  and  $n = 1$ . We obtain a length that increases much faster with lower temperature, than previously predicted. The difference is most clear, when the thermal length gets comparable to the system size, i.e.  $l_T \approx 1$ .

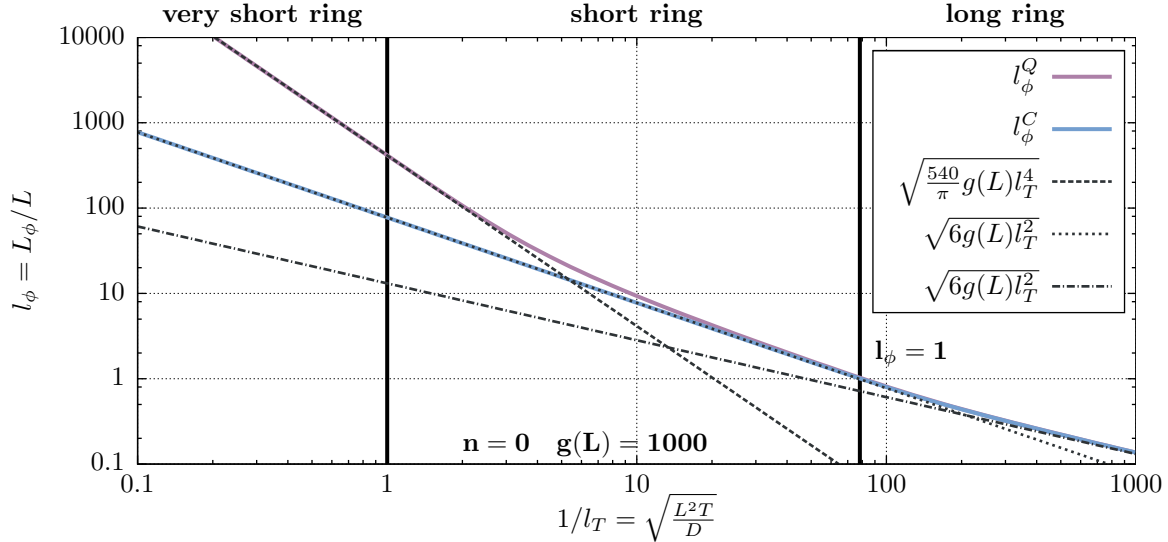


Figure 4.10: The relative dephasing length  $l_\phi = L_\phi/L$  for quantum noise (Q) and classical noise (C) for  $g(L) = 1000$  and  $n = 0$ . The three regimes and their corresponding asymptotic expressions, see table 4.1, have been included for comparison.

# Chapter 5

## Corrections to the conductivity

### 5.1 Weak localization correction to the conductivity in a quasi-1d ring

The total correction to the conductivity is given by (3.74):

$$\Delta\sigma = -\frac{2e^2D}{\pi} \sum_{n=-\infty}^{\infty} \int_0^{\infty} dt P_n(r, r, t) e^{-F_n(t)}. \quad (5.1)$$

where

$$F_n(t) = \frac{1}{2} \langle \phi^2 \rangle_{V, R_{t,n}} \quad (5.2)$$

is the Cooperon decay function, given by the phase difference of two time reversed random walks, averaged over electronic noise and random walks with winding number  $n$ , which we calculated for classical noise and quantum noise, including the Pauli principle, in the last two chapters.  $P_n(r, r, t)$  is given by (3.71):

$$P_n(r, r, t) = \frac{1}{\sqrt{4\pi Dt}} e^{-(nL)^2/4Dt} \quad (5.3)$$

and corresponds to the probability density of a random walk on the ring with winding number  $n$  to return to its origin at time  $t$ . We have to sum over all  $n$  and integrate over all times  $t$ , since all trajectories contribute.<sup>1</sup>

It is convenient to express this formula in terms of the relative length scales and the dimensionless conductance, defined in (3.90) and (3.91). Then we can write the corrections as

$$\Delta g(L) = \frac{\Delta\sigma}{e^2L} = -\frac{2}{\pi^{3/2}} \int_0^{\infty} dl_t \sum_{n=-\infty}^{\infty} e^{-(n/2l_t)^2} e^{-F_n(l_t, l_T, g(L))}. \quad (5.4)$$

---

<sup>1</sup>Taking into account all times in the integral, we automatically include trajectories which violate the condition  $Tt \gg 1$ . Thus, in the following, we have to make sure that the integral over  $t$  from 0 to  $1/T$  gives only a small contribution.

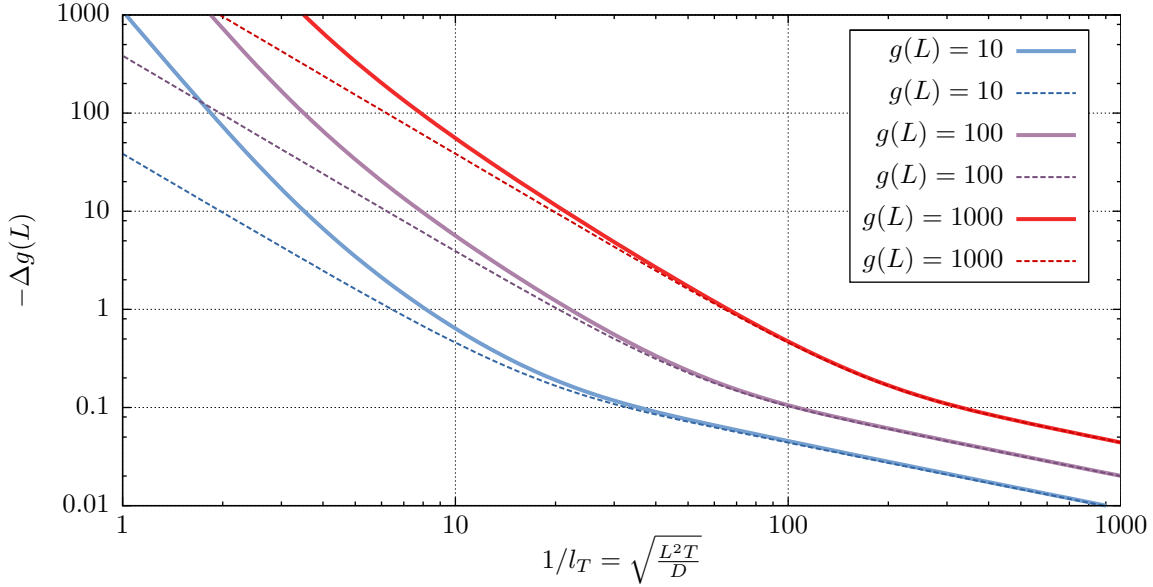


Figure 5.1: The full correction to the conductance without a magnetic field, given by (5.1) for different values of  $g(L)$ . Solid lines are calculated using quantum noise, dashed lines using classical noise.

Note that in the metallic regime, we always have  $g(L) \gg 1$ . Inserting into this formula our expressions  $F^C$  from (3.95) and  $F^Q$  from (4.11), and plotting against the inverse relative temperature length  $1/l_T \sim \sqrt{T}$ , we obtain figure 5.1. The difference between the classical and our improved treatment of electronic noise is clearly visible for low temperatures.

From the figure we identify again three regimes:

- The **long ring** regime: If  $l_\phi \ll 1$ , we have  $l_T \ll 1$ , see table 4.1. Trajectories  $l_t \ll 1$  contribute most to the conductance integral, here the  $n = 0$  mode is dominating, thus we obtain, using (C.9):

$$\begin{aligned}
 -\Delta g(L) &\approx \frac{2}{\pi^{3/2}} \int_0^\infty dl_t \exp\left(-\frac{1}{g(L)} \frac{\sqrt{\pi}}{4} \frac{l_t^3}{l_T^2}\right) \\
 &= \frac{4}{9} \sqrt{\frac{3}{\pi}} \frac{1}{\Gamma(2/3)} \sqrt[3]{g(L) \frac{4}{\sqrt{\pi}} l_T^2} \sim \sqrt[3]{g(L) l_T^2}.
 \end{aligned} \tag{5.5}$$

Note that since  $l_\phi = \sqrt[3]{g(L) l_T^2}$ , see table 4.1, this is equivalent to the known result:

$$-\Delta\sigma \sim e^2 L_\phi. \tag{5.6}$$

- The **short ring** regime: If  $l_\phi \gg 1$  and still  $l_T \ll 1$ , trajectories with  $l_t \gg 1$  dominate and we have to sum over all  $n$ , since higher modes are not neglectable any more. We

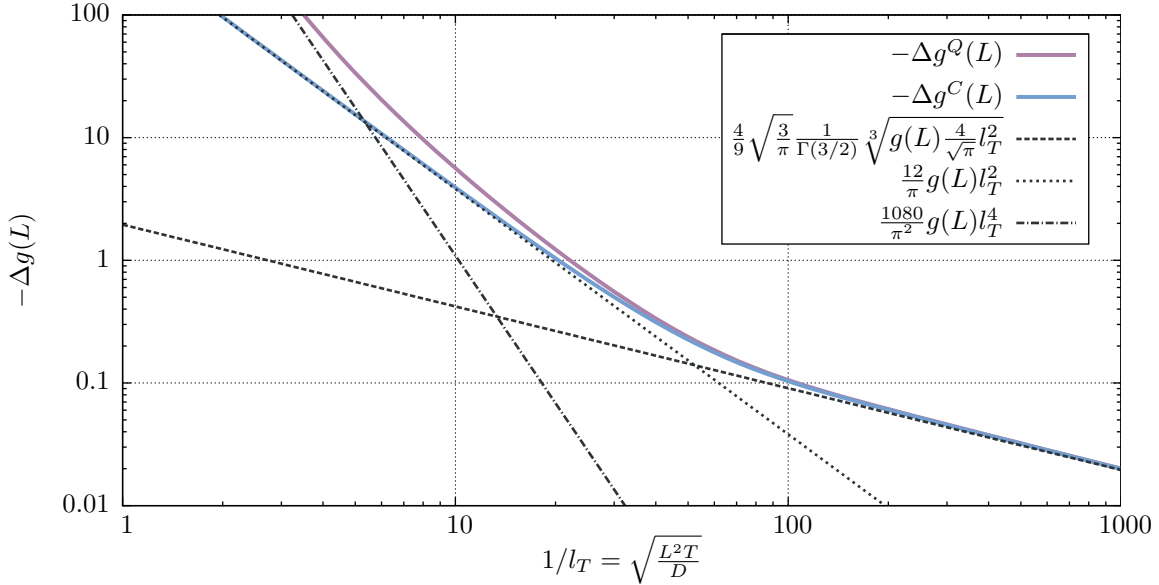


Figure 5.2: The full correction to the conductance for quantum noise (Q) and classical noise (C) without a magnetic field, given by (5.1) for  $g(L) = 100$ . Shown in comparison to the asymptotic expressions (5.5), (5.7) and (5.8). Already at  $l_T < 1$  the correction is larger than  $g(L)$  itself, thus, the very small ring regime cannot be reached.

obtain:

$$\begin{aligned}
 -\Delta g(L) &\approx \frac{2}{\pi^{3/2}} \int_0^\infty dl_t \sum_{n=-\infty}^\infty \exp\left(-\frac{n^2}{(2l_t)^2}\right) \exp\left(-\frac{1}{g(L)} \frac{1}{6} \frac{l_t^2}{l_T^2}\right) \\
 &= \frac{\sqrt{6g(L)l_T^2}}{\pi} \coth\left(\frac{1}{2\sqrt{6g(L)l_T^2}}\right) \sim g(L) l_T^2
 \end{aligned} \tag{5.7}$$

(The integral has been done using (C.10) and then the sum using (C.16).)

- The **very short ring** regime: If  $l_\phi \gg 1$  and  $l_T \gg 1$ , we obtain:

$$\begin{aligned}
 -\Delta g(L) &\approx \int_0^\infty dl_t \sum_{n=-\infty}^\infty \exp\left(-\frac{n^2}{2l_t^2}\right) \exp\left(-\frac{1}{g(L)} \frac{\pi}{540} \frac{l_t^2}{l_T^4}\right) \\
 &= \frac{\sqrt{540g(L)l_T^4}}{\pi^{3/2}} \coth\left(\frac{\sqrt{\pi}}{2\sqrt{540g(L)l_T^4}}\right) \sim g(L) l_T^4
 \end{aligned} \tag{5.8}$$

The 3 regimes are identified and compared to the asymptotic expressions in figure 5.2. We see that the absolute value of the corrections to the conductivity become larger than the conductivity itself, when we approach the quantum regime, i.e.  $l_T \ll 1$ , at low

temperatures. Indeed, from (5.7) or (5.8) we obtain:

$$\boxed{\frac{\Delta\sigma}{\sigma_0} \equiv \frac{\Delta g(L)}{g(L)} \ll 1 \quad \Rightarrow \quad l_T \ll 1}. \quad (5.9)$$

Requiring that the corrections stay small thus means that we cannot have a thermal length larger than the system length. Thus, the very short ring regime cannot be reached in a weak localization experiment.

Another way of understanding this is the following: In the long ring regime or, equivalently, the infinite system, the corrections can be written in the general form:

$$-\frac{\Delta\sigma}{\sigma_0} \sim \frac{1}{\rho_0} \int_0^\infty dt \frac{1}{\sqrt{Dt}} e^{-t/\tau_\phi} \sim \frac{1}{g(L_\phi)}, \quad (5.10)$$

since  $\rho_0 D \sim \sigma_0/e^2$ , see (1.3). Thus, a common requirement for the validity of weak-localization is

$$\boxed{g(L_\phi) \gg 1} \quad \text{for the infinite system.} \quad (5.11)$$

For the short (or very short) ring on the other hand we obtain:

$$\begin{aligned} \frac{\Delta\sigma}{\sigma_0} &= \sum_{n=-\infty}^{\infty} \frac{\Delta\sigma_n}{\sigma_0} \sim \sum_{n=-\infty}^{\infty} \frac{e^2 L}{\sigma_0} \int_0^\infty dt e^{\sim -(n/l_t)^2} e^{-(l_t/l_\phi)^2} \\ &\sim \frac{1}{g(L_\phi)} \sum_{n=0}^{\infty} \exp\left(-\frac{|n|}{l_\phi}\right), \end{aligned} \quad (5.12)$$

since we have to do the sum over all winding numbers here. We may thus require in analogy to the infinite system:

$$\boxed{g(L_\phi) \gg l_\phi = L_\phi/L} \quad \text{for the ergodic system,} \quad (5.13)$$

where the term ‘ergodic system’ stands for systems where the electron trajectories, on average, explore the system completely.

$g(L_\phi) = g(L)/l_\phi$  may now be obtained from the usual condition

$$F_n(l_\phi, l_T, g(L)) \equiv 1. \quad (5.14)$$

The results for this are summarized in table 5.1.

Plugging in the result for  $g(L_\phi)$  of the short or very short ring regimes into (5.14), we necessarily obtain  $l_T \gg 1$ , implying that the very short ring regime is incompatible with the condition that the corrections to the conductivity in the weak localization regime are small. Nevertheless, it may be expected that our new results may be of relevance for understanding the onset of the regime of strong localization, or the transition to a zero dimensional system. We will investigate these possibilities in the near future.

In this thesis we will now focus on possibilities how the small corrections in the long or short ring regime can be verified experimentally.

	Condition	Dominating decay function	$-\Delta g(L)$	$g(L_\phi)$
<b>long ring</b>	$l_\phi \ll 1, l_T \ll 1$	$F_n(t) \sim \frac{1}{g(L)} \frac{l_\phi^3}{l_T^2}$	$\sim \sqrt[3]{g(L)l_T^2}$	$l_\phi^2/l_T^2$
<b>short ring</b>	$l_\phi \gg 1, l_T \ll 1$	$F_n(t) \sim \frac{1}{g(L)} \frac{l_\phi^2}{l_T^2}$	$\sim g(L)l_T^2$	$l_\phi/l_T^2$
<b>very short ring</b>	$l_\phi \gg 1, l_T \gg 1$	$F_n(t) \sim \frac{1}{g(L)} \frac{l_\phi^2}{l_T^4}$	$\sim g(L)l_T^4$	$l_\phi/l_T^4$

Table 5.1: The 3 regimes of the conductance. The very short ring regime cannot be reached, since it would necessarily lead to  $\Delta g(L) > g(L)$ .

## 5.2 Magneto-conductance measurements

The most common method for extracting the weak localization correction from the total conductivity is to use magneto-conductance measurements, i.e. measuring the conductance against the magnetic field strength of an external field. Since the weak-localization correction is quickly destroyed by any mechanism that destroys the time reversal symmetry, the corrections will vanish for high enough magnetic fields and thus giving us the opportunity to subtract the constant background from the total conductance.

An external magnetic field enters our setup, described by equation (5.1), in two ways:

1. by destroying the phase coherence of the Cooperon and thus providing another infrared cutoff,

$$e^{-t/\tau_B}, \quad (5.15)$$

where  $\tau_B = 2/(DL_S^2 e^2 B^2)$  for a wire of circular cross section with radius  $L_S$ , for details, see [26]. (In fact, the Cooperon decay due to this effect is not exactly exponential, but can be well approximated by it, see Eq. (1.141) of [9] and the following discussion.)

2. by the flux of the magnetic field through the ring, i.e. the Aharonov-Bohm effect,

$$e^{in\theta} \quad (5.16)$$

where  $\theta = 4\pi\phi/\phi_0$  is the reduced flux ( $\phi_0 = 2\pi/e$ ). The reason for this is simple: If the vector potential is azimuthal to the wire and we assume that  $L_S \ll L$ , then it is constant inside the ring and we have no Lorentz force. Then the eikonal approximation becomes exact and the phase picked up by the Cooperon is simply given by  $2eB\pi L^2$  (The factor of 2 originates from the forward and backward path of the Cooperon and  $\pi L^2$  is the area penetrated by the flux.) The oscillations in the

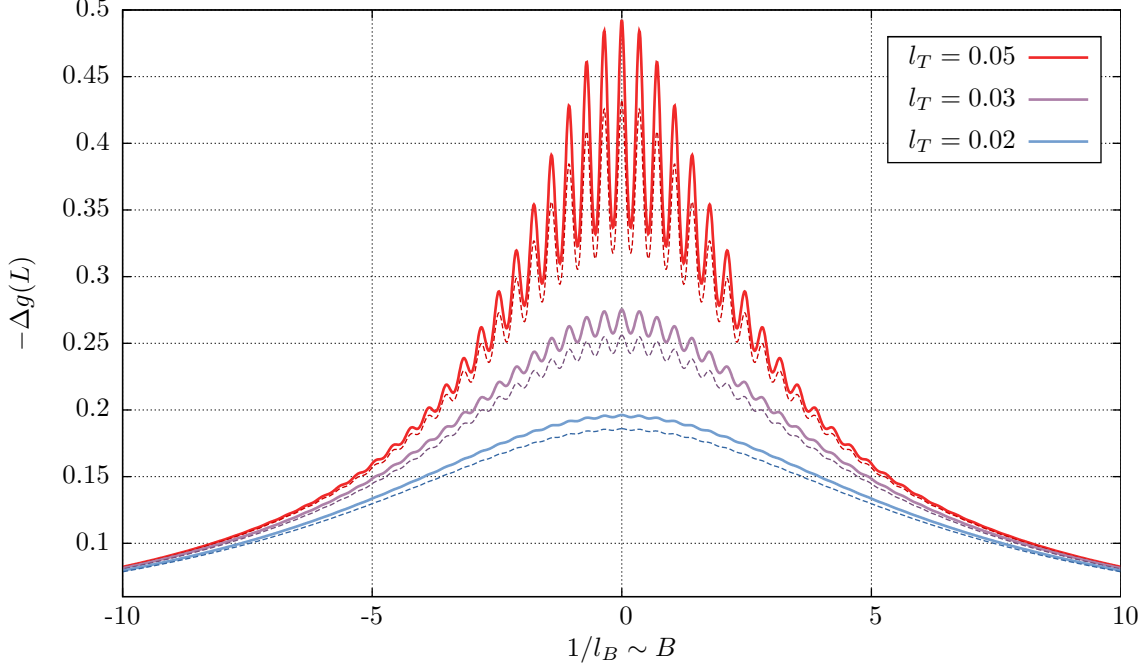


Figure 5.3: Plots of the dimensionless magneto-conductance for  $g(L) = 10$  and  $l_S = 0.5$ . Dotted lines are calculated using classical noise, solid lines using quantum noise.

conductivity due to this effect are known as Altshuler-Aharonov-Spivak oscillations, see [27].

We conclude that the conductivity correction in a magnetic field can be written as:

$$\Delta\sigma = -\frac{2e^2D}{\pi} \sum_{n=-\infty}^{\infty} \int_0^{\infty} dt P_n(r, r, t) e^{-F_n(t)} e^{-t/\tau_B} e^{in\theta}. \quad (5.17)$$

Using the dimensionless variables from (3.90) and (3.91) and introducing:

$$l_B = \frac{\sqrt{D\tau_B}}{L} \quad \text{and} \quad l_S = \frac{L_S}{L}, \quad (5.18)$$

we can write the correction to the dimensionless conductance, depending on a magnetic field ( $l_B \sim 1/B$ ), as:

$$\Delta g = \frac{\Delta\sigma}{e^2L} = -\frac{2}{\pi^{3/2}} \int_0^{\infty} dl_t \sum_{n=-\infty}^{\infty} e^{-(n/2l_t)^2} e^{-(l_t/l_B)^2} e^{-F_n(l_t)} \cos(2^{3/2}\pi n/l_B l_S). \quad (5.19)$$

This function is shown in figure 5.3, for reasonable parameters. One clearly observes the zero mode as the envelope of this function and the first mode as the visible oscillations.

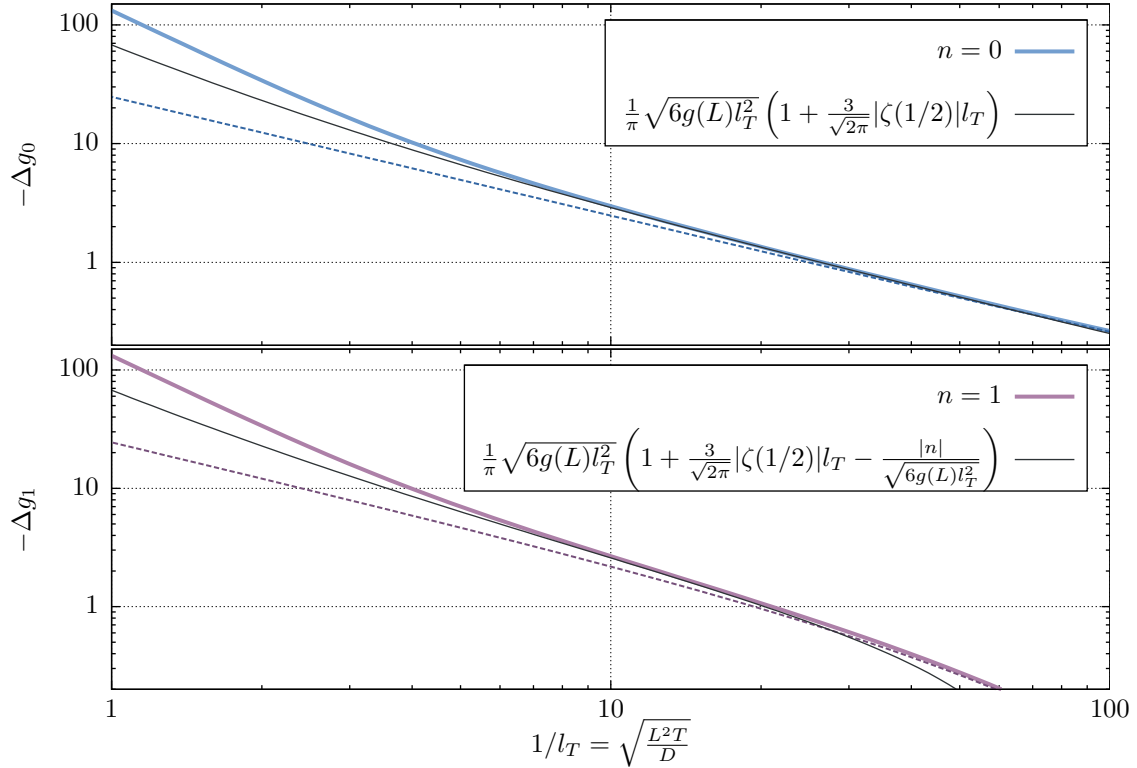


Figure 5.4: The  $n = 0$  and  $n = 1$  mode of the magneto-conductance in comparison to formula (5.21) and (5.22) for  $g(L) = 100$ . Dotted lines are calculated using classical noise, solid lines using quantum noise.

Higher modes give an exponentially smaller contribution to the corrections and are suppressed, as long as  $l_\phi$  is smaller than 1. For the opposite case  $l_\phi \gg 1$ , all winding numbers play a role. Using this setup, it might be possible to subtract the background and the envelope from the experimental data and obtain a curve only for one specific mode of the corrections.

### 5.3 Possible experimental realization

Since the regime of the very small ring is not experimentally accessible, we consider the first correction to the small ring regime, given by (4.27):

$$F_n^Q(t) = \frac{1}{g(L)} \frac{1}{6} \frac{l_t^2}{l_T^2} \left( 1 - \frac{6}{\sqrt{2\pi}} |\zeta(1/2)| l_T \right). \quad (5.20)$$

for all  $n$  and where we kept only the leading correction due to quantum noise, i.e. low temperature. Using magneto-conductance measurements we can now extract a specific winding number from the total conductance. In this regime the correction to the  $n = 0$

harmonic of the magneto-conductance is given from (5.4) by:

$$\begin{aligned} -\Delta g_0(L) &= \frac{1}{\pi} \sqrt{\frac{6g(L)l_T^2}{\left(1 - \frac{6}{\sqrt{2\pi}}|\zeta(1/2)|l_T\right)}} \\ &\approx \frac{1}{\pi} \sqrt{6g(L)l_T^2} \left(1 + \frac{3}{\sqrt{2\pi}}|\zeta(1/2)|l_T\right), \end{aligned} \quad (5.21)$$

while for the  $n > 0$  harmonics, we obtain:

$$\begin{aligned} -\Delta g_1(L) &\approx \frac{1}{\pi} \sqrt{6g(L)l_T^2} \left(1 + \frac{3}{\sqrt{2\pi}}|\zeta(1/2)|l_T\right) \exp\left(-|n| \sqrt{\frac{\left(1 + \frac{3}{\sqrt{2\pi}}|\zeta(1/2)|l_T\right)}{6g(L)l_T^2}}\right) \\ &\approx \frac{1}{\pi} \sqrt{6g(L)l_T^2} \left(1 + \frac{3}{\sqrt{2\pi}}|\zeta(1/2)|l_T - \frac{|n|}{\sqrt{6g(L)l_T^2}}\right). \end{aligned} \quad (5.22)$$

A comparison of these results to a numerical evaluation is given in figure 5.4.

To first order, the corrections are the same for all modes  $n$  individually. The prefactor of this correction is given by  $\frac{3}{\sqrt{2\pi}}|\zeta(1/2)| \approx 1.75$ . We see that the relative correction of the conductance is here directly proportional to  $l_T$ , which is the ratio of the thermal length to the system size. This should be checked experimentally for a ring, where electron trajectories explore the system completely, which requires a relatively small size and low temperatures. Note though that until now, we considered only an isolated ring, which obviously does not correspond to a real transport experiment.

### 5.3.1 The effect of connecting wires

To carry out a transport experiment with a metallic ring, we have to connect the ring to wires, through which a current can be injected. Even classically, the conductance of the whole system becomes here non-local and has to be obtained from Kirchhoff laws. The Cooperon must then be weighted properly in the conductance integral over all possible trajectories, see [3].

But more importantly, the Cooperon is itself a non-local object, which depends on the geometry of the system. In particular, the spatial dependence of the correlator for electron-electron interactions, (3.47), is modified and does not obey the convenient symmetry properties of a ring any more, which lead us to our results in chapter 3.7.

In the regime where we expect large corrections due to quantum noise, i.e. for a very small ring, where the decoherence length is larger than the system size, we expect the connected wires to strongly affect our previous results. A detailed calculation of the corrections in this case seems difficult.

However, there is the possibility of connecting a very small ring to leads via tunneling contacts. Then, as long as the dwelling time  $\tau_d$  (i.e. the inverse tunneling probability



Figure 5.5: Some orbits contributing to the magneto-conductance in a grid. Left: Contributing to the first harmonic, Right: Contributing to the second harmonic. (Taken from [28])

per time) in the ring is much larger than the decoherence time, a measurement of the decoherence length in the regimes where quantum noise plays an important role might be possible. We will study this setup in more detail elsewhere.

### 5.3.2 Recent experiments in a grid

Ferrier et al. describe in [28] a method to extract the decoherence length  $L_\phi$  from the magneto-conductance oscillations of a grid fabricated from a GaAs/GaAlAs 2D electron gas (2DEG). In such a grid setup, different kinds of electron trajectories contribute to weak localization, but since the frequency of the oscillations of the conductance depends on the area enclosed by the trajectories, only specific classes of trajectories correspond to each Fourier mode of the corrections, see for example figure 5.5. Still, the contribution of this classes of trajectories add up in a non-trivial way and a detailed analysis of their results would go beyond the scope of this thesis.

In [22] these authors were able to measure for the first time a geometrical dependence of the decoherence length  $L_\phi$  in this setup. They looked at the oscillating part of the magneto-conductance, i.e. modes  $n > 0$  and extracted  $L_\phi$  for different temperatures. When the temperature was *high* enough, so that  $L_\phi \lesssim L$ , where  $L$  is the circumference of a grid cell, they obtained a temperature dependence of the form

$$L_\phi \sim T^{-1/2}. \quad (5.23)$$

In this regime the trajectories are on average shorter than the circumference of a grid cell, thus the oscillating part of the conductance will be dominated by trajectories which enclose one grid cell exactly once, corresponding to a well-defined ring, thus, this corresponds to the long ring regime and  $n = 1$ , see table 4.1.

For *lower* temperatures, the behavior they obtained for the oscillating part was similar to the long ring regime with  $n = 0$ :

$$L_\phi \sim T^{-1/3}. \quad (5.24)$$

We assume, that this is due to the fact, that trajectories with large tails (e.g. the second trajectory of 5.5) dominate the decoherence and thus the result is equivalent to an infinite wire here.

For both of these cases we have shown that our improved treatment of the electronic noise leads only to small corrections to the decoherence length. We thus conclude that magneto-conductance measurements in a grid are unsuitable to demonstrate variations due to quantum noise.

# Chapter 6

## Conclusions

We calculated in detail the decoherence of the Cooperon by electron-electron interactions in a disordered quasi one dimensional metallic ring in all relevant regimes including first order correction terms. The results have been summarized in table 4.1. We were able to confirm the results of Ludwig and Mirlin [2] for a ring in the case of classical noise and Marquardt and von Delft [4] for an infinite wire in the case of quantum noise and bring them together.

Using our improved treatment of electronic noise, we could show that previous calculations should be modified at low temperatures and small system sizes. When the thermal length approaches the ring size, new quantum corrections to the Cooperon decay function have to be taken into account. It should be noted that these corrections cannot dominate without leaving the regime of weak localization (that is the regime of validity of our theory).

An interesting challenge for future work consists in devising experimental setups where these corrections are significant enough to be observed.



# Appendix A

## Asymptotic evaluation of the Cooperon decay function

### A.1 Classical noise

The Cooperon decay function for classical noise is given by (3.95):

$$F_n^C(t) = \frac{1}{g(L)} \frac{l_t^2}{l_T^2} \left[ \frac{1}{6} - \int_0^1 dx \left( \sum_{k=1}^{\infty} \frac{\cos(2\pi knx)}{(k\pi)^2} e^{-(\pi k)^2 (2l_t)^2 x(1-x)} \right) \right]. \quad (\text{A.1})$$

$l_t$  and  $n$  are the only parameters modifying the form of this function.

#### A.1.1 The long ring $l_t \ll 1$ :

$n = 0$  mode:

In (A.1), we can expand the second term using (C.19) and then do the integral over  $x$  using (C.3) and obtain:

$$F_{n=0}^C(t)_{l_t \ll 1} = \frac{1}{g(L)} \frac{\sqrt{\pi} l_t^3}{4 l_T^2} \left( 1 - \frac{4l_t}{3\sqrt{\pi}} \right). \quad (\text{A.2})$$

$n > 0$  modes:

Here we can simply expand the exponential in the second term since the sum converges for  $k \sim 1$ . Then the first term of the expansion vanishes, because the  $x$  integral is over  $n$  full periods of cosine. For the next term we can use the delta representation of the infinite sum over cosine in the form (C.14) and obtain:

$$F_{n>0}^C(t)_{l_t \ll 1} = \frac{1}{g(L)} \frac{1}{6} \frac{l_t^2}{l_T^2} \left( 1 - 2l_t^2 \left( 1 - \frac{6}{n} \sum_{k=1}^n \left( \frac{k}{n} - \frac{k^2}{n^2} \right) \right) \right). \quad (\text{A.3})$$

The sum can be done using (C.11) and (C.12). We obtain:

$$\boxed{F_{n>0}^C(t)_{l_t \ll 1} = \frac{1}{g(L)} \frac{1}{6} \frac{l_t^2}{l_T^2} \left( 1 - 2 \frac{l_t^2}{n^2} \right)}. \quad (\text{A.4})$$

### A.1.2 The short ring $1 \ll l_t$ :

$n = 0$  mode:

Here, we do the integral over  $x$  using (C.4) and then use the asymptotic expansion (C.17) and obtain:

$$\boxed{F_{n=0}^C(t)_{1 \ll l_t} = \frac{1}{g(L)} \frac{1}{6} \frac{l_t^2}{l_T^2} \left( 1 - \frac{1}{30l_t^2} \right)}. \quad (\text{A.5})$$

$n > 0$  modes:

Since  $l_t \gg 1$ , the exponential function will be non-negligibly small only for  $x \lesssim 1/l_t^2 \ll 1/2$ , thus we can replace  $x(1-x)$  by  $x$  in the exponent, extend the integral to  $\infty$  and scale by the factor  $k\pi$ :

$$F_{n>0}^C(t)_{1 \ll l_t} = \frac{1}{g(L)} \frac{1}{6} \frac{l_t^2}{l_T^2} \left[ 1 - 12 \int_0^\infty dx \sum_{k=1}^\infty \frac{\cos(2nx)}{(k\pi)^3} e^{-(k\pi)(2l_t)^2 x} \right]. \quad (\text{A.6})$$

Now, we can do the integral over  $x$  using (C.6) and then the sum over  $k$  using (C.15):

$$F_{n>0}^C(t)_{1 \ll l_t} = \frac{1}{g(L)} \frac{1}{6} \frac{l_t^2}{l_T^2} \left[ 1 - \frac{2l_t^4}{n^4} \left( \frac{n^2}{l_t^2} + 12l_t^2 - 6n \coth \left( \frac{n}{2l_t^2} \right) \right) \right]. \quad (\text{A.7})$$

For  $n \ll 2l_t^2$  we can expand  $\coth(x) = 1/x + x/3 - x^3/45$  to third order and obtain

$$\boxed{F_{2l_t^2 \gg n > 0}^C(t)_{1 \ll l_t} = \frac{1}{g(L)} \frac{1}{6} \frac{l_t^2}{l_T^2} \left( 1 - \frac{1}{30l_t^2} \right)}, \quad (\text{A.8})$$

independent of  $n$  and in agreement with (A.5). In the opposite case,  $n \gg 2l_t^2$ , we replace  $\coth$  by 1 and obtain

$$F_{n \gg 2l_t^2}^C(t)_{1 \ll l_t} = \frac{1}{g(L)} \frac{1}{6} \frac{l_t^2}{l_T^2} \left( 1 - 2 \frac{l_t^2}{n^2} \right). \quad (\text{A.9})$$

Since large winding numbers are not accessible to the experimentalist anyways, this small correction is of no physical relevance.

## A.2 Quantum noise

The Cooperon decay function for quantum noise is given by (4.15):

$$F^Q(t) = -\frac{1}{g(L)} \frac{l_t^2}{l_T^2} \int_0^1 dx \tilde{z}_Q(x) \left( \sum_{k=1}^{\infty} \frac{\cos(2\pi knx)}{(k\pi)^2} e^{-(\pi k)^2 (2l_t)^2 x(1-x)} \right), \quad (\text{A.10})$$

where  $\tilde{z}_Q(x)$  is given by (D.7).  $F^Q(t)$  depends on  $l_T$ ,  $l_t$  and  $n$  non-trivially.

### A.2.1 The long ring $l_T \ll l_t \ll 1$

$n = 0$  mode:

Since  $l_t \ll 1$ , we can use (C.19) to expand the sum. The first order in the expansion vanishes because of (D.12)). The leading term from third order is given by the first correction term of the classical result, see (A.2). Altogether, we obtain:

$$F_{n=0}^Q(t)_{l_T \ll l_t \ll 1} = \frac{1}{g(L)} \frac{2}{\sqrt{\pi}} \frac{l_t^3}{l_T^2} \left[ \int_0^1 dx \tilde{z}(x) \sqrt{x(1-x)} - \frac{\sqrt{\pi}}{6} l_t + \mathcal{O}\left(\frac{l_T^2}{l_t}\right) \right]. \quad (\text{A.11})$$

Now, we may write  $\tilde{z}(x) = (\tilde{z}(x) - 1) + 1$ . Then, the +1 term can be evaluated using (C.3). For the  $\tilde{z} - 1$  term we can expand  $\sqrt{x(1-x)} \approx (x^{1/2} - x^{3/2}/2)$  since the integrand is non-negligible only for  $x \lesssim 1/\alpha = \pi l_T^2/l_t^2 \ll 1$ :

$$F_{n=0}^Q(t)_{l_T \ll l_t \ll 1} = \frac{1}{g(L)} \frac{l_t^3}{l_T^2} \left[ \frac{\sqrt{\pi}}{4} + \frac{2}{\sqrt{\pi}} \int_0^1 dx [\tilde{z}(x) - 1] (x^{1/2} - x^{3/2}/2) - \frac{1}{3} l_t + \mathcal{O}\left(\frac{l_T^2}{l_t}\right) \right]. \quad (\text{A.12})$$

The second integral can now be evaluated using (D.11):

$$F_{n=0}^Q(t)_{l_T \ll l_t \ll 1} = \frac{1}{g(L)} \frac{\sqrt{\pi}}{4} \frac{l_t^3}{l_T^2} \left( 1 - \frac{2^{3/2}}{\pi} |\zeta(1/2)| \frac{l_T}{l_t} - \frac{4}{3\sqrt{\pi}} l_t - \mathcal{O}\left(\frac{l_T^3}{l_t^3}\right) + \mathcal{O}\left(\frac{l_T^2}{l_t}\right) \right). \quad (\text{A.13})$$

The leading result is given by:

$$\boxed{F_{n=0}^Q(t)_{l_T \ll l_t \ll 1} = \frac{1}{g(L)} \frac{\sqrt{\pi}}{4} \frac{l_t^3}{l_T^2} \left( 1 - \frac{2^{3/2}}{\pi} |\zeta(1/2)| \frac{l_T}{l_t} - \frac{4}{3\sqrt{\pi}} l_t \right)}. \quad (\text{A.14})$$

$n > 0$  modes:

We use the same trick as in the last chapter and write  $\tilde{z}(x) = (\tilde{z}(x) - 1) + 1$ . The integral over the +1 term has already been calculated for classical noise, see (A.4). In the  $\tilde{z}(x) - 1$  term we can replace the upper border of integration by  $1/n$ , assuming  $n \ll l_t^2/l_T^2$ . The

contribution from modes  $n$  larger than this will be negligibly small since  $l_t^2/l_T^2 \gg 1$ . Now we expand  $\exp(-x) \approx 1 - x$  and obtain:

$$F_{n>0}^Q(t)_{l_T \ll l_t \ll 1} = -\frac{1}{g(L)} \frac{l_t^2}{l_T^2} \int_0^{1/n} dx [\tilde{z}_Q(x) - 1] \left( \sum_{k=1}^{\infty} \frac{\cos(2\pi knx)}{(k\pi)^2} (1 - (\pi k)^2 (2l_t)^2 x(1-x)) \right) - \frac{1}{g(L)} \frac{1}{6} \frac{l_t^2}{l_T^2} \left( 2 \frac{l_t^2}{n^2} \right). \quad (\text{A.15})$$

For the first term of the expansion, we can do the sum over  $k$  using (C.13) while for the second we use (C.14) and observe that the integral over the delta functions vanishes. Thus we are left with:

$$F_{n>0}^Q(t)_{l_T \ll l_t \ll 1} = -\frac{1}{g(L)} \frac{l_t^2}{l_T^2} \int_0^{1/n} dx [\tilde{z}(x) - 1] (1/6 - nx + n^2 x^2) - \frac{2}{g(L)} \frac{l_t^4}{l_T^2} \int_0^1 dx [\tilde{z}(x) - 1] (x - x^2) - \frac{1}{g(L)} \frac{1}{6} \frac{l_t^2}{l_T^2} \left( 2 \frac{l_t^2}{n^2} \right). \quad (\text{A.16})$$

Now we use (D.11):

$$F_{n>0}^Q(t)_{l_T \ll l_t \ll 1} = \frac{1}{g(L)} \frac{1}{6} \frac{l_t^2}{l_T^2} \left( 1 - \frac{6}{\pi} \frac{n l_T^2}{l_t^2} + \mathcal{O}\left(\frac{n^2 l_T^4}{l_t^4}\right) \right) - \frac{1}{g(L)} \frac{2}{\pi} \frac{l_t^4}{l_T^2} \left( \frac{l_T^2}{l_t^2} - \mathcal{O}\left(\frac{l_T^4}{l_t^4}\right) \right) - \frac{1}{g(L)} \frac{1}{6} \frac{l_t^2}{l_T^2} \left( 2 \frac{l_t^2}{n^2} \right). \quad (\text{A.17})$$

Finally, we obtain:

$$F_{n>0}^Q(t)_{l_T \ll l_t \ll 1} = \frac{1}{g(L)} \frac{1}{6} \frac{l_t^2}{l_T^2} \left( 1 - \frac{6}{\pi} \frac{n l_T^2}{l_t^2} - 2 \frac{l_t^2}{n^2} - \frac{12}{\pi} \frac{l_T^2}{l_t^2} \right). \quad (\text{A.18})$$

### A.2.2 The short ring $l_T \ll 1 \ll l_t$

$n = 0$  mode:

Like in the previous section, we write  $\tilde{z}_Q(x) = (\tilde{z}_Q(x) - 1) + 1$  and obtain:

$$F_{n=0}^Q(t)_{l_T \ll 1 \ll l_t} = -\frac{1}{g(L)} \frac{l_t^2}{l_T^2} \int_0^1 dx [\tilde{z}_Q(x) - 1] \sum_{k=1}^{\infty} \frac{1}{(k\pi)^2} e^{-(k\pi)^2 (2l_t)^2 x(1-x)} - \frac{1}{g(L)} \frac{1}{6} \frac{l_t^2}{l_T^2} \left( \frac{1}{30} \frac{1}{l_t^2} \right), \quad (\text{A.19})$$

where we used the classical result for the +1 term, see (A.5). Now we can use the fact that  $l_t^2/l_T^2 \gg l_t^2$ , thus we can again use (C.19) to second order:

$$F_{n=0}^Q(t)_{l_T \ll 1 \ll l_t} = \frac{1}{g(L)} \frac{1}{6} \frac{l_t^2}{l_T^2} + \frac{1}{g(L)} \frac{2}{\sqrt{\pi}} \frac{l_t^3}{l_T^2} \int_0^1 dx [\tilde{z}_Q(x) - 1] \sqrt{x-x^2} - \frac{1}{g(L)} \frac{1}{6} \frac{l_t^2}{l_T^2} \left( \frac{1}{30} \frac{1}{l_t^2} \right). \quad (\text{A.20})$$

The remaining integral can be evaluated using (D.11) and we obtain:

$$F_{n=0}^Q(t)_{l_T \ll 1 \ll l_t} = \frac{1}{g(L)} \frac{1}{6} \frac{l_t^2}{l_T^2} \left( 1 - \frac{6}{\sqrt{2\pi}} |\zeta(1/2)| l_T - \frac{1}{30} \frac{1}{l_t^2} - \mathcal{O}\left(\frac{l_T^3}{l_t^2}\right) \right). \quad (\text{A.21})$$

The leading term is given by:

$$\boxed{F_{n=0}^Q(t)_{l_T \ll 1 \ll l_t} = \frac{1}{g(L)} \frac{1}{6} \frac{l_t^2}{l_T^2} \left( 1 - \frac{6}{\sqrt{2\pi}} |\zeta(1/2)| l_T - \frac{1}{30} \frac{1}{l_t^2} \right)}. \quad (\text{A.22})$$

**$n > 0$  modes:**

Using the same arguments as in the previous section, we obtain

$$F_{n>0}^Q(t)_{l_T \ll 1 \ll l_t} = -\frac{1}{g(L)} \frac{l_t^2}{l_T^2} \int_0^1 dx [\tilde{z}_Q(x) - 1] \sum_{k=1}^{\infty} \frac{\cos(2\pi k n x)}{(k\pi)^2} e^{-(k\pi)^2 (2l_t)^2 x(1-x)} - \frac{1}{g(L)} \frac{1}{6} \frac{l_t^2}{l_T^2} \left( \frac{1}{30} \frac{1}{l_t^2} \right), \quad (\text{A.23})$$

where we assumed  $n < 2l_t^2$  for the last term, see (A.6). In the remaining integral, as long as  $n < l_t^2$ , the argument of cosine is the smallest, thus we expand and then use (C.18) and (C.19):

$$F_{n>0}^Q(t)_{l_T \ll 1 \ll l_t} = -\frac{1}{g(L)} \frac{l_t^2}{l_T^2} \int_0^1 dx [\tilde{z}_Q(x) - 1] \left( \frac{1}{6} - \frac{2l_t}{\sqrt{\pi}} \sqrt{x(1-x)} + 2l_t^2 x(1-x) \right) - \frac{1}{g(L)} \frac{l_t^2}{l_T^2} \int_0^1 dx [\tilde{z}_Q(x) - 1] \left( \frac{n^2 x^2}{l_t \sqrt{\pi} \sqrt{x(1-x)}} \right) - \frac{1}{g(L)} \frac{1}{6} \frac{l_t^2}{l_T^2} \left( \frac{1}{30} \frac{1}{l_t^2} \right). \quad (\text{A.24})$$

Selecting the largest terms using (D.11), we obtain:

$$F_{n>0}^Q(t)_{l_T \ll 1 \ll l_t} = \frac{1}{g(L)} \frac{1}{6} \frac{l_t^2}{l_T^2} \left( 1 - \frac{1}{30} \frac{1}{l_t^2} - \frac{6}{\sqrt{2\pi}} |\zeta(1/2)| l_T + \mathcal{O}(l_T^2) - \mathcal{O}\left(\frac{n^2 l_T^3}{l_t^4}\right) \right). \quad (\text{A.25})$$

The dependence on  $n$  is very weak, thus we have the same results as for the  $n = 0$  mode, (A.22):

$$F_{n>0}^Q(t)_{l_T \ll 1 \ll l_t} = \frac{1}{g(L)} \frac{1}{6} \frac{l_t^2}{l_T^2} \left( 1 - \frac{6}{\sqrt{2\pi}} |\zeta(1/2)| l_T - \frac{1}{30} \frac{1}{l_t^2} \right). \quad (\text{A.26})$$

### A.2.3 The very short ring $1 \ll l_T \ll l_t$

Here we can calculate all modes at the same time. The exponential function is much more strongly peaked than  $\tilde{z}_C$ , thus we can Taylor expand  $\tilde{z}_C$  and the argument of the exponential, change the upper boundary of the integral to  $\infty$  and scale by a factor of  $k\pi$ :

$$F_n^Q(t)_{l_t \gg l_T \gg 1} = \frac{1}{g(L)} \frac{l_t^2}{l_T^2} \int_0^\infty dx \left[ \frac{2\pi l_t^2}{3l_T^2} - 1 \right] \sum_{k=1}^\infty \frac{\cos(2nx)}{(k\pi)^3} e^{-(k\pi)(2l_t)^2 x}. \quad (\text{A.27})$$

Now, we can do the integral over  $x$ , using (C.6) and then evaluate the sum, using (C.15):

$$F_n^Q(t)_{l_t \gg l_T \gg 1} = \frac{1}{g(L)} \frac{l_t^2}{l_T^2} \left[ \frac{2\pi l_t^2}{3l_T^2} - 1 \right] \left( \frac{l_t^4}{6n^4} \left( \frac{n^2}{l_t^2} + 12l_t^2 - 6n \coth\left(\frac{n}{2l_t^2}\right) \right) \right), \quad (\text{A.28})$$

just like in (A.7). As long as  $n \ll 2l_t^2$ , we obtain, independent of  $n$ :

$$F_n^Q(t)_{1 \ll l_T \ll l_t} = \frac{1}{g(L)} \frac{l_t^2}{l_T^4} \frac{\pi}{540} \left( 1 - \frac{3}{2\pi} \frac{l_T^2}{l_t^2} \right). \quad (\text{A.29})$$

# Appendix B

## Comments on the numerical evaluation of the Cooperon decay function

The full Cooperon decay function is given by:

$$F(t) = -\frac{1}{g(L)} \frac{l_t^2}{l_T^2} \int_0^1 dx z(x) \left( \sum_{k=1}^{\infty} \frac{\cos(2\pi knx)}{(k\pi)^2} e^{-(\pi k)^2 (2l_t)^2 x(1-x)} \right). \quad (\text{B.1})$$

A direct numerical evaluation of the integral and the sum is difficult, because  $z(x)$  is peaked at the borders of integration and not negligible in-between.

Instead, it is easy to show that (B.1) can be written in the form

$$F(t) = \frac{1}{g(L)} \frac{l_t}{l_T^2} \sum_{k=1}^{\infty} \left[ \frac{1}{(k\pi)^3} \frac{\sqrt{\pi}}{2} \text{Im} \left[ w \left( \frac{n}{2l_t} + i\pi k l_t \right) \right] + \frac{l_t}{(k\pi)^2} q(l_t, l_T, k, n) \right] \quad (\text{B.2})$$

where  $w(z)$  is the complex error function, also known as the Faddeeva function, defined by

$$w(z) = e^{-z^2} \text{erfc}(-iz). \quad (\text{B.3})$$

Several algorithms for a fast evaluation of this function exist. In this thesis a modified version from the Matpack library <sup>1</sup> has been used, which is freely available under the GNU Public License (GPL) <sup>2</sup>.

The function  $q$  is equal to 1 for classical noise and for quantum noise we obtain:

$$q(l_t, l_T, k, n) = - \int_0^1 dx (\tilde{z}_Q(x) - 1) \cos(2\pi kn) e^{-(\pi k)^2 (2l_t)^2 x(1-x)}. \quad (\text{B.4})$$

---

<sup>1</sup><http://users.physik.tu-muenchen.de/gammel/matpack/>

<sup>2</sup><http://www.gnu.org/licenses/old-licenses/gpl-2.0.txt>

## **72 B. Comments on the numerical evaluation of the Cooperon decay function**

Since  $(\tilde{z}_Q(x) - 1)$  is strongly peaked around zero, the integral can be cut appropriately, then the integrand is smooth and can be evaluated numerically without any problems. In this thesis the integration algorithm QAWO from the GNU Scientific Library <sup>3</sup> has been used, which is also freely available under the GPL.

After integration, the sum over  $k$  can be done straightforwardly and cut when the desired precision has been reached.

---

<sup>3</sup><http://www.gnu.org/software/gsl/>

# Appendix C

## Mathematical Formulas

### C.1 Table of integrals and sums

$$\sum_{n=-\infty}^{\infty} f(n) = \sum_{m=-\infty}^{\infty} \int_{-\infty}^{\infty} dy f(y) e^{2\pi i m y}. \quad (\text{C.1})$$

$$\int_{-\infty}^{\infty} dy \cos(2\pi k y) e^{-\alpha y^2} = \sqrt{\frac{\pi}{\alpha}} e^{-k^2 \pi^2 / \alpha} \quad (\text{C.2})$$

$$\int_0^1 dx \sqrt{x(1-x)} = \frac{\pi}{8} \quad (\text{C.3})$$

$$\int_0^1 dx e^{-\alpha^2 x(1-x)} = \frac{\sqrt{\pi}}{\alpha} e^{-(\frac{\alpha}{2})^2} \operatorname{erfi}\left(\frac{\alpha}{2}\right) \quad (\text{C.4})$$

$$\int_0^1 dx x^2 e^{-\alpha^2 x(1-x)} = \frac{1}{2} \frac{1}{\alpha^2} + \frac{\sqrt{\pi}}{4} \frac{1}{\alpha} e^{-(\frac{\alpha}{2})^2} \operatorname{erfi}\left(\frac{\alpha}{2}\right) - \frac{\sqrt{\pi}}{2} \frac{1}{\alpha^3} e^{-(\frac{\alpha}{2})^2} \operatorname{erfi}\left(\frac{\alpha}{2}\right) \quad (\text{C.5})$$

$$\int_0^{\infty} dx \cos(\alpha x) e^{-\beta x} = \frac{\beta}{\beta^2 + \alpha^2} \quad (\text{C.6})$$

$$\int_0^{\infty} \frac{x \coth(x) - 1}{\sinh(x)^2} x^s = \begin{cases} 1/2 & s = 0 \\ \frac{\sqrt{2\pi}}{8} |\zeta(1/2)| & s = 1/2 \\ 1/2 & s = 1 \\ \pi^2/12 & s = 2 \end{cases} \quad (\text{C.7})$$

$$\int_0^{\infty} dx \frac{1}{\sqrt{x}} e^{-\alpha x - \beta/x} = \sqrt{\frac{\pi}{\alpha}} e^{-2\sqrt{\alpha\beta}} \quad (\text{C.8})$$

$$\int_0^{\infty} dx e^{-\alpha x^3} = \frac{2\sqrt{3}\pi}{\sqrt[3]{\alpha} \Gamma(2/3)} \quad (\text{C.9})$$

$$\int_0^{\infty} dx e^{-\alpha/x^2 - \beta x^2} = \frac{1}{2} \sqrt{\frac{\pi}{\alpha}} \exp\left(-2\sqrt{\alpha\beta}\right) \quad (\text{C.10})$$

$$\sum_{k=1}^n k = \frac{n(n+1)}{2} \quad (\text{C.11})$$

$$\sum_{k=1}^n k^2 = \frac{n(n+1)(2n+1)}{6} \quad (\text{C.12})$$

$$\sum_{k=1}^{\infty} \frac{\cos(2\pi kx)}{(k\pi)^2} = \frac{1}{6} - x + x^2 \quad x \in [0, 1] \quad (\text{C.13})$$

$$\sum_{k=1}^{\infty} \cos(2\pi kx) = \frac{1}{2} (\delta(x+m) - 1) \quad m \in \mathbb{Z} \quad (\text{C.14})$$

$$\sum_{k=1}^{\infty} \frac{1}{(k\pi)^2} \frac{1}{\alpha^2 (k\pi)^2 + \beta^2} = \frac{3\alpha^2 + \beta^2 - 3\alpha\beta \coth(\beta/\alpha)}{6\beta^4} \quad (\text{C.15})$$

$$\sum_{k=1}^{\infty} e^{-\alpha k} = \frac{1}{e^{\alpha} - 1} \quad (\text{C.16})$$

## C.2 Asymptotic expansions

$$e^{-x^2} \operatorname{erfi}(x) \approx \frac{1}{\sqrt{\pi x}} \quad x \gg 1 \quad (\text{C.17})$$

$$\sum_{k=1}^{\infty} e^{-k^2 \pi x} \approx \frac{1}{2\sqrt{x}} - \frac{1}{2} \quad x \ll 1 \quad (\text{C.18})$$

with exponential accuracy, see [29]; and by integration, we also have:

$$\sum_{k=1}^{\infty} \frac{1}{(k\pi)^2} e^{-k^2 \pi x} \approx \frac{1}{6} - \frac{\sqrt{x}}{\pi} + \frac{x}{2\pi} \quad x \ll 1 \quad (\text{C.19})$$



# Appendix D

## Special functions

### D.1 The function $\tilde{\Omega}(x)$

The function  $\Omega(x)$  is given by:

$$\Omega(x) = x(1-x)^2 \quad x \in [0, 1]. \quad (\text{D.1})$$

Now, we define

$$\tilde{\Omega}(x) = \Omega(\tilde{x}), \quad x = \tilde{x} + k \in \mathbb{R}, \quad (\text{D.2})$$

where  $k \in \mathbb{Z}$  is chosen such that always  $\tilde{x} \in [0, 1]$ , making it a periodic function for all  $x \in \mathbb{R}$ . The function is shown in Figure D.1. Note that for small  $x$ , we have:

$$\tilde{\Omega}(x) = x\theta(x) \quad x \ll 1 \quad (\text{D.3})$$

and that its average value is given by:

$$\int_0^1 \tilde{\Omega}(x) dx = \frac{1}{12}. \quad (\text{D.4})$$

Because of  $\tilde{\Omega}$ 's periodicity, we may use the discrete Fourier transform:

$$\tilde{\Omega}(k) = \int_0^1 dx \tilde{\Omega}(x) e^{2\pi i k x} \quad (\text{D.5})$$

to write it as a sum:

$$\tilde{\Omega}(x) = \frac{1}{12} - \frac{1}{2} \sum_{k=1}^{\infty} \frac{3 \sin(2\pi k x) + \pi k \cos(2\pi k x)}{(k\pi)^3}. \quad (\text{D.6})$$

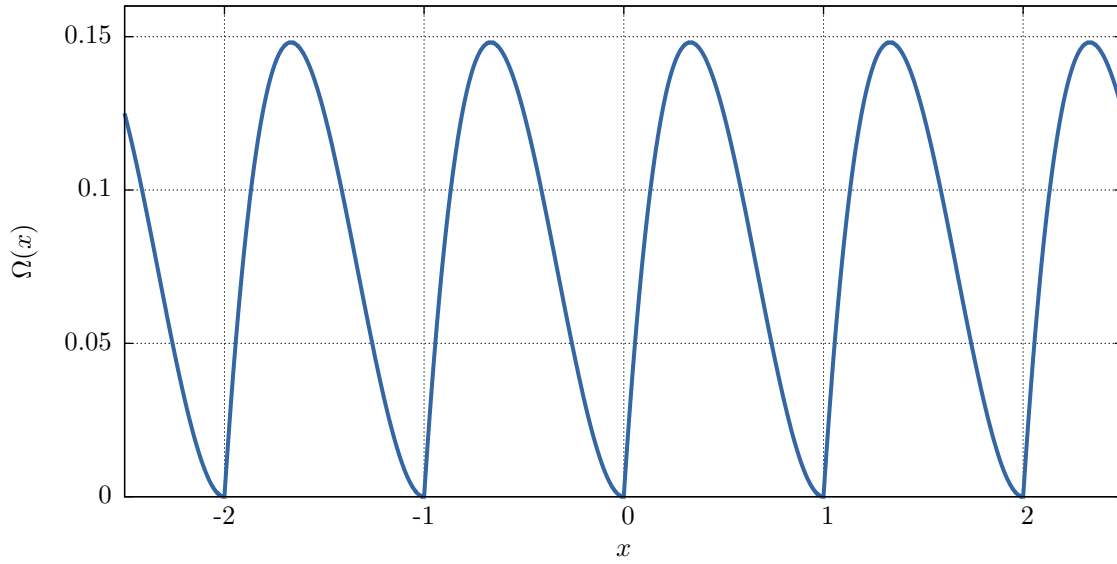


Figure D.1: The function  $\tilde{\Omega}(x)$ .

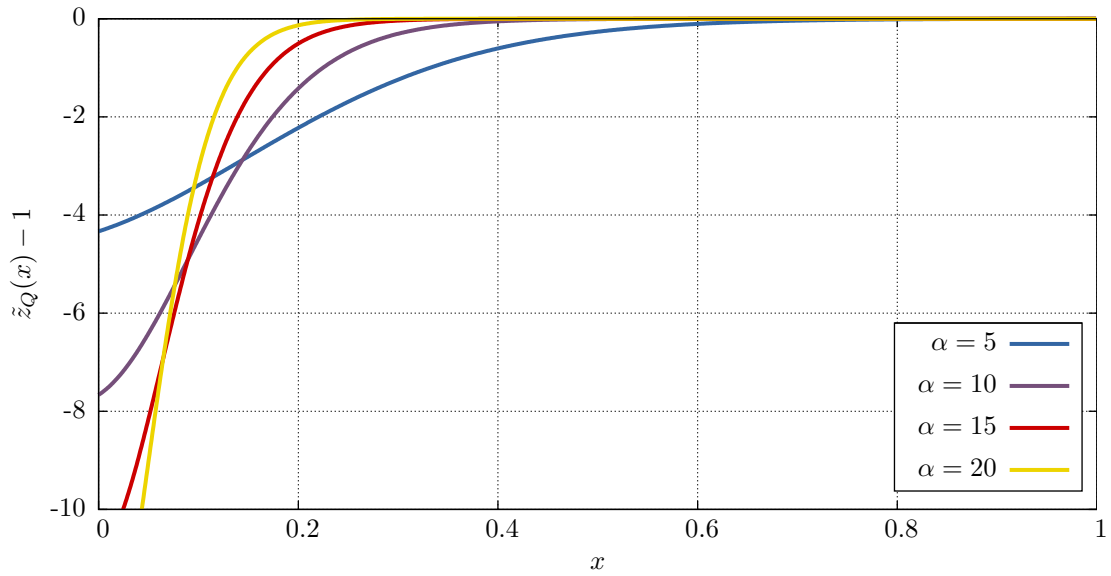


Figure D.2: The function  $\tilde{z}_Q(x) - 1$  for different values of  $\alpha = \pi T t > 1$ .

## D.2 The function $\tilde{z}_Q(x)$

Defined by:

$$\tilde{z}_Q(x) = u(\alpha x) - 2\alpha(1-x)w(\alpha x), \quad (\text{D.7})$$

where

$$w(x) = \frac{x \coth(x) - 1}{\sinh(x)^2}, \quad u(x) = \coth(x) - \frac{x^2}{\sinh(x)^2} \quad (\text{D.8})$$

and

$$\alpha = \pi T t = \pi l_t^2 / l_T^2 \gg 1, \quad (\text{D.9})$$

because of (4.10). This function is shown in Figure D.2.

We are interested in the limit  $\alpha \gg 1$ . Here,  $\tilde{z}(x)$  approaches 1 exponentially fast for  $x > 1/\alpha$ . Thus, in integrals of the type

$$\int_0^1 dx [\tilde{z}_Q(x) - 1] f(x), \quad (\text{D.10})$$

we can extend the upper border of integration to  $\infty$  as long as  $f(x)$  is increasing much slower than  $e^x$ . This allows us to do the following integrals using (C.7) and  $d/dx [u(x)] = 2w(x)$ , for  $\alpha \gg 1$ :

$$\int_0^1 dx [\tilde{z}_Q(x) - 1] x^s = \begin{cases} -1 & s = 0 \\ -\frac{1}{\sqrt{\alpha}} \frac{\sqrt{2\pi}}{4} |\zeta(1/2)| + \mathcal{O}\left(\frac{1}{\alpha^{3/2}}\right) & s = 1/2 \\ -\frac{1}{\alpha} + \frac{\pi^2}{12} \frac{1}{\alpha^2} & s = 1 \\ -\mathcal{O}\left(\frac{1}{\alpha^{3/2}}\right) & s = 3/2 \\ -\frac{\pi^2}{6} \frac{1}{\alpha^2} + \mathcal{O}\left(\frac{1}{\alpha^3}\right) & s = 2, \end{cases} \quad (\text{D.11})$$

to obtain an expansion in  $1/\alpha$  for  $f(x)$  being a polynomial of order  $< 3$ . Note that the first equation implies:

$$\int_0^1 dx \tilde{z}_Q(x) = 0, \quad (\text{D.12})$$

which actually holds for all  $\alpha$ .



# Bibliography

- [1] B. L. Altshuler, A. G. Aronov, and D. E. Khmelnitsky. Effects of electron-electron collisions with small energy transfers on quantum localisation. *Journal of Physics C: Solid State Physics*, 15(36):7367–7386, 1982.
- [2] T. Ludwig and A. D. Mirlin. Interaction-induced dephasing of Aharonov-Bohm oscillations. *Physical Review B (Condensed Matter and Materials Physics)*, 69(19):193306–4, May 2004.
- [3] C. Texier and G. Montambaux. Dephasing due to electron-electron interaction in a diffusive ring. *Physical Review B (Condensed Matter and Materials Physics)*, 72(11):115327–20, 2005.
- [4] F. Marquardt, J. von Delft, R. A. Smith, and V. Ambegaokar. Decoherence in weak localization. I. Pauli principle in influence functional. *Physical Review B (Condensed Matter and Materials Physics)*, 76(19):195331–27, November 2007.
- [5] J. von Delft, F. Marquardt, R. A. Smith, and V. Ambegaokar. Decoherence in weak localization. II. Bethe-Salpeter calculation of the cooperon. *Physical Review B (Condensed Matter and Materials Physics)*, 76(19):195332–17, November 2007.
- [6] G. Bergmann. Weak localization in thin films: a time-of-flight experiment with conduction electrons. *Physics Reports*, 107(1):1–58, May 1984.
- [7] S. Chakravarty and A. Schmid. Weak localization: The quasiclassical theory of electrons in a random potential. *Physics Reports*, 140(4):193–236, July 1986.
- [8] E. Akkermans and G. Montambaux. *Mesoscopic Physics of Electrons and Photons*. Cambridge University Press, 1 edition, May 2007.
- [9] T. Dittrich. *Quantum Transport and Dissipation*. Wiley-VCH Verlag GmbH, February 1998.
- [10] F. Marquardt. Lecture notes ”Mesoskopische Physik” about weak-localization: <http://homepages.physik.uni-muenchen.de/~Florian.Marquardt/mesolecture/>.
- [11] G. Rickayzen. *Green’s Functions and Condensed Matter*. Academic Pr, June 1981.

- 
- [12] B. L. Altshuler and A. G. Aronov. Electron-Electron Interactions In Disordered Conductors. *Modern Problems in Condensed Matter Science*, 10:1, 1985. edited by A. L. Efros and M. Pollak (North-Holland, Amsterdam, 1985).
- [13] R. P. Feynman and A. R. Hibbs. *Quantum Mechanics and Path Integrals*. McGraw-Hill Companies, June 1965.
- [14] A. M. Zagoskin. *Quantum Theory of Many-Body Systems: Techniques and Applications*. Springer, 1 edition, March 1998.
- [15] A. L. Fetter and J. D. Walecka. *Quantum Theory of Many-Particle Systems*. Dover Publications, June 2003.
- [16] R. Kubo. Statistical-Mechanical Theory of Irreversible Processes. I. General Theory and Simple Applications to Magnetic and Conduction Problems. *Journal of the Physical Society of Japan*, 12:570–586, 1957.
- [17] H. B. Callen and T. A. Welton. Irreversibility and Generalized Noise. *Physical Review*, 83(1):34, July 1951.
- [18] H. Nyquist. Thermal Agitation of Electric Charge in Conductors. *Physical Review*, 32(1):110, July 1928.
- [19] P. Nozieres and D. Pines. *Theory Of Quantum Liquids*. Westview Press, November 1999.
- [20] W. Eiler. Electron-electron interaction and weak localization. *Journal of Low Temperature Physics*, 56(5):481–498, 1984.
- [21] G. Montambaux and E. Akkermans. Nonexponential Quasiparticle Decay and Phase Relaxation in Low-Dimensional Conductors. *Physical Review Letters*, 95(1):016403–4, July 2005.
- [22] M. Ferrier, A. C. H. Rowe, S. Gueron, H. Bouchiat, C. Texier, and G. Montambaux. Geometrical Dependence of Decoherence by Electronic Interactions in a GaAs/GaAlAs Square Network. *Physical Review Letters*, 100(14):146802–4, April 2008.
- [23] J. von Delft. Influence Functional for Decoherence of Interacting Electrons in Disordered Conductors. *cond-mat/0510563*, October 2005. *International Journal of Modern Physics B*, 22, 727-833 (2008).
- [24] R. P. Feynman and F. L. Vernon. The theory of a general quantum system interacting with a linear dissipative system. *Annals of Physics*, 24:118–173, October 1963.
- [25] U. Sivan, Y. Imry, and A. G. Aronov. Quasi-Particle Lifetime in a Quantum Dot. *Europhys. Lett.*, 28(2):115–120, October 1994.

- 
- [26] B. L. Altshuler and A. G. Aronov. Magnetoresistance of thin films and of wires in a longitudinal magnetic field. *JETP Letters*, 33(10):499–501, May 1981.
- [27] B. L. Altshuler, A. G. Aronov, and B. Z. Spivak. The Aaronov-Bohm effect in disordered conductors. *JETP Letters*, 33(2):94–97, 1981.
- [28] M. Ferrier, L. Angers, A. C. H. Rowe, S. Guron, H. Bouchiat, C. Texier, G. Montambaux, and D. Mailly. Direct Measurement of the Phase-Coherence Length in a GaAs/GaAlAs Square Network. *Physical Review Letters*, 93(24):246804, December 2004.
- [29] H. M. Edwards. *Riemann's Zeta Function*. Dover Publications, dover ed edition, June 2001.



# Acknowledgments

I want to thank everybody who helped me in writing this thesis.

In particular, my close advisor Dr. Oleg Yevtushenko, who guided me through most of this work. Without his patience and experience this would not have been possible.

Also, I want to thank my advisors Prof. Dr. Jan von Delft and Dr. Florian Marquardt for the opportunity to join their group, bringing up this topic and supporting me in numerous patient discussions. They provided the fundamentals of this work and gave a physical meaning to the results.

Furthermore, I want to thank my advisor Prof. Dr. Wilhelm Zwerger for providing the necessary support from the Technical University of Munich.

I also want to acknowledge the support of my numerous colleagues at the Arnold Sommerfeld Center, who provided a stimulating and challenging environment.

Moreover, I had the great honor to discuss our results with Professor Boris Altshuler and Prof. Dr. Alexander Mirlin, who I want to thank for their insightful comments.



## Erklärung

des Diplomanden

Name:

Vorname:

Mit der Abgabe der Diplomarbeit versichere ich, dass ich die Arbeit selbständig verfasst und keine anderen als die angegebenen Quellen und Hilfsmittel benutzt habe.

.....

(Ort, Datum)

.....

(Unterschrift)